Local invariants of fronts in 3-manifolds

Thesis submitted in accordance with the requirements of
the University of Liverpool for the degree of Doctor in Philosophy

by

Suliman Alsaeed

November 2014

Abstract

An invariant is a quantity which remains unchanged under certain classes of transformations. A wave front (or a front) in a 3-manifold is the image of a surface under a Legendrian map. The aim of this thesis is the description of all local invariants of fronts in 3-manifolds.

The front invariants under consideration are those whose increments in generic homotopies are determined entirely by diffeomorphism types of local bifurcations of the fronts. Such invariants are dual to trivial codimension 1 cycles supported on the discriminant in the space of corresponding Legendrian maps.

We describe the spaces of the discriminantal cycles (possibly non-trivial) for various orientation and co-orientation settings of the fronts in an arbitrary oriented 3-manifold, both for the integer and mod2 coefficients. For the majority of these cycles we find homotopy-independent interpretations which guarantee the triviality required. In particular, in the case of framed fronts we show that all integer local invariants of Legendrian maps without corank 2 points are essentially exhausted by the numbers of points of isolated singularity types of the fronts.

Dedication

All my thanks to Allah for helping me bring this work to a successful completion

To

My mother, without her continuous support and prayers, I could not complete this process

To

My siblings, Rima, Youssef, Abdulrahman, Rasha, Abdullah, Maryam, Munira and my beloved nieces and nephews, Bdoor, Sultana, Jojo, Ibrahim, Ahmad M, Jory and Ahmad Y for supporting me constantly by their unlimited love and encouragement

Contents

Acknowledgments

I would like to give special thanks to my supervisor Victor Goryunov who has provided me essential knowledge and expertise throughout the progress of my thesis. His insights and feedback into my work have been invaluable and provided me vital techniques, skills and knowledge to complete my final project.

Many thanks to, everyone in the Department of Mathematical Sciences at the University of Liverpool, in particular to my second supervisor, Anna Pratoussevitch for her support and kind words. I am also thankful to my colleagues whom I have great gratitude for their friendship throughout my time at the University of Liverpool. A spacial thanks to Fawaz Alharbi, Nasser Bin Turki, Andrew Monaghan, Heather Riley, Graham Reeve, Katy Gallagher, Nada Alhabib, Joel Haddley, Poj Lertchoosakul, Kalyan Banerjee and Jenna Birch for their moral support and encouragement over the years.

I would like to thank Umm al-Qura university for giving me the chance to continue my studies. In addition, I would like to thank the Saudi cultural Bureau in London for their support during my studies abroad.

I am especially grateful to all my friends who have been around these past few years, who have been helping and supporting me at different occasions. In particular, all my friends from Flat 18, Muflih, Mosleh, Hammad, Sulaiman, Berkan and many, many others...

At last, by the fact of completing this thesis, I am immensely indebted to all my family members for their constant support and encouragement throughout the duration of my studies.

Introduction

Consider a set A of mathematical objects with an equivalence relation E on it. We say that a function on A is *an E-invariant* or just *an invariant* if its restriction to each E-equivalence class is constant. For example, A may be a linear space and the equivalence may be upto a certain group of linear transformations acting on A.

0.1 General approach

Another example, model for this thesis is that A is a set of maps generic in certain sense and equipped with certain topology, and each equivalence class is a connected component of A. Moreover, it may happen that we are able to add to A – consistently with the topology – a set Σ of non-generic maps. In all the situations we will be considering, the set Σ will be of real codimension 1 in $\Omega = A \cup \Sigma$. We will call $\Sigma \subset \Omega$ *the discriminant*. In most of our cases Σ will be *co-orientable* in Ω, that is, if U and V are two local connected components of $\Omega \setminus \Sigma$ near a generic point $\sigma \in \Sigma$ then we will be able to distinguish locally between U and V, and nominate one of them positive and the other negative. The side of Σ facing the positive component is usually also called *positive*. In

such a co-oriented case, assuming that our invariants take values in an abelian group S, we are able to extend an invariant I previously defined on $\Omega \setminus \Sigma$ to the set Σ_1 of generic points of Σ by setting the value $I(\sigma)$ to be *the jump of* I, that is, the difference of the values of I on the neighboring positive and negative components of $\Omega \setminus \Sigma$. The restriction to Σ_1 of the extension of I will be denoted I' and called *the derivative of* I (since it is analogues to the discrete derivative).

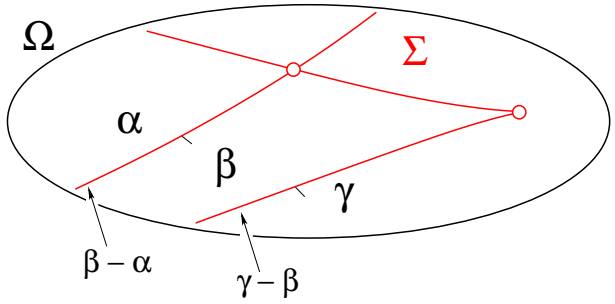

Figure 1: Values of an invariant on $\Omega \setminus \Sigma$ and its extension on Σ_1.

Another problem considered in this thesis is: is there any invariant on $\Omega \setminus \Sigma$ whose extension to Σ_1 coincides with a given function on Σ_1? In a sense, the question is about integrating a given derivative.

An approach to this question comes from the following model situation. Let us take a plane for the space Ω and a graph $\Gamma \subset \mathbb{R}^2$ for Σ (see Figure 2). We assume that only finitely many edges meet at any vertex of Γ, and Γ is a closed subset of $\mathbb{R}^2$ (in particular Γ may have edges going to infinity). The edges of Γ are playing the role of the set Σ_1, in particular they are co-oriented in the plane. The vertices of Γ are playing the role of the strata of Σ of codimension 2 in Ω.

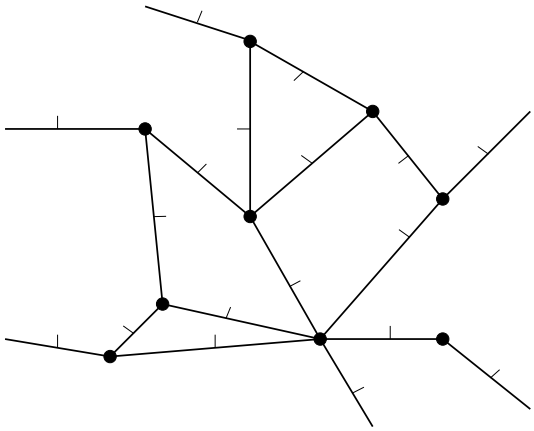

Figure 2: Embedded graph in the plane.

Consider a function ϕ on the set of edges of Γ having a constant value x_i on the edge X_i. What are the conditions on the x_i for ϕ to be the derivative I' of a locally constant function I on $\mathbb{R}^2 \setminus \Gamma$?

Assume such an I exists. Then for any two points f_0 and f_1 in $\Omega \setminus \Gamma$,

$$I(f_1) = I(f_0) + \sum x_i \langle \gamma, X_i \rangle,$$

where γ is a generic path in $\mathbb{R}^2$ from f_0 to f_1 and $\langle \gamma, X_i \rangle$ the intersection number of γ with the edge X_i: a transversal crossing of X_i by γ contributes to it $+1$ if the crossing is in the co-orienting direction and -1 otherwise. If the value $I(f_0)$ is given, the quantity $I(f_1)$ is path-independent if and only if the value $\sum x_i \langle \omega, X_i \rangle$ is zero for any generic loop ω in $\mathbb{R}^2$, that is, the intersection number of ω with the closed 1-chain $\sum x_i \bar{X}_i$ must vanish (the $\bar{X}_i$ is the closure of X_i). The intersection number is well-defined if and only if $\sum x_i \bar{X}_i$ is a cycle, that is, every vertex Y_j of Γ enters its boundary with coefficient zero. This is equivalent to the total jump of the invariant along a small loop around the Y_j to be zero (see Figure 3).

Figure 3: Left: co-oriented edges entering a vertex of a planar graph, labelled with the increments of an invariant across them. The total increment $a-b+c$ of the invariant along the loop shown must be zero.
Right: if we orient the edges consistently and take their sum with the coefficients equal to the increments then $a-b+c$ is the coefficient with which the central point enters the boundary of the sum.

Since the plane is co-orientable the boundary conditions on $\sum x_i \bar{X}_i$ just described are the only conditions needed for existence of an invariant. However, if Ω is, for example, a torus then $\sum x_i \bar{X}_i$ must also have zero intersection number with each generator of $H_1(\Omega; S)$. (In the latter case we say that the cycle $\sum x_i \bar{X}_i$ is *trivial*).

The study of invariants of smooth maps via their derivatives (including those of order higher than 1) has its staring point in knot theory. It was further developed in works of Arnold and Goryunov for some other cases. We shall start with a brief overview of their earlier results on such invariants.

0.2 Knot and link invariants

In 1989, V. Vassiliev and M. Goussarov introduced the notion of finite type knot invariants (a.k.a. Vassiliev invariants). Vassiliev's approach is based on the study of discriminants in (infinite-dimensional) spaces of smooth maps from one manifold into another. By definition, the discriminant consists of all maps with non-stable singularities.

For example, consider the space of all smooth maps from the circle into oriented three-space, $\Psi = \{f : S^1 \to \mathbb{R}^3\}$, equipped – like any other space of maps in this thesis – with the Whitney C^∞ topology (see [11], page 11). If f is an embedding, then its image is a knot. The complement to the set of all embeddings is the discriminant $\Gamma \subset \Psi$. It consists of all smooth maps from S^1 into $\mathbb{R}^3$ that have singularities, either local, where $f' = 0$, or nonlocal, when f is not injective. Two knots are equivalent if and only if they can be joined by a path in the space Ψ that does not intersect the discriminant. Therefore, knot types are in one-to-one correspondence with the connected components of $\Psi \setminus \Gamma$.

Definition 0.2.1. A *knot invariant* with values in an abelian group S is a locally constant map from $\Psi \setminus \Gamma$ to S.

The simplest degeneration is when the only singularity of f is a double point of the image. We call a double point *generic* if the velocities of the two branches meeting at it are non-proportional. Generic points of the k-tuple self-intersection of Γ are maps whose only singularises are k generic double points. We will denote by $\Gamma_k \subset \Gamma$ the set of all such maps. Points of $\bigcup_{k\geq 1} \Gamma_k$ will be called *singular knots*.

The stratum Γ_1 is co-oriented in Ψ. Namely, a double point of the image may be perturbed in two ways as shown below.

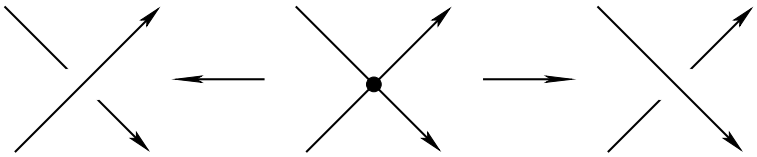

We call the local perturbation on the right *positive* and on the left *negative*, and use the same names for the corresponding sides of Γ_1 in Ψ. This assignment of the names dose not depend on the choice of the orientation of the source circle.

Any knot invariant can be extended to singular knots (but not to the rest of Γ) by means of the *Vassiliev skein relation* [3]:

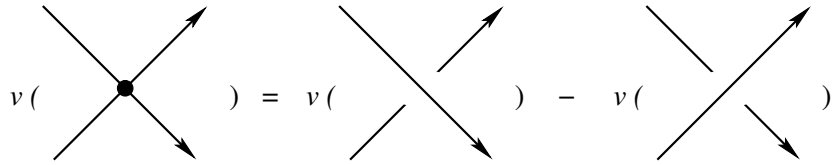

Here v is a knot invariant with values in some abelian group, the left-hand side is the value of v on a singular knot K (shown in a neighbourhood of a double point) and the right-hand side is the difference of the values of v on (possibly singular) knots obtained from K by replacing the double point with a positive and a negative crossing respectively.

Using the Vassiliev skein relation recursively, we extend any knot invariant to knots with an arbitrary number of double points. There are many ways to do this, since we can choose to resolve double points in an arbitrary order. However, the result is independent of such a choice [3]. The restriction of an

extended knot invariant to the stratum Γ_k is called the *kth order index* of the invariant.

Definition 0.2.2. [1] A knot invariant is said to be a *Vassiliev invariant* of order (or degree) at most n if its extension vanishes on all singular knots with more than n double points. A Vassiliev invariant is said to be of order (degree) n if it is of order at most n but not of order at most $n-1$.

Example 1. Consider a generic point of Γ_2, and a germ Π of a plane transversal to Γ_2 in Ψ at this point. The local intersection of Π with Γ is shown in Figure 2. It consists of four co-oriented Γ_1 rays. The figure also shows the local behavior of the corresponding maps near the two singular point of the unperturbed map.

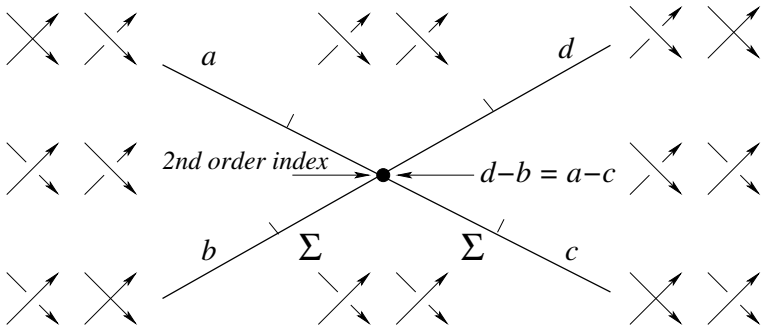

Figure 4: Order 2 index assignment from order 1 index values.

Let a, b, c, d be the values of the extension of a knot invariant to the local Γ_1 components, that is, the values of *the first order index* of the invariant. The value of *the second order index* of the invariant at the central Γ_2 point is $a-c$. This is also equal to $d-b$ since the total increment of the invariant along a

small circle around the center must be zero: $-a-b+c+d=0$. Similar order k indices are assigned to connected components of the set Γ_k.

Example 2. There are no non-constant integer-valued knot invariants of order 1, that is, for which the 2nd order index vanishes. Indeed, any singular knot with exactly one generic double point can be unknotted to the curve ∞ by a sequence of crossing changes, that is, joined to the ∞ by a generic path in $\Gamma_1 \cup \Gamma_2$. The value of an order 1 invariant along this path does not change. Therefore, any first order invariant has the same value on the whole of Γ_1. In particular, this value is equal to the increment of the invariant in the following bifurcation.

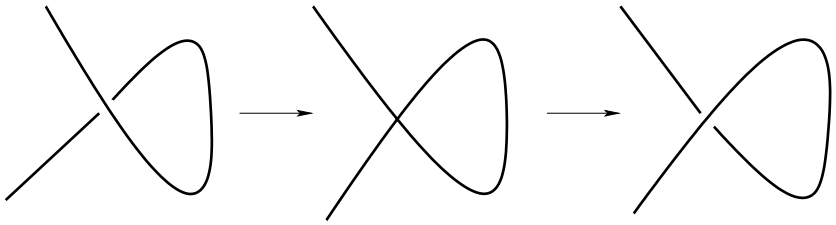

The knots types on the left and right here are the same, hence the increment is zero.

0.2.1 Linking number

The linking number is an example of a non-constant order 1 Vassiliev invariant of two-component oriented links in oriented $\mathbb{R}^3$ or S^3. It has an analog for framed knots, called the *self-linking number*.

The linking number $l(A,B)$ of two oriented closed spatial curves A and B is the number of times A winds around B. To give a precise definition, choose

an oriented disk D_A immersed in the space so that its oriented boundary is the curve A. The linking number $l(A, B)$ is then defined as the intersection number of D_A and B.

The linking number may be read from a link diagram. In general, there are two types of crossing points in a link diagram, positive and negative:

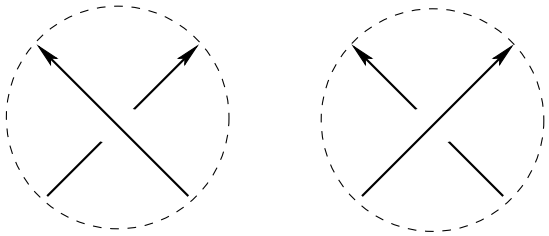

Negative Crossing *Positive Crossing*

The *local writhe* of a crossing is defined as $+1$ or -1 for positive or negative crossings, respectively. The *writhe* (or *total writhe*) of a diagram is the sum of the writhes of all crossing points, or, equivalently, the difference between the number of positive and negative crossings.

Let I be the set of crossing points of a link diagram involving branches of both components of the two oriented closed spatial curves A and B. Then I is a disjoint union of two subsets I_B^A (points where A passes over B) and I_A^B (where B passes over A).

Proposition 0.2.1. *[3]*

$$l(A, B) = \sum_{p \in I_B^A} w(p) = \sum_{p \in I_A^B} w(p) = 1/2 \sum_{p \in I} w(p),$$

where $w(p) = \pm 1$ *is the local writhe of the crossing point.*

Lemma 0.2.1. *[3] The linking number of an oriented two component link is a Vassiliev invariant of order 1.*

Indeed, a local change of a crossing from the negative to the positive increases the linking number by 1. Hence the first order index of the linking number is constant, and therefore its second order index vanishes.

0.3 Planar curve invariants

After Vassilev's introduction of finite types invariants, similar approach has been developed to invariants of (spacial) smooth maps in a range of other low dimensions. In this section we present Arnold's work on regular curves and planar fronts.

0.3.1 Regular curves

A *regular curve* is a smooth immersion of an (oriented) circle into the plane. Let Φ be the space of all such regular curves. A generic immersion has only ordinary double points of transversal self-intersection. All non-generic immersions form a discriminant $\Theta \subset \Phi$. To explain the nature of Arnold's results we follow his way and star with an example.

Consider two curves of Figure 5. They belong to the same component of the space of immersions (see Section 0.3.1.1). Hence there exists a one-parameter family of immersions connecting these two generic immersions [13].

The immersions in this connecting path are certainly not generic for certain values of the parameter labeling the immersions. If the path is generic, three

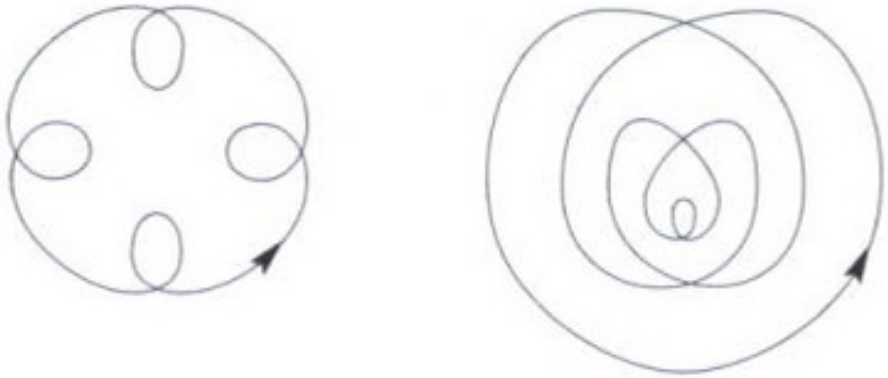

Figure 5: Two representatives of one component of the space of regular planar curves [13].

types of events (Figure 6) can occur: *triple point of the immersion*, and *self-tangencies* of two types: *direct self-tangencies* (when the two tangent branches are oriented by the same tangent vector) and the *inverse self-tangencies* (when the velocity are opposite). We are going to describe Arnold's planar curve invariants J^+, J^- and St. Comparison of their values on the curves of Figure 5 implies

Proposition 0.3.1. *[13] The number of triple crossings on any generic path connecting the two curves shown in Figure 5 is at least six. The number of the direct self-tangencies and the number of inverse self-tangencies are also greater than or equal to six.*

So we have there discriminantal strata of codimension 1 in the space Φ of all immersions of a circle into the plane corresponding to *triple points*, *direct self-tangencies* and *inverse self-tangencies*.

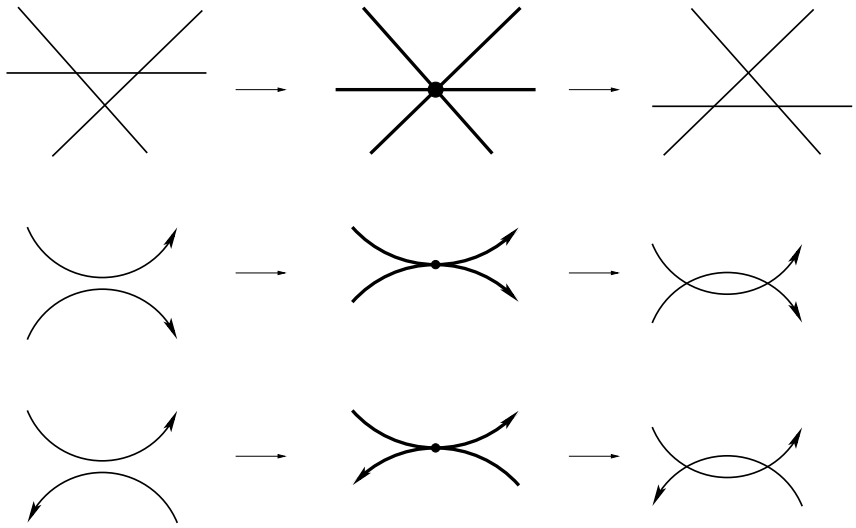

Figure 6: Triple point and self-tangencies bifurcations, direct and inverse.

Lemma 0.3.1. *[7] Each of these three strata of the discriminant is co-orientable in* Φ.

Arnold defines the co-orientation of the self-tangencies discriminant as follows. A direct self-tangency bifurcation is called *positive* if the number of double points of the curve *increases*. An inverse self-tangency bifurcation is called *positive* if the number of double points *decreases*.

The positive side of the triple point stratum in Φ is chosen by the following rule.

A crossing of the triple point stratum by a generic path in Φ gives rise to the *vanishing triangles* (the dying triangle, which existed just before the crossing, and the newborn triangle appearing just after it). We assign signs to the triangles as set in Figure 7.

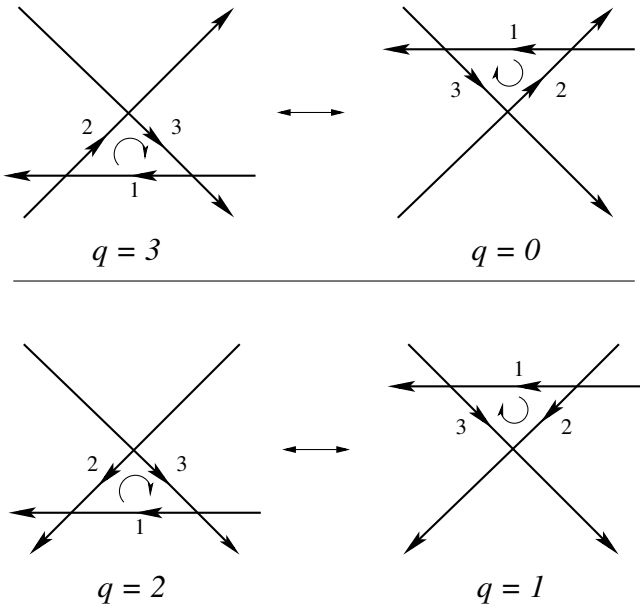

Figure 7: Vanishing triangles and their sings $(-1)^q$.

In words, the rule is as follows. Fix an orientation on the source circle. A triple point has three preimages on the circle and their cyclic order is well defined. Hence one obtains a well-defined orientation of the vanishing triangles (given by the cyclic order in which the immersed curve visits its sides). On the other hand, each side has its own direction (since the circle is oriented). This direction may coincide with the direction defined by the above cyclic order or may be opposite to it. Let q be the number of the sides of the vanishing triangle whose directions coincide with that given by the cyclic order.

Definition 0.3.1. The *sign* of a triangle is set to be $(-1)^q$.

We are now call a triple point bifurcation *positive* if the newborn triangle is positive, and hence the dying one is negative.

Remark 1. The coorientation of the triple point discriminantal stratum involves global information about the image. We will avoid such a situation in our study of fronts in 3-manifolds.

Remark 2. None of the three co-orientations depends on the orientation of the source circle or of the plane.

0.3.1.1 Invariants St, J^+ and J^-

The *index* of an immersion of an oriented circle into the an oriented plane is the degree of the mapping $S^1 \to S^1$ sending a point of the circle to the direction of the velocity of the immersion at the point. The Whitney Theorem [4] says that the connected components of the space Φ are numbered by the values of the index.

Consider one of these components, that is, the space of immersions of a fixed index.

Theorem 0.3.1. *[7] There exists a unique (up to an additive constant) invariant of generic curves of a fixed index, whose value remains unchanged under a crossing of a self-tangency stratum of the discriminant, but increases by one under a positive crossing of a triple point stratum of the discriminant.*

The invariant is denoted by St (Strangeness), when normalized by the following conditions:

$$St(K_0) = 0, \quad St(K_{i+1}) = i \quad (i = 0, 1, ...), \tag{1}$$

where K_0 is the infinity curve and K_{i+1} is the simplest curve with i double points (see Figure 8). The curve K_j has index $\pm j$ depending on the orientation.

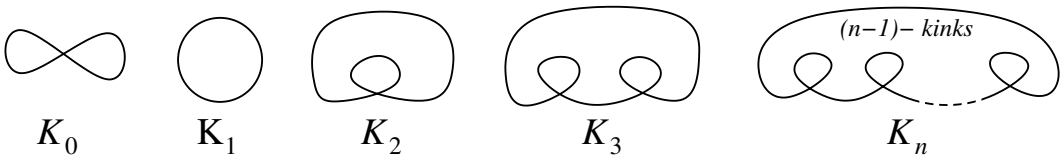

Figure 8: The standard curves K_j.

Theorem 0.3.2. *[7] There exists a unique (up to an additive constant) invariant of generic curves of a fixed index, whose value remains unchanged under a crossing of an inverse self-tangency or of a triple point stratum of the discriminant, but increases by two under a positive crossing of a direct self-tangency stratum of the discriminant.*

This invariant is denoted by J^+, when normalized by the following conditions:

$$J^+(K_0) = 0, \quad J^+(K_{i+1}) = -2i \quad (i = 0, 1, ...). \tag{2}$$

Theorem 0.3.3. *[7] There exists a unique (up to an additive constant) invariant of generic curves of a fixed index, whose value remains unchanged under a crossing of a direct self-tangency or of a triple point stratum of the discriminant, but decreases by two under a positive crossing of an inverse self-tangency stratum of the discriminant.*

This invariant is denoted by J^-, when normalized by the following conditions:

$$J^-(K_0) = -1, \quad J^-(K_{i+1}) = -3i \quad (i = 0, 1, ...). \tag{3}$$

The choice of the values of the basic invariants on the curves K_j is dictated by the request of the invariants behaving well under the following operation.

Consider two regular curves, one in the left half plane and the other in the right half plane (see Figure 9). Connect them with a bridge not intersecting the two curves assuming that the orientations of the surviving parts of the original curves are inherited in the orientation of the resulting curve. (Notice that this is not always possible, for example if the both curves are the standard circles K_1 with opposite orientations.) The resulting curve is called *the connected sum* of the two original.

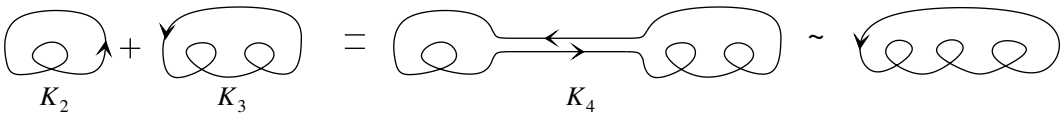

Figure 9: The connected sum of two immersions.

Definition 0.3.2. An invariant I is said to be *additive* if

$$I(A + B) = I(A) + I(B)$$

whenever the connected sum $A + B$ of curves A and B is defined.

Theorem 0.3.4. *[13] All three basic invariants are additive under the connected sum of immersions.*

Notice that the summation is not an operation on the classes of immersions, since the bridge may be different. However, the basic invariants are additive under any choice of the bridge [13].

0.3.2 Planar fronts

Arnold also obtained a natural generalization of the invariants of regular planar curves to the case of generic planar wave fronts [12, 13]. A generic planar

front is a curve whose only singularities are transversal double points and semi-cubical cusps. The complete list of their generic one-parameter bifurcations consist of *triple points, self-tangencies, cusp births and cusp crossings* (Figure 10).

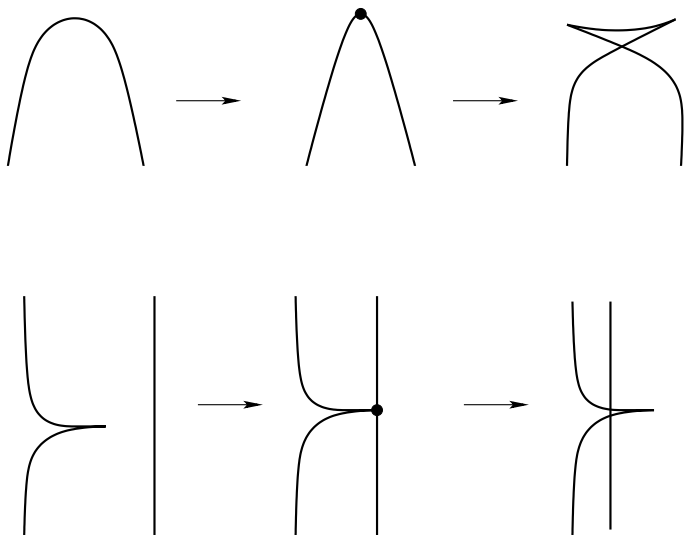

Figure 10: Cusp birth and cusp crossing.

We are not going into details of Arnold's results on this topic, but rather concentrate on their refinements due to Francesca Aicardi [5], who described all local additive invariants of oriented and co-orientated one-component plane wave fronts. The word *local* here means that their increment under generic crossings of the discriminant depends – we would say nearly – only on the behavior of the family of fronts in neighborhoods of the points of the preimage circle sent to the points involved in the bifurcation. For all basic definitions related to fronts and for the description of the space of corresponding Legendrian maps see our Chapter 1.

First of all, Aicardi showed that there are five basic invariants independent of the orientations of fronts and of the plane as well as of the co-orientation of fronts:

(i) n: the number of double points;

(ii) λ: the number of cusp points;

(iii) J^+: responsible [5] for the direct self-tangencies;

(iv) J^-: responsible for the inverse self-tangencies;

(v) Sp: responsible for the triple points and cusp crossings.

Here the direct and inverse self-tangencies are understood in the co-orientation sense (see Figure 11).

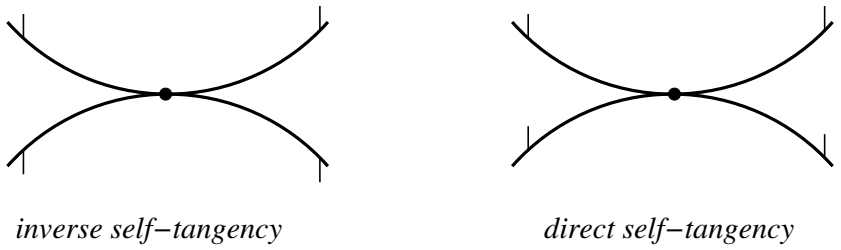

Figure 11: Inverse and direct self-tangencies of co-oriented fronts.

The invariants J^+, J^-, and Sp of wave fronts reduce to the invariants J^+, J^-, and St for wave fronts without cusps, that is, to the Arnold invariants of smooth closed plane curves. Hence, Aicardi actually allows certain global information about a front, which we will avoid in our own work as promised in Remark 1.

The number of integer-valued linearly independent additive local invariants of generic oriented and co-oriented wave fronts in an oriented plane is equal to 10. One of these invariants is the *Maslov index* [5]. The *Maslov index* of a generic planar wave front is calculated as the difference between the numbers of positive and negative cusps of the front (see Figure 12). A cusp is said to be *positive*, if its outgoing branch belongs to the co-orienting half-plane. Otherwise a cusp is said to be *negative*.

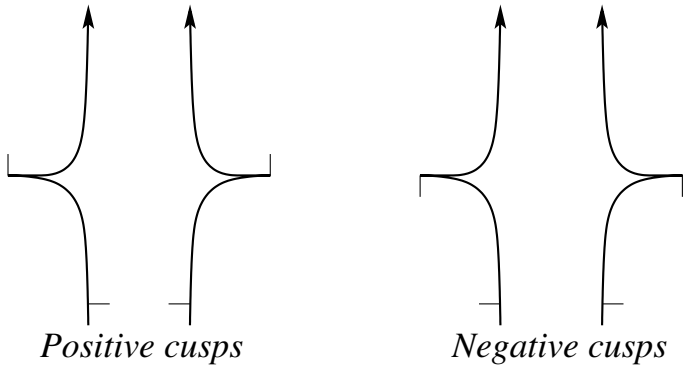

Figure 12: Cusp types.

To describe the other additive invariants, Aicardi introduced 6 new invariants which she denoted $f^+, f^-, \lambda^\uparrow, \lambda^\downarrow, p^\uparrow, p^\downarrow$.

The invariant $f^+(f^-)$ counts the double points where two positive (negative) branches of the fronts intersect. Here we call a *branch positive* if its orientation followed by its co-orientation gives the positive orientation of the plane, and *negative* otherwise.

The invariant $\lambda^\uparrow(\lambda^\downarrow)$ is the number of cusps at which the orientation of the plane defined by the two branches of an oriented front leaving the cusp

point (first along the incoming branch, second along the outgoing branch) is positive (negative).

The invariants $p^{\uparrow}$ and $p^{\downarrow}$ count the numbers of cusp crossings of certain types (see [5] for the rather complicated rules) in generic 1-parameter families. These six new invariants satisfy the relations

$$\lambda^{\uparrow} + \lambda^{\downarrow} = \lambda, \qquad f^{+} + f^{-} - J^{+} + J^{-} - \frac{1}{2}\lambda = n,$$

hence, from the linear independence point of view, only four of them are really new.

0.4 Surfaces in 3-manifolds

0.4.1 Maps of surfaces to $\mathbb{R}^3$

Local invariants of mappings of oriented surfaces into $\mathbb{R}^3$ were classified by Victor Goryunov [16]. Locally, the image of a generic mapping of a fixed closed (that is, compact without boundary) surface M to $\mathbb{R}^3$ is either a smooth sheet, or transversal intersection of either 2 or 3 smooth sheets, or the Whitney umbrella (the image of the map $(x, y) \longmapsto (x, y^2, xy)$). Mappings with more complicated images form the discriminantal hypersurface in the space of all C^{∞} maps from M to $\mathbb{R}^3$.

Goryunov showed that the space of integer-valued local invariants of mappings of an oriented surface into oriented $\mathbb{R}^3$ is 3-dimensional, with the following basic invariants:

(1) I_t, the number of triple points;

(2) $I_p/2$, half the number of pinch points;

(3) $I_\int$, the integral invariant.

The meanings of the first two invariants are clear. However, we need to remind the detailed description of the integral invariant $I_\int$ since its analog will be introduced for oriented fronts in $\mathbb{R}^3$ in our Chapter 4.

Let $\mathrm{Im}f$ be the image of a generic mapping of a surface $f : M \to \mathbb{R}^3$. Take a point u in $\mathbb{R}^3$ not on the image. Consider a small 2-sphere centered at u. It is oriented as the boundary of the oriented three-ball it bounds. The radial contraction of the image of f onto the sphere defines the composition mapping from M to the sphere. We denote by $deg(u)$ the degree of this mapping. The surface $\mathrm{Im}f$ subdivides the ambient 3-space into a finite number of connected components D. The value $deg(u)$ is constant on each of them. We denote the corresponding value by $deg(D)$.

We define the integral of the function deg against the Euler characteristic χ setting, in its established notation from [16]:

$$\int_{\mathbb{R}^3 \setminus \mathrm{Im}f} deg(u) d\chi(u) = \sum_D deg(D) d\chi(D),$$

where D runs through all connected components of $\mathbb{R}^3 \setminus \mathrm{Im}f$.

There are 8 (respectively 3) local connected components of the complement to the front around a triple point t (respectively a pinch point p). We set the degrees $deg(t)$ and $deg(p)$ to be the arithmetical means of the corresponding 8 or 3 degrees. The number $deg(t)$ is a semi-integer that also coincides with the arithmetical mean of the degrees of any two opposite local components.

The value $deg(p)$ is the degree of the largest of the three components around p.

We finally set

$$I_{\int}(f) = \int_{\mathbb{R}^3 \setminus \mathrm{Im} f} deg(u) d\chi + \sum_t deg(t) + \frac{1}{2} \sum_p deg(p),$$

where t and p run thought all triple and pinch points of the image.

0.4.2 Maps between 3-manifolds

In 2011 Victor Goryunov classified order 1 invariants of maps between 3-manifolds [17]. He showed that in the oriented case the space of integer invariants has rank 7 for any source and target. The mod2 setting, with $\mathbb{R}^3$ as the target, adds another 4 linearly independent invariants. One of them combines the self-linking of the cuspidal edge of the critical value set with the number of connected components of the edge [17]. Two other of these four invariants are similar combinations for the two links constructed from the self-intersection of critical value set and parts of its cuspidal edge [6]. Goryunov also analyzed general non-oriented settings and obtained either exact descriptions or rank estimates for the spaces of integer- and mod2-valued invariants.

0.5 Results of the thesis

All the terminology of contact geometry used in this section will be explained in detail in Chapter 1.

In this thesis we classify local invariants of fronts in 3-manifolds. Let $\pi : E \to B$ be a Legendrian bundle. Consider a Legendrian immersion $i : L \to E$ of a manifold L. The restriction of the projection π to L, that is, $\pi \circ i : L \to B$, is said to be a *Legendrian map*. Legendrian maps are maps to a manifold of dimension 1 greater than the dimension of the source. Throughout the thesis we assume that the target of a Legendrian map is a 3-manifold. We denote by $\mathcal{L}(M, N)$ the space of all appropriate Legendrian maps $M^2 \to N^3$ (see Chapter 1), where M is a fixed closed (that is, compact without boundary) surface and N has no boundary. The image of such a map is called a *wave front* or just a *front*.

The only singularities of generic fronts in N are transversal intersections of either two or three smooth sheets, cuspidal edges and their transversal intersections with smooth sheets, and swallowtails (see Figure 13).

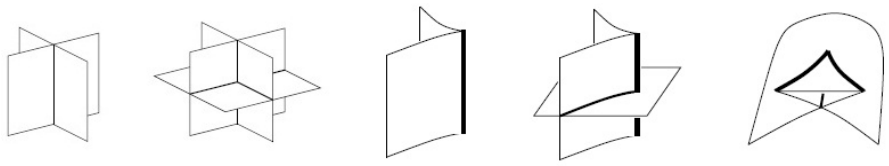

Figure 13: Local singularities of stable fronts in a 3-manifold.

Maps whose fronts have more complicated singularities form the *discriminantal* hypersuface Ξ in $\mathcal{L}$. The discriminant subdivides $\mathcal{L}$ into connected components. Our aim is to find a complete list of what we call the local invariants, for various orientation and co-orientation settings.

The invariants we study are order 1 local. Our notion of locality is slightly more rigid than the one from Section 0.3 used by Arnold. Here is our formal

definition.

Definition 0.5.1. We say that an invariant is *local* of order 1 if every increment of the invariant in a generic homotopy of fronts is determined entirely by the diffeomorphism type of the local bifurcation of the front at a crossing of Ξ.

Since no higher order invariants will be involved, we call such invariants just local. We make no difference in the exposition between local invariants of Legendrian maps $M \to N$ and of fronts in N parametrised by M: bifurcations of the Legendrian maps are considered in terms of bifurcations of their fronts.

Up to a choice of an additive constant (individual for each connected component of $\mathcal{L}$), any numerical local invariant I is defined by its *derivative* $I' = \sum x_i X_i$, where the X_i are discriminantal strata of codimension 1 in $\mathcal{L}$ and co-oriented in $\mathcal{L}$, and the x_i are the local increments of I along paths crossing the X_i in the co-orienting direction. This linear combination is a trivial codimension 1 cycle in $\mathcal{L}$: its intersection index with any loop in $\mathcal{L}$ must be zero. Therefore, construction of such linear combinations (without an a priori knowledge of the invariants) splits into two parts:

a) establishing conditions on linear combinations of the codimension 1 strata to be cycles (we call them *discriminantal cycles*), and

b) checking the triviality of the discriminantal cycles.

The first part is a singularity theory task and does not depend on the choice of M and N (except for their orientability) and of a particular connected component of $\mathcal{L}(M, N)$. Indeed the boundaries of X_i consist of discriminantal

strata Y_j of codimension 2 in $\mathcal{L}$. The fact that a particular Y_j enters the boundary of $\sum x_i X_i$ with the coefficient zero is equivalent to the vanishing of the intersection number of $\sum x_i X_i$ with a small loop around Y_j (see Figure 3). Such small loops are realized as loops in representatives Π of germs of planes transversal to the Y_j. Therefore, generic two-parameter deformations of codimension 2 degenerations of fronts in 3-manifolds must be considered and their bifurcation diagrams (that is, intersections of the representatives Π with the discriminant Ξ) must be studied.

Part b) above is straightforward if we are able to give an integral (that is, homotopy-free) interpretation of a relevant invariant. However, in more complicated situations knowledge of the fundamental group of a particular connected component of $\mathcal{L}(M, N)$ may be required to show that the intersection index of any non-contractible loop in this component with the discriminantal cycle vanishes.

In the thesis we describe integer and mod2 invariants for ***framed and oriented fronts, framed but not oriented fronts*** and lastly ***oriented fronts with no framing***. Each case will be presented in a separate chapter. We should notice that we opt for the word 'framed' in this context (instead of the traditional 'co-orientated') to avoid confusion with co-orientations of discriminantal strata in the space $\mathcal{L}(M, N)$. None of our results depends on a component choice in $\mathcal{L}(M, N)$, and, therefore, we always refer to the space $\mathcal{L}$ or $\mathcal{L}(M, N)$ as a whole, without mentioning its particular connected components. All invariants are considered up to a choice of additive constants on these components.

The thesis is organized as follows.

Chapter 1: we recall basic definitions concerning contact geometry and Legendrian singularities. We also explain where the framing and co-orientation of fronts are coming from.

Chapter 2: we list local singularities of generic framed and oriented fronts in oriented 3-manifolds. Our first main result, Theorem 2.3.1, states that for framed and oriented fronts in any oriented 3-dimensional manifold the space of integer discriminantal cycles has rank 19. We explain the geometric meaning of basic integer cycles. The second part of our first main result is Theorem 2.3.2, which concerns the $\mathbb{Z}_2$ setting of the same problem. This time the space of discriminantal cycles has rank 20: in addition to mod2 reductions of the integer cycles, we have the cycle counting the parity of the number of direct self-tangencies of fronts in generic homotopies.

Chapter 3: we start with describing stable singularities of framed fronts which are under consideration in this chapter. Our second main result, Theorem 3.3.1 states that for framed fronts in any oriented 3-manifold the space of integer discriminantal cycles has rank 6. This space contains a rank 5 subspace which is spanned essentially by the derivatives of the invariants counting the numbers of points of fronts of various stable isolated singularity types. These are triple points of a front, two types of swallowtails, and two types of intersections of cuspidal edges with smooth sheets. A sixth basic discriminantal cycle corresponds to an algebraic count of corank 2 points of Legendrian maps $M \to N$ in generic homotopies. The mod2 setting adds another 2 basic cycles which are responsible for counting the parities of numbers of direct and opposite self-tangencies of fronts in generic homotopies.

Chapter 4: we consider oriented fronts with no framing. We describe stable singularities of oriented fronts. We then state our third main result, Theorem 4.3.1, claiming that the space of integer discriminantal cycles of oriented fronts in any oriented 3-manifold has rank 7. Similarly, this space contains a rank 6 subspace which is spanned essentially by the derivatives of the integral invariant (similar to that in Section 0.4.1) and invariants counting the numbers of points of fronts of various stable isolated singularity types. In Theorem 4.3.2, we state that the space of mod2 discriminantal cycles, in the same setting, has rank 11. The 4 additional basic cycles correspond to the linking and self-linking numbers of the links defined by the edges of the front, and also to the parity of the number of self-tangencies in generic one-parameter families of fronts.

Chapter 1

Basic Concepts

1.1 Contact manifolds

A smooth field of tangent hyperplanes on a manifold M is defined locally as the field of zeros of a differential 1-form. Assume the manifold is $(2n+1)$-dimensional and the 1-form is α. The hyperplane field is called *non-degenerate at a point of* M if at this point $\alpha \wedge (d\alpha)^n$ is not zero.

Definition 1.1.1. A *contact structure* on a smooth manifold M^{2n+1} is a field of tangent hyperplanes which is non-degenerate at any point. The planes of the field are called *contact planes*, and the corresponding local 1-form α is called a *contact form*.

Example 3. The linear space $\mathbb{R}^{2n+1}$ with coordinates $(p_1, \ldots, p_n; q_1, \ldots, q_n; z)$ has the standard contact structure given by the form

$$\alpha = dz - \sum_{i=1}^{n} p_i dq_i.$$

In this case $\mathbb{R}^{2n+1}$ is considered as the 1-jet space $J^1(\mathbb{R}^n_q, \mathbb{R}^1_z)$ of functions on $\mathbb{R}^n$, with the $p_i = \frac{\partial z}{\partial q_i}$.

Definition 1.1.2. An odd-dimensional manifold M^{2n+1} equipped with a contact form α is called a *contact manifold*.

1.2 Legendrian submanifolds

Definition 1.2.1. A submanifold of a contact manifold is said to be *integral* if its tangent space at every point belongs to the contact plane.

Definition 1.2.2. A *Legendrian submanifold* of a contact manifold is an integral submanifold of maximal dimension (that is, equal to n [11] for a $(2n+1)$-dimensional contact manifold).

Legendrian submanifolds we consider in this thesis are allowed to be *immersed* which is more general than in the traditional definition in [11].

Example 4. The plane $\{p = \text{constant}, z = \text{constant}\}$ in the standard contact space from Example 3 is Legendrian.

Definition 1.2.3. A *Legendrian fibration* is a fibration with Legendrian fibres.

Example 5. The standard $\mathbb{R}^{2n+1}$ fibred by the map $(p, q, z) \mapsto (q, z)$.

Definition 1.2.4. The projection of an (immersed) Legendrian submanifold of the total space of Legendrian fibration to the base space of this fibration is called a *Legendrian map*.

Definition 1.2.5. The image of a Legendrian map is called *the front* of the map.

1.2.1 Generating families

Locally, any Legendrian submanifold is a Legendrian submanifold in $J^1(\mathbb{R}^n_q, \mathbb{R}_z)$ defined by a family $F(x, q)$ of functions in $x \in \mathbb{R}^k$ with parameters $q \in \mathbb{R}^n$ as follows:

$$L = \{(p, q, z) : \exists x : F_x = 0, p = F_q, z = F\}.$$

The smoothness of L is ensured if the rank of the matrix $(F_x)_{x,q}$ of the second derivatives at the base point must be equal to k (dimension of x). The family F of functions in x depending on the parameter q is called a *generating family* of this Legendrian submanifold.

Before we give examples we recall the A, D, E simple function singularities. In a neighbourhood of a degenerate 0-modal critical point 0, every function $f : (\mathbb{R}^n, 0) \to (\mathbb{R}, 0)$ is stably $V-$equivalent to one of the following functions germs [11]:

A_k	D_k	E_6	E_7	E_8
x^{k+1}, $k \geq 1$	$x^2y + y^{k-1}$, $k \geq 4$	$x^3 + y^4$	$x^3 + xy^3$	$x^3 + y^5$

Example 6. A truncated V-versal deformation of the A_2 singularity, $F(x, q) = x^3 + qx$, is a generating family for a parameterized Legendrian curve in $\mathbb{R}^3_{p,q,z}$:

$$q = -3x^2, \quad p = x, \quad z = -2x^3.$$

The front is the image of the Legendrian map

$$(x) \mapsto (q = -3x^2, z = -2x^3)$$

which is a cusp in the (q, z)-plane.

In higher dimensions, the germ of a Legendrian submanifold under the same name is a cylinder over the curve in 3-space.

All through this thesis our fronts will be in a 3-dimensional manifold, and in all our local normal forms, we will be using the traditional local model for this dimension which is the space $J^1(\mathbb{R}^2, \mathbb{R})$ of 1-jets of functions on the plane fibred over $J^0(\mathbb{R}^2, \mathbb{R}) \simeq \mathbb{R}_u \times \mathbb{R}^2_{v,w}$. The contact form here is $\alpha = du - V\,dv - W\,dw$, where V, W are coordinates along the fibres of the fibration. For the orientation of the 3-space we take $du \wedge dv \wedge dw$.

In $J^1(\mathbb{R}^2_{v,w}, \mathbb{R}_u)$ a germ of a Legendrian surface L is defined by its *generating family of functions* $F(x, v, w)$:

$$L = \{(u, v, w, V, W) \,|\, \exists x : F_x = 0, u = F, V = F_v, W = F_w\}\,.$$

Sometimes it is convenient to refer to this surface as defined by a *generating family* $u = F(x, v, w)$ *of hypersurfaces*. The minimal dimension of the variable x here is the corank of the derivative of the projection $L \to \mathbb{R}^3_{u,v,w}$ at the base point.

An equivalence of two Legendrian maps $L_j \to E_j \to B_j$, $j = 1, 2$, is a commutative diagram

$$\begin{array}{ccccc} L_1 & \to & E_1 & \to & B_1 \\ \downarrow & & \varphi\downarrow & & \downarrow \\ L_2 & \to & E_2 & \to & B_2 \end{array}$$

in which φ is a contactomorphism (a diffeomorphism which sends one contact structure to the other), and the other two vertical arrows are diffeomorphisms. In terms of local generating families $\Phi(x, u, v, w) = 0$ of hypersurfaces

this corresponds to the V-equivalence of functions Φ preserving the fibration $(x, u, v, w) \mapsto (u, v, w)$.

1.3 Framed and oriented fronts

In the next three chapters we will be considering *framed* and/or *oriented* fronts. The orientation of a front will be coming from the orientation of the compact surface M in the Legendrian map $M \to N$. We show the orientation of the front at its regular points by a co-orientation, so that this co-orientation followed by the orientation of the front is the orientation of N.

The framing of the fronts will be coming from the consideration of Legendrian surfaces in the ST^*N: their projections to N provide our framed fronts.

In more details, a contact element of the 3-manifold N is a hyperplane in the tangent space to N at a point. A contact element with one of its sides in the tangent space distinguished is usually called co-oriented, but we have already mentioned that we will call it *framed*. The set of all framed contact elements of N is the spherisation ST^*N of the cotangent bundle of N.

A point of ST^*N is a pair (ν, Π) consisting of a point $\nu \in N$ and a framed hyperplane $\Pi \subset T_\nu N$. In the tangent space to ST^*N at (ν, Π), consider the hyperplane mapped to Π under the projection $\rho : ST^*N \to N$. The field of all such hyperplanes is the standard contact structure on ST^*N, and the projection ρ is a Legendrian fibration. The fronts in N of (immersed) Legendrian submanifolds L of ST^*N are naturally framed, at least at their regular points:

at a point $p \in L \subset ST^*N$, there is a framed contact 4-plane $\mathcal{P}$ tangent to L which is projected by ρ to a contact element of N tangent to the front $\rho(L)$ at $\rho(p)$ and inheriting the framing from that of $\mathcal{P}$. Our fronts will be framed this way.

Remark 3. We would like once again to emphasise the use of the terminology in this thesis which may be somehow non-traditional:

- a *front's framing* at a point is a choice of the positive side of the 2-plane tangent to the front at this point (this is, what is usually called a co-orientation of the front);
- *our* co-orientation of a front is a tool to inform about *the orientation* of the projected Legendrian surface (see the first paragraph of this section);
- we will be also using *another co-orientation*, that of the discriminantal strata of codimension 1 in the space of all our Legendrian maps: the direction of this co-orientation is a fixed choice of one of the two possible directions in the corresponding generic 1-parameter local bifurcation of a front. All such bifurcations will be depicted and their positive directions will be explicitly specified.

Chapter 2

Local invariants of framed oriented fronts

In this chapter we take our fronts to be framed and oriented as explained in Section 1.3. In all our figures, we assume that the ambient 3-space is taken with the right orientation (that is, the standard one). When writing the normal forms of generating families we are considering the contact structure on $J^1(\mathbb{R}^2_{v,w}, \mathbb{R}_u)$ which is mentioned in the previous chapter. Very frequently in our figures we will be allowing various choices of the framing and orientation like it is shown in Figure 2.1, where we are using $\alpha = \pm$ for the framing direction and $\beta = \pm$ for showing the orientation.

In all our notations, the upper signs will be representing framings and the lower orientations.

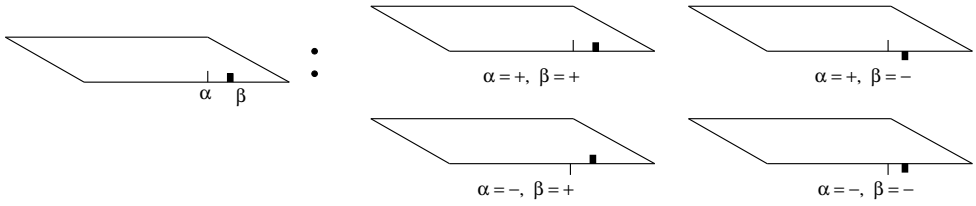

Figure 2.1: Framing and showing the orientation of a smooth sheet.

2.1 Stratification of generic framed oriented fronts in oriented 3-manifolds

A regular point of a generic front $\mathcal{F}$ corresponds to an A_1 singularity of a function in a generating family. Hence the set of all such points will be denoted A_1. Irregular points of $\mathcal{F}$ are:

- A_1^2, transversal intersections of two smooth sheets. Taking the local region of the ambient space into which the framings of both sheets are directed, we distinguish 3 types of such strata $A^2_{1,\beta_1\beta_2}$ with $\beta_1\beta_2 = ++, +-$ or $--$ shown Figure 2.2;

- A_1^3, same for three sheets. Considering the local quadrant of the ambient space into which the framings of all three sheets are directed, we get 4 types here: $A^3_{1,\beta_1\beta_2\beta_3}$, with $\beta_1\beta_2\beta_3 = +++, ++-, +--, ---$. Very frequently it will be convenient to allow permutations of the subscripts with the understanding that, for example $A^3_{1,-++} = A^3_{1,+-+} = A^3_{1,++-}$;

- $A_{2\pm}$, cuspidal edges. The sign in the edge notation indicates the co-orientation (Figure 2.4). We notice that the front framing defines the

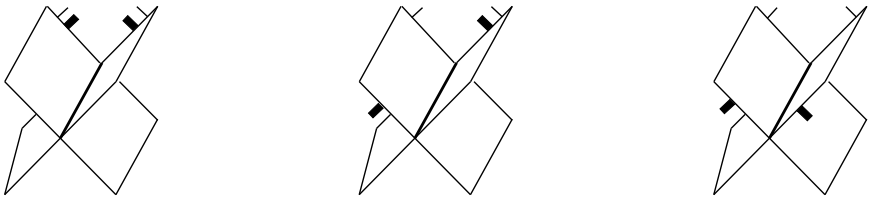

Figure 2.2: Types of stable singularities of framed oriented fronts: $A^2_{1,++}$, $A^2_{1,+-}$ and $A^2_{1,--}$.

natural orientation of the edge as shown in Figure 2.3;

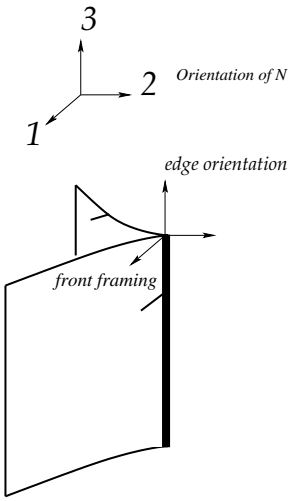

Figure 2.3: Edge orientation.

- A_2A_1, transversal intersections of cuspidal edges with regular sheets. There are 8 types which differ by the sign of the edge, and the framing and co-orientation of the smooth sheet. If the framing or the co-orientation of the sheet coincide with the edge orientation we decorate

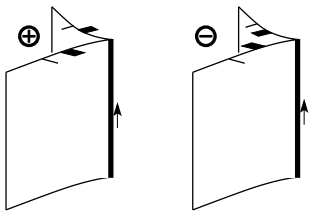

Figure 2.4: Types of A_2 singularities.

the A_1 with a plus, and if it is opposite we decorate with a minus as shown in Figure 2.5. In the left of the figure we show the general case $A_{2\sigma}A_{1,\beta}^{\ \alpha}$;

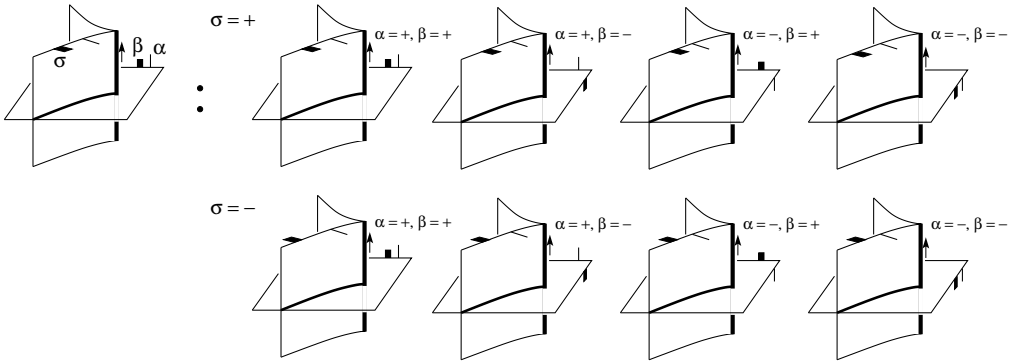

Figure 2.5: Various A_2A_1 points of a front.

- $A_{3,\pm}^{\ \pm}$, swallowtail points. There are four types of swallowtails in this setting shown in Figure 2.6.

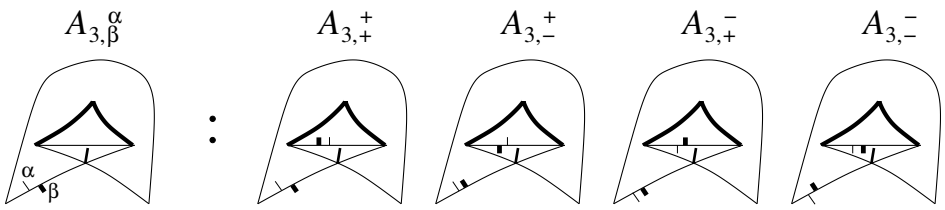

Figure 2.6: Types of A_3 singularities.

2.2 Local invariants

As it was said in the Introduction, a local invariant I defines its *derivative* $I' = \sum_i x_i X_i$, where the $X_i \subset \Xi$ are the strata of codimension 1 in $\mathcal{L}$ we are able to distinguish for the needs of Definition 0.5.1, and the x_i are the local increments of I along generic paths in $\mathcal{L}$ crossing the X_i in the co-orienting direction. On the other hand, I is defined by I' on each connected component $\mathcal{L}_j$ of $\mathcal{L}$ up to a choice of 'a constant of integration', that is, up to an arbitrary choice of the value of I at a non-discriminantal base point in $\mathcal{L}_j$.

Since the total increment of I along any loop in $\mathcal{L}_j$ vanishes, the derivative $\sum_i x_i X_i$ must be a trivial codimension 1 cycle in $\mathcal{L}_j$. The vanishing of the total increment on contractible loops (that is, the derivative being a cycle, maybe non-trivial) is equivalent to its vanishing on small loops in $\mathcal{L}$ around codimension 2 strata of the discriminant. Finding the relevant cyclicity constraints on the increments x_j is the problem on which we concentrate in this thesis. Cycles of the form $\sum_i x_i X_i$ will be called *discriminantal*.

One of the ways to establish the triviality of a cycle $I' = \sum_i x_i X_i$ is to find

an *integral* (that is, path-independent) interpretation of its antiderivative I in terms of the geometry of individual fronts.

Example 7. It is clear that the number of isolated singularities of $\mathcal{F}$ of a particular type is a local invariant. We introduce notations for such invariants:

$I_{t_{\beta_1\beta_2\beta_3}}$, *the number of triple points* $A^3_{1,\beta_1\beta_2\beta_3}$;

$I_{s^{\alpha}_{\beta}}$, *the number of swallowtails* $A_{3,\beta}{}^{\alpha}$;

$I^{\sigma}_{c^{\alpha}_{\beta}}$, *the number of* $A_{2\sigma}A_{1,\beta}{}^{\alpha}$ *points*;

Another three obvious local invariants in $\mathbb{R}^3$ or S^3 are

I_{ℓ}, *the linking number of the oriented link formed by the positive cuspidal edges of* $\mathcal{F}$ *with the similar link formed by the negative edges* (as shown in Figure 2.7);

$I_{\ell'_+}$, *the self-linking number of the oriented framed link formed by the positive edges of* $\mathcal{F}$.

$I_{\ell'_-}$, *the self-linking number of the oriented framed link formed by the negative edges of* $\mathcal{F}$.

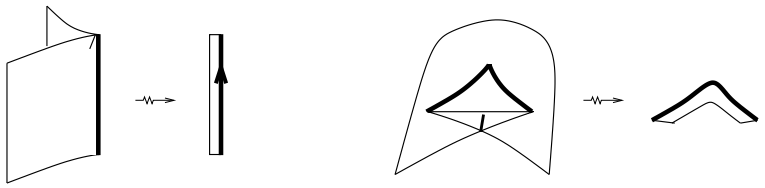

Figure 2.7: Constructing an oriented framed link (equivalently, a ribbon) from the cuspidal edge of a framed front.

We will also introduce a few candidates for local invariants. Firstly, $I^+_{\Sigma^2}$, $I^-_{\Sigma^2}$, which are responsible for counting the algebraic number of corank 2 points of Legendrian maps in homotopies. We do not have their integral interpretations, we only know their derivatives. Secondly, I_{opp} and I_{dir}. We call a self-tangency of two smooth sheets: *direct* when the framings of the sheets at the touching point coincide, and *opposite* when they do not. The invariant I_{opp} is responsible for counting the number of opposite tangencies of two smooth sheets, and the invariant I_{dir} is responsible for counting the parity of direct tangencies of two smooth sheets in homotopies. In all four cases the derivatives of these invariants may happen to be non-trivial cycles in $\mathcal{L}$.

2.3 Classification of the discriminantal cycles and invariants

We now formulate the main results of this Chapter. Their proofs are in Section 2.6. All statements in this section refer to any compact oriented surface M and oriented 3-manifold N. Both M and N have no boundary.

The first main result of this chapter is

Theorem 2.3.1. *The space of integer (with $\mathbb{Z}$ coefficients) discriminantal cycles in $\mathcal{L}(M,N)$ has rank 19. Its basis is formed by the derivatives of the invariants*

$$I_{t_{+++}}, \quad I_{t_{++-}}, \quad I_{t_{+--}}, \quad I_{t_{---}},$$

$$I_{s^+_+}, \quad I_{s^+_-}, \quad I_{s^-_+}, \quad I^+_{\Sigma^2},$$

$$((I_{s^+_-} - I_{s^-_-}) - (I^+_{\Sigma^2} + I^-_{\Sigma^2}))/2, \quad ((I_{s^+_+} - I_{s^-_+}) - (I^+_{\Sigma^2} + I^-_{\Sigma^2}))/2$$

$$I^+_{c^+_-}, \quad I^+_{c^-_+}, \quad I^+_{c^-_-}, \quad I^-_{c^+_+}, \quad I^-_{c^+_-}, \quad (I^+_{c^+_-} + I^+_{c^-_+} + I^-_{c^+_-} + I_{s^+_-} + I_{s^-_+} - I^-_{c^-_+})/2,$$

$$(I_{\ell'_+} + I_{\ell'_-} + I_{s^+_-} + I_{s^-_+})/2, \quad ((I_{s^+_+} + I^+_{c^+_-} + I^+_{c^-_+} + I^+_{\Sigma^2} - I_\ell))/2, \quad I_{opp}.$$

Let $\mathcal{L}_1 \subset \mathcal{L}(M,N)$ be the set of all Legendrian maps without corank 2 points. Discriminantal cycles in $\mathcal{L}_1$ do not contain any summands of $I^{+'}_{\Sigma^2}$, $I^{-'}_{\Sigma^2}$. Our proof of Theorem 2.3.1 yields

Corollary 2.3.1. *The space of integer discriminantal cycles in $\mathcal{L}_1(M,N)$ has rank 17. Its basis is formed by the derivatives of the invariants*

$$I_{t_{+++}}, \quad I_{t_{++-}}, \quad I_{t_{+--}}, \quad I_{t_{---}},$$

$$I_{s^+_+}, \quad I_{s^+_-}, \quad (I_{s^+_-} - I_{s^-_-})/2, \quad (I_{s^+_+} - I_{s^-_+})/2,$$

$$I^+_{c^+_-}, \quad I^+_{c^-_+}, \quad I^+_{c^-_-}, \quad I^-_{c^+_+}, \quad I^-_{c^+_-}, \quad (I^+_{c^+_-} + I^+_{c^-_+} + I^-_{c^+_-} + I_{s^+_-} + I_{s^-_+} - I^-_{c^-_+})/2,$$

$$(I_{\ell'_+} + I_{\ell'_-} + I_{s^+_-} + I_{s^-_+})/2, \quad ((I_{s^+_+} + I^+_{c^+_-} + I^+_{c^-_+} - I_\ell))/2, \quad I_{opp}.$$

Corollary 2.3.2. *The space of all integer local invariants on $\mathcal{L}_1(M,\mathbb{R}^3)$ has rank 16 or 17.*

The exact value of the rank here depends on I'_{opp} being or not being a trivial cycle.

Theorem 2.3.2. *The space of mod2 discriminantal cycles in $\mathcal{L}(M,N)$ has rank 20. Its basis is formed by I'_{dir} and the reduced basic derivatives of Theorem 2.3.1.*

Depending on how many of the linear combinations of the mod2 discriminantal cycles I'_{dir}, I'_{opp} and $I^{+'}_{\Sigma^2}$, $I^{-'}_{\Sigma^2}$ turn out to be trivial, we have

Corollary 2.3.3. *The space of $\mathbb{Z}_2$-valued local invariants of framed and oriented fronts in $\mathbb{R}^3$ or S^3 parametrised by M has rank at least 16 and at most 20.*

2.4 Codimension 1 bifurcations

To prove our main results, we first of all need a description of all codimension 1 discriminantal strata in $\mathcal{L}(M, N)$. Therefore we will now list all generic 1-parameter families of our Legendrian maps, in terms of the local bifurcations of their fronts. We co-orient the strata in $\mathcal{L}$ wherever we can do this by local means. We chose the *positive* side of the strata to be in the direction of the positive base of the 1-parameter (multi)versal unfolding. As long as only corank 1 singularities are concerned, the fronts in 3-manifolds do not differ locally from the critical value sets of maps between 3-manifolds. Therefore, in that part, our list is not too far from the relevant part of the list from [17] but has a crucial difference in the strata decorations.

2.4.1 Multi-germs

First of all, we have interactions of generic singularities which involve certain tangencies and further intersection. They differ by the framings and orientations of the participating smooth sheets and the signs of the edges and swallowtails. The notations of such bifurcations are listed below, with T used for the tangency of the participating strata. Very frequently a finite bounded region is born in a bifurcation. In such cases, the notation of the transformation is based on the framings and coorientations of the faces of this region

(plus is used for the outside direction). Letters e and h distinguish between elliptic and hyperbolic versions of similar bifurcations. The figures illustrate only one particular type from the range.

So, we have:

- $TA_{1,\ \beta_1\beta_2}^{2,e,\alpha_1\alpha_2}$, $[\alpha_i, \beta_i = \pm]$, elliptic tangency of two smooth sheets. We choose α_i and β_i to be positive if the framing/coorientation are outside the bounded region *after* the bifurcation, and minus otherwise as it shown in Figure 2.8. The two faces are not ordered here. We co-orient the $TA_1^{2,e}$ stratum in $\mathcal{L}$ as follows. Assume we have the coordinates (u, v, w) in the ambient space, where the equation of the first sheet of the $TA_1^{2,e}$ family is $v = u^2 + w^2 - \lambda$, and the equation of the second (horizontal) sheet is $v = 0$ and λ is the family parameter. The tangency degeneration of $TA_1^{2,e}$ occurs when $\lambda = 0$. We chose the positive side of $TA_1^{2,e}$ stratum to be in the positive direction of λ as shown in Figure 2.8

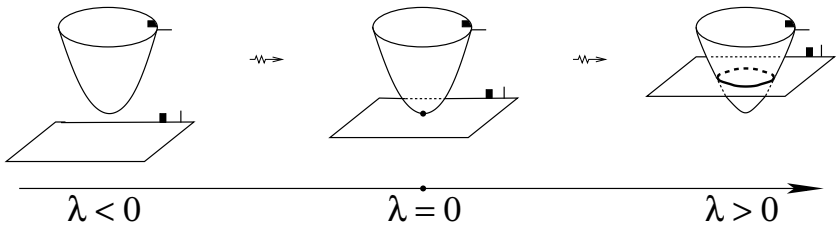

Figure 2.8: The $TA_{1,\ +-}^{2,e,++}$ bifurcation.

- $TA_{1,\beta_1\beta_2}^{2,h,r}$, $[r = \{0, 1\}, \beta_i = \pm]$, same, but hyperbolic. We write $r = 1$ if the sheets are framed to the same side, and $r = 0$ if the framings are

opposite (see Figure 2.9). In such bifurcation we do not have a finite bounded region. So, the stratum is decorated by the sheets arrangement at the center. It is easier to illustrate all types of $TA_1^{2,h}$ by their behavior at the center of a transversal planar section (see Figure 2.10). We set $\beta_i = +$ if the sheet is co-oriented to the framing side. If $r = 1$ and β_1 and β_2 coincide, we fail to locally co-orient the stratum in $\mathcal{L}$, which means that the two directions across $TA^{2,h,1}_{1,++}$ and $TA^{2,h,1}_{1,--}$ strata in $\mathcal{L}$ are indistinguishable.

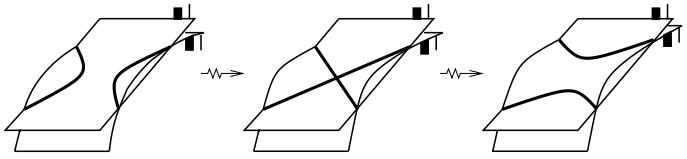

Figure 2.9: The $TA^{2,h,0}_{1,++}$ bifurcation.

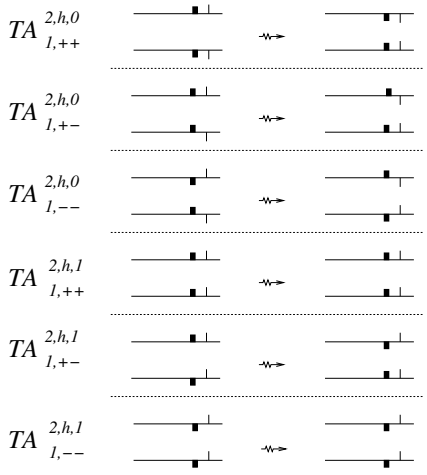

Figure 2.10: Sheets arrangement at the center of positive $TA_1^{2,h}$ moves.

- $TA^{3,\alpha_1\alpha_2\alpha_3}_{1,\beta_1\beta_2\beta_3}$, $[\alpha_i, \beta_i = \pm]$, three smooth sheets are pairwise transversal to each other, but the line of intersection of any two of them is tangent to the third sheet at the moment of bifurcation. The faces here are not ordered. Similarly we set α_i and β_i plus if the framing/co-orientation are outside the bounded region *after* the bifurcation, and minus otherwise (see Figure 2.11).

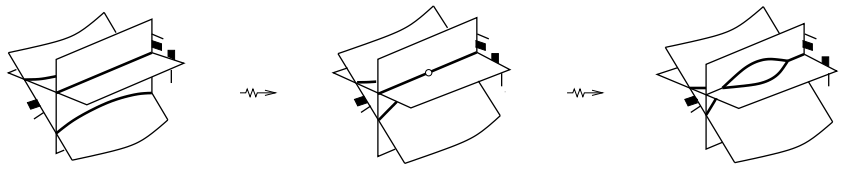

Figure 2.11: The $A^{3,--+}_{1,---}$ bifurcation.

- $A^{4,\alpha_1\alpha_2\alpha_3\alpha_4}_{1,\beta_1\beta_2\beta_3\beta_4}$, $[\alpha_i, \beta_i = \pm]$, intersection of four smooth sheets. The α_i and β_i indicate respectively the framings and co-orientations of the faces of the tetrahedral region appearing *after* the bifurcation. We set them plus if the framing/co-orientation are outside the tetrahedron, and minus otherwise. The faces here are ordered up to even permutations. Namely, we label i the vertex of the newborn tetrahedron opposite the ith face, and we assume that the frame $\overline{12}$, $\overline{13}$, $\overline{14}$ gives the orientation of the ambient space (see Figure 2.12). We assume here that the positive move does not decrease the number of faces framed outwards, and if this number is 2 (that is, is not changed in the bifurcation) then the number of faces co-oriented outwards increases. Therefore with the ordering as described, we have 19 types of the A^4_1 strata (see the table in Section

2.4.3), two of which – $A^{4,++--}_{1,++--}$ and $A^{4,++--}_{1,--++}$ – are not co-orientable in $\mathcal{L}$.

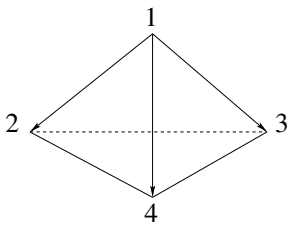

Figure 2.12: The ordering from vertex 1.

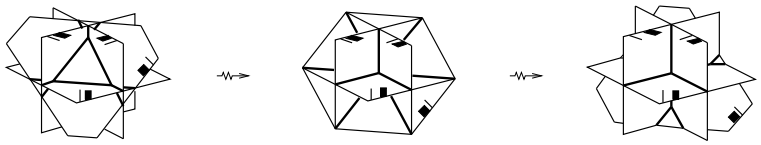

Figure 2.13: The $A^{4,+++-}_{1,+++-}$ bifurcation.

- $A_{2\pm}A^{2,\alpha_1\alpha_2}_{1,\beta_1\beta_2}$, $[\alpha_i, \beta_i = \pm]$, a cuspidal edge meets the intersection of two smooth sheets. The signs α_i, β_i are the signs of the A_2A_1 points after the bifurcation, in the order in which the points are locally on the cuspidal edge if we follow the edge orientation (see Figure 2.14).

- $A^{2,e,\pm}_{2,\beta_1\beta_2}$, $[\beta_i = \pm]$, two edges of given signs meet face-to-face. During the bifurcation the crossing sign of the two local oriented edges changes. The upper sign in the notation of the stratum is the crossing sign after the bifurcation, whereas the lower indices β_i (unordered) indicate the signs of the edges involved in the bifurcation as shown in Figure 2.15.

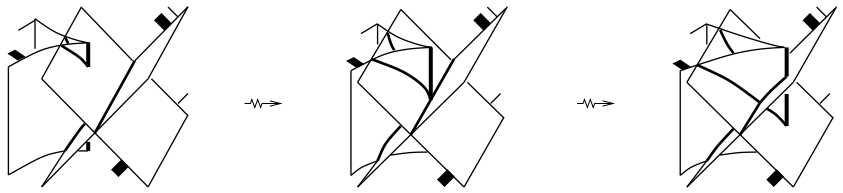

Figure 2.14: The $A_{2-}A^{2,++}_{1,-+}$ bifurcation.

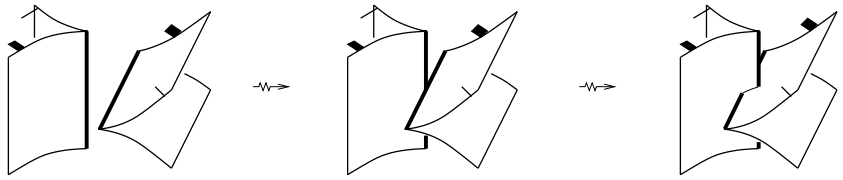

Figure 2.15: The $A^{2,e,+}_{2,+-}$ bifurcation.

- $A^{2,h}_{2,\beta_1\beta_2}$, $[\beta_i = \pm]$, one of the edges is overtaking the other. We set the positive side of the bifurcation to be the one with the positive crossing of the edges. Similarly, the lower indices β_i indicate the signs of the edges involved in the bifurcation (see Figure 2.16): β_1 is the sign of the edge crossed after the transition.

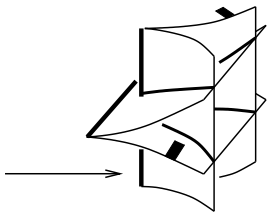

Figure 2.16: Positive $A^{2,h}_{2,+-}$ move.

- $A_{3,\pm}{}^{\pm}A_{1,\pm}{}^{\pm}$, a smooth sheet passes through a swallowtail. The swallowtail types were explained earlier. We decorate the smooth sheet A_1

with minuses if –at the end– the framing/co-orientation are facing the swallowtail point, and with pluses otherwise (see Figure 2.17).

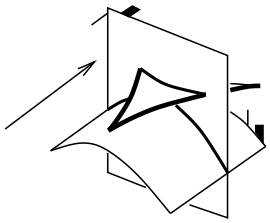

Figure 2.17: Positive $A_{3,-}^{\ +}A_{1,+}^{\ -}$ move.

- $TA_{2\pm}A_{1,\pm}^{e,\pm}$, a cuspidal edge becomes tangent to a smooth sheet so that the two local components of $\mathcal{F}$ do not intersect before the bifurcation. We decorate the smooth sheet A_1 with pluses, if the framing/co-orientation are outside the finite bounded region on the right, and with minuses otherwise (see Figure 2.18).

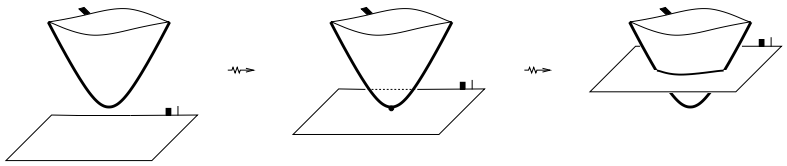

Figure 2.18: The $TA_{2+}A_{1,+}^{e,+}$ bifurcation.

- $TA_{2\pm}A_{1,\pm}^{h,\pm}$, the hyperbolic version of the previous. Similarly, we decorate the smooth sheet A_1 with pluses if the framing/co-orientation are towards the edge before the bifurcation, and with minuses otherwise (see Figure 2.19).

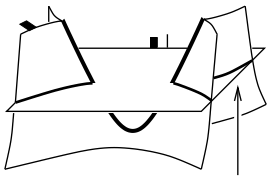

Figure 2.19: Positive $TA_{2-}A^{h,+}_{1,+}$ move.

2.4.2 Uni-germs

Our normal forms for generic 1-parameter uni-germ transformations follow [10, 21], and their illustrations in Figure 2.20 correspond to [12].

The sign of the real parameter λ in the local normal forms for the generating families below co-orients the strata in $\mathcal{L}$.

- $A^{e,\alpha}_{3,\beta} : \alpha u = x^4 + (v^2 - \lambda)x^2 + wx$, birth of cuspidal lips, with the swallowtails of the signs in the notation $[\alpha, \beta = \pm]$.

- $A^{h,\alpha}_{3,\beta} : \alpha u = x^4 + (\lambda - v^2)x^2 + wx$, beaks bifurcation on the edge, with the swallowtails of the signs in the notation $[\alpha, \beta = \pm]$.

- ${A_{4,\beta}}^{\alpha} : \alpha u = x^5 + \lambda x^3 + vx^2 + wx$, here α indicates the sign of the *local writhe of the cuspidal edge* after the bifurcation, and β is the sign of the edge.

- $D^{\sigma}_{4,\beta} : u = \alpha x^2 y + y^3 - \lambda y^2 + vy + wx$, the swallowtails after the bifurcation are ${A_{3,\beta}}^{+}$. The σ in the D_4 notation refers to the sign of the singularity with the normal form $\pm x^2 y + y^3$.

Altogether, we have 145 codimension 1 strata in $\mathcal{L}$, four of which we have failed to co-orient.

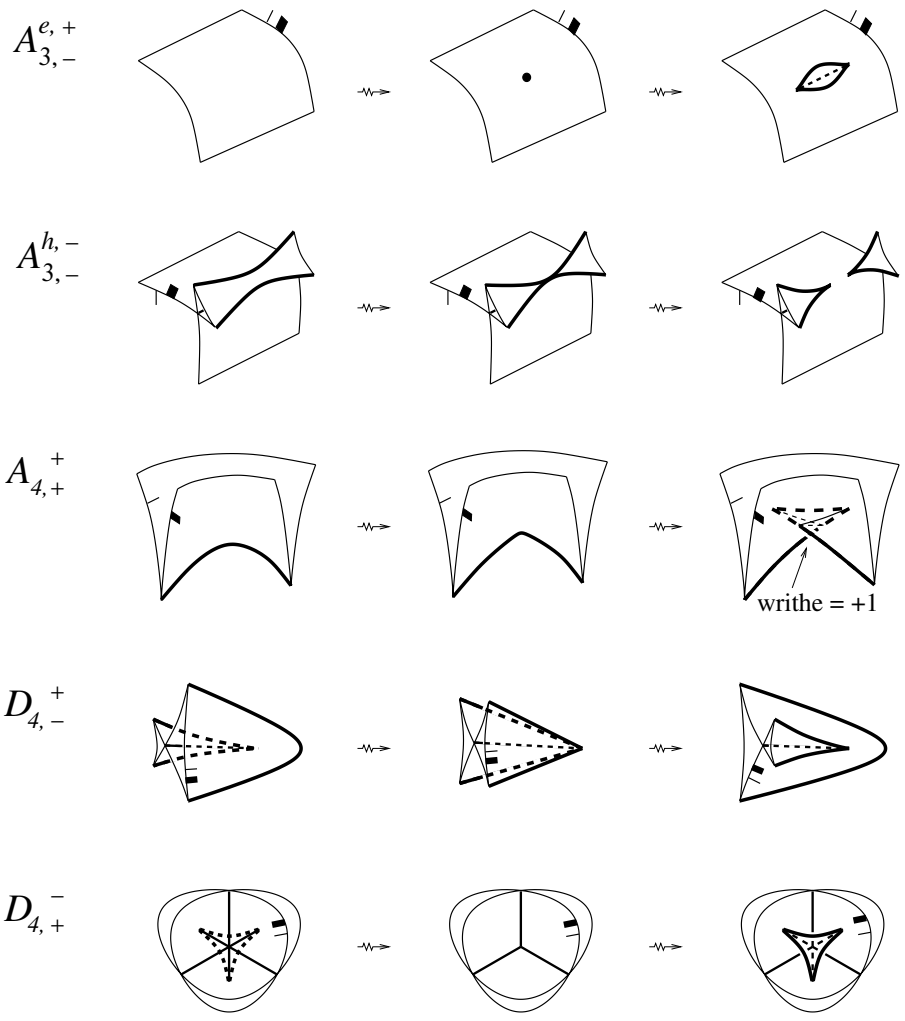

Figure 2.20: Codimension 1 uni-germs.

2.4.3 The integer invariants in terms of linear combinations of the strata

We will write the integer invariants in terms of what we call the big strata. Each big stratum is a sum of elementary ones across which any invariant has equal increments. The notation of a big stratum will be by one of its elementary summands which will usually be the first summand in the table below. Strata for which the increments may be non-zero only in the mod2 case will be kept in square brackets.

No.	Big Stratum Notation	Class
1	$[A^{4,++++}_{1,++++}]$	$A^{4,++++}_{1,++++} + A^{4,+++-}_{1,+++-} + [A^{4,++--}_{1,++--}]$
	$A^{4,++++}_{1,+++-}$	$A^{4,++++}_{1,+++-} + A^{4,+++-}_{1,++++} + A^{4,++--}_{1,++--} + A^{4,++-+}_{1,++-+}$
	$A^{4,++++}_{1,++--}$	$A^{4,++++}_{1,++--} + A^{4,+++-}_{1,++-+} + A^{4,+++-}_{1,+---} + A^{4,++-+}_{1,+--+} + A^{4,++--}_{1,++++}$
	$A^{4,++++}_{1,+---}$	$A^{4,++++}_{1,+---} + A^{4,+++-}_{1,+--+} + A^{4,+++-}_{1,----} + A^{4,++--}_{1,+-++}$
	$[A^{4,++++}_{1,----}]$	$A^{4,++++}_{1,----} + A^{4,+++-}_{1,---+} + [A^{4,++--}_{1,--++}]$
6	$TA^{3,+++}_{1,+++}$	$TA^{3,+++}_{1,+++} + TA^{3,++-}_{1,++-} + TA^{3,+--}_{1,+--} + TA^{3,---}_{1,---}$
	$TA^{3,+++}_{1,++-}$	$TA^{3,+++}_{1,++-} + TA^{3,++-}_{1,+++} + TA^{3,++-}_{1,+--} + TA^{3,+--}_{1,++-} + TA^{3,+--}_{1,---} + TA^{3,---}_{1,+--}$
	$TA^{3,+++}_{1,+--}$	$TA^{3,+++}_{1,+--} + TA^{3,++-}_{1,+-+} + TA^{3,++-}_{1,---} + TA^{3,+--}_{1,+++} + TA^{3,+--}_{1,-+-} + TA^{3,---}_{1,++-}$
	$TA^{3,+++}_{1,---}$	$TA^{3,+++}_{1,---} + TA^{3,++-}_{1,--+} + TA^{3,+--}_{1,-++} + TA^{3,---}_{1,+++}$

No.	Big Stratum Notation	Class
10	$TA^{2,e,++}_{1,\ ++}$	$TA^{2,e,++}_{1,\ ++} + TA^{2,h,0}_{1,++} - TA^{2,e,--}_{1,\ --}$
	$TA^{2,e,++}_{1,\ +-}$	$TA^{2,e,++}_{1,\ +-} + TA^{2,h,0}_{1,+-} - TA^{2,e,--}_{1,\ +-}$
	$TA^{2,e,++}_{1,\ --}$	$TA^{2,e,++}_{1,\ --} + TA^{2,h,0}_{1,--} - TA^{2,e,--}_{1,\ ++}$
	$TA^{2,e,+-}_{1,\ ++}$	$TA^{2,e,+-}_{1,\ ++} + TA^{2,h,1}_{1,+-} - TA^{2,e,+-}_{1,\ --}$
	$[TA^{2,e,+-}_{1,\ +-}]$	$TA^{2,e,+-}_{1,\ +-} + [TA^{2,h,1}_{1,++}]$
	$[TA^{2,e,+-}_{1,\ -+}]$	$TA^{2,e,+-}_{1,\ -+} + [TA^{2,h,1}_{1,--}]$
16	$A_{2^+}A^{2,++}_{1,++}$	$A_{2^+}A^{2,++}_{1,++} + A_{2^+}A^{2,+-}_{1,+-} + A_{2^+}A^{2,--}_{1,--} + A_{2^+}A^{2,-+}_{1,-+}$
	$A_{2^+}A^{2,++}_{1,+-}$	$A_{2^+}A^{2,++}_{1,+-} + A_{2^+}A^{2,+-}_{1,--} + A_{2^+}A^{2,--}_{1,-+} + A_{2^+}A^{2,-+}_{1,++}$
	$A_{2^+}A^{2,++}_{1,-+}$	$A_{2^+}A^{2,++}_{1,-+} + A_{2^+}A^{2,+-}_{1,++} + A_{2^+}A^{2,--}_{1,+-} + A_{2^+}A^{2,-+}_{1,--}$
	$A_{2^+}A^{2,++}_{1,--}$	$A_{2^+}A^{2,++}_{1,--} + A_{2^+}A^{2,+-}_{1,-+} + A_{2^+}A^{2,--}_{1,++} + A_{2^+}A^{2,-+}_{1,+-}$
	$A_{2^-}A^{2,++}_{1,++}$	$A_{2^-}A^{2,++}_{1,++} + A_{2^-}A^{2,+-}_{1,+-} + A_{2^-}A^{2,--}_{1,--} + A_{2^-}A^{2,-+}_{1,-+}$
	$A_{2^-}A^{2,++}_{1,+-}$	$A_{2^-}A^{2,++}_{1,+-} + A_{2^-}A^{2,+-}_{1,--} + A_{2^-}A^{2,--}_{1,-+} + A_{2^-}A^{2,-+}_{1,++}$
	$A_{2^-}A^{2,++}_{1,-+}$	$A_{2^-}A^{2,++}_{1,-+} + A_{2^-}A^{2,+-}_{1,++} + A_{2^-}A^{2,--}_{1,+-} + A_{2^-}A^{2,-+}_{1,--}$
	$A_{2^-}A^{2,++}_{1,--}$	$A_{2^-}A^{2,++}_{1,--} + A_{2^-}A^{2,+-}_{1,-+} + A_{2^-}A^{2,--}_{1,++} + A_{2^-}A^{2,-+}_{1,+-}$
24	$A_{3,+}{}^{+}A_{1,+}{}^{+}$	$A_{3,+}{}^{+}A_{1,+}{}^{+} + A_{3,+}{}^{+}A_{1,-}{}^{-}$
	$A_{3,+}{}^{+}A_{1,-}{}^{+}$	$A_{3,+}{}^{+}A_{1,-}{}^{+} + A_{3,+}{}^{+}A_{1,+}{}^{-}$
	$A_{3,-}{}^{+}A_{1,+}{}^{+}$	$A_{3,-}{}^{+}A_{1,+}{}^{+} + A_{3,-}{}^{+}A_{1,-}{}^{-}$
	$A_{3,-}{}^{+}A_{1,-}{}^{+}$	$A_{3,-}{}^{+}A_{1,-}{}^{+} + A_{3,-}{}^{+}A_{1,+}{}^{-}$
	$A_{3,+}{}^{-}A_{1,+}{}^{+}$	$A_{3,+}{}^{-}A_{1,+}{}^{+} + A_{3,+}{}^{-}A_{1,-}{}^{-}$
	$A_{3,+}{}^{-}A_{1,-}{}^{+}$	$A_{3,+}{}^{-}A_{1,-}{}^{+} + A_{3,+}{}^{-}A_{1,+}{}^{-}$
	$A_{3,-}{}^{-}A_{1,+}{}^{+}$	$A_{3,-}{}^{-}A_{1,+}{}^{+} + A_{3,-}{}^{-}A_{1,-}{}^{-}$
	$A_{3,-}{}^{-}A_{1,-}{}^{+}$	$A_{3,-}{}^{-}A_{1,-}{}^{+} + A_{3,-}{}^{-}A_{1,+}{}^{-}$

No.	Big Stratum	Class
32	$TA_{2^+}A^{e,+}_{1,+}$	$TA_{2^+}A^{e,+}_{1,+} + TA_{2^+}A^{h,-}_{1,-}$
	$TA_{2^+}A^{e,+}_{1,-}$	$TA_{2^+}A^{e,+}_{1,-} + TA_{2^+}A^{h,-}_{1,+}$
	$TA_{2^+}A^{e,-}_{1,+}$	$TA_{2^+}A^{e,-}_{1,+} + TA_{2^+}A^{h,+}_{1,-}$
	$TA_{2^+}A^{e,-}_{1,-}$	$TA_{2^+}A^{e,-}_{1,-} + TA_{2^+}A^{h,+}_{1,+}$
	$TA_{2^-}A^{e,+}_{1,+}$	$TA_{2^-}A^{e,+}_{1,+} + TA_{2^-}A^{h,-}_{1,-}$
	$TA_{2^-}A^{e,+}_{1,-}$	$TA_{2^-}A^{e,+}_{1,-} + TA_{2^-}A^{h,-}_{1,+}$
	$TA_{2^-}A^{e,-}_{1,+}$	$TA_{2^-}A^{e,-}_{1,+} + TA_{2^-}A^{h,+}_{1,-}$
	$TA_{2^-}A^{e,-}_{1,-}$	$TA_{2^-}A^{e,-}_{1,-} + TA_{2^-}A^{h,+}_{1,+}$
40	$A^{e/h,+}_{3,\ +}$	$A^{e,+}_{3,+} + A^{h,+}_{3,+}$
	$A^{e/h,+}_{3,\ -}$	$A^{e,+}_{3,-} + A^{h,+}_{3,-}$
	$A^{e/h,-}_{3,\ +}$	$A^{e,-}_{3,+} + A^{h,-}_{3,+}$
	$A^{e/h,-}_{3,\ -}$	$A^{e,-}_{3,-} + A^{h,-}_{3,-}$

Lemma 2.4.1. *In terms of the above big strata the derivatives of the numbers of points of isolated singularity types of generic fronts and of the edge (self)-linking numbers are:*

$$
\begin{aligned}
I_{t_{+++}} &: 2TA^{3,+++}_{1,+++} + A_{2+}A^{2,++}_{1,++} + A_{2-}A^{2,++}_{1,++} + A^{+}_{3,-}A^{+}_{1,+} + A^{-}_{3,+}A^{+}_{1,+},\\
I_{t_{++-}} &: 2TA^{3,+++}_{1,++-} + A_{2+}A^{2,++}_{1,++} + A_{2+}A^{2,++}_{1,+-} + A_{2+}A^{2,++}_{1,-+} + A_{2-}A^{2,++}_{1,++}\\
&\quad + A_{2-}A^{2,++}_{1,+-} + A_{2-}A^{2,++}_{1,-+} + A^{+}_{3,-}A^{+}_{1,-} + A^{-}_{3,+}A^{+}_{1,-},\\
I_{t_{+--}} &: 2TA^{3,+++}_{1,+--} + A_{2+}A^{2,++}_{1,+-} + A_{2+}A^{2,++}_{1,-+} + A_{2+}A^{2,++}_{1,--} + A_{2-}A^{2,++}_{1,+-}\\
&\quad + A_{2-}A^{2,++}_{1,-+} + A_{2-}A^{2,++}_{1,--} + A^{+}_{3,+}A^{+}_{1,+} + A^{-}_{3,-}A^{+}_{1,+},\\
I_{t_{---}} &: 2TA^{3,+++}_{1,---} + A_{2+}A^{2,++}_{1,--} + A_{2-}A^{2,++}_{1,--} + A^{+}_{3,+}A^{-}_{1,-} + A^{-}_{3,-}A^{+}_{1,-},
\end{aligned}
$$

$$
\begin{aligned}
I_{s^+_+} &: 2A^{e/h,+}_{3,\ +} + A^{+}_{4,+} + A^{-}_{4,+} + D^{+}_{4,+} + 3D^{-}_{4,+},\\
I_{s^+_-} &: 2A^{e/h,+}_{3,\ -} + A^{+}_{4,-} + A^{-}_{4,-} + D^{+}_{4,-} + 3D^{-}_{4,-},\\
I_{s^-_+} &: 2A^{e/h,-}_{3,\ +} + A^{-}_{4,+} + A^{+}_{4,+} - D^{+}_{4,-} - 3D^{-}_{4,-},\\
I_{s^-_-} &: 2A^{e/h,-}_{3,\ -} + A^{-}_{4,-} + A^{+}_{4,-} - D^{+}_{4,+} - 3D^{-}_{4,+},\\
I^+_{c^+_+} &: A^{+}_{3,+}A^{+}_{1,+} + A^{-}_{3,+}A^{+}_{1,+} + TA_{2+}A^{e,+}_{1,+} + TA_{2+}A^{e,-}_{1,-} + 2A^{2,e,+}_{2,++} + A^{2,e,+}_{2,+-}\\
&\quad + A^{2,h}_{2,++} + A^{2,h}_{2,+-} + A^{+}_{4,+},\\
I^+_{c^+_-} &: A^{+}_{3,+}A^{+}_{1,-} + A^{-}_{3,+}A^{+}_{1,-} + TA_{2+}A^{e,+}_{1,-} + TA_{2+}A^{e,-}_{1,+} + 2A^{2,e,+}_{2,++} + A^{2,e,+}_{2,+-}\\
&\quad + A^{2,h}_{2,++} + A^{2,h}_{2,+-} + A^{+}_{4,+},\\
I^+_{c^-_+} &: A^{+}_{3,+}A^{+}_{1,-} + A^{-}_{3,+}A^{+}_{1,-} + TA_{2+}A^{e,-}_{1,+} + TA_{2+}A^{e,+}_{1,-} + 2A^{2,e,-}_{2,++} + A^{2,e,-}_{2,+-}\\
&\quad - A^{2,h}_{2,++} - A^{2,h}_{2,-+} + A^{-}_{4,+},\\
I^+_{c^-_-} &: A^{+}_{3,+}A^{+}_{1,+} + A^{-}_{3,+}A^{+}_{1,+} + TA_{2+}A^{e,-}_{1,-} + TA_{2+}A^{e,+}_{1,+} + 2A^{2,e,-}_{2,++} + A^{2,e,-}_{2,+-}\\
&\quad - A^{2,h}_{2,++} - A^{2,h}_{2,-+} + A^{-}_{4,+},\\
I^-_{c^+_+} &: A^{+}_{3,-}A^{+}_{1,+} + A^{-}_{3,-}A^{+}_{1,+} + TA_{2-}A^{e,+}_{1,+} + TA_{2-}A^{e,-}_{1,-} + 2A^{2,e,+}_{2,--} + A^{2,e,+}_{2,+-}\\
&\quad + A^{2,h}_{2,--} + A^{2,h}_{2,-+} + A^{+}_{4,-},\\
I^-_{c^+_-} &: A^{+}_{3,-}A^{+}_{1,-} + A^{-}_{3,-}A^{+}_{1,-} + TA_{2-}A^{e,+}_{1,-} + TA_{2-}A^{e,-}_{1,+} + 2A^{2,e,+}_{2,--} + A^{2,e,+}_{2,+-}\\
&\quad + A^{2,h}_{2,--} + A^{2,h}_{2,-+} + A^{+}_{4,-},\\
I^-_{c^-_+} &: A^{+}_{3,-}A^{+}_{1,-} + A^{-}_{3,-}A^{+}_{1,-} + TA_{2-}A^{e,-}_{1,+} + TA_{2-}A^{e,+}_{1,-} + 2A^{2,e,-}_{2,--} + A^{2,e,-}_{2,+-}\\
&\quad - A^{2,h}_{2,--} - A^{2,h}_{2,+-} + A^{-}_{4,-},\\
I^-_{c^-_-} &: A^{+}_{3,-}A^{+}_{1,+} + A^{-}_{3,-}A^{+}_{1,+} + TA_{2-}A^{e,-}_{1,-} + TA_{2-}A^{e,+}_{1,+} + 2A^{2,e,-}_{2,--} + A^{2,e,-}_{2,+-}\\
&\quad - A^{2,h}_{2,--} - A^{2,h}_{2,+-} + A^{-}_{4,-},\\
I_\ell &: A^{2,e,+}_{2,+-} - A^{2,e,-}_{2,+-} + A^{2,h}_{2,+-} + A^{2,h}_{2,-+},\\
I_{\ell'_+} &: 2A^{2,e,+}_{2,++} + 2A^{2,h}_{2,++} - 2A^{2,e,-}_{2,++} + A^{+}_{4,+} - A^{-}_{4,+},\\
I_{\ell'_-} &: 2A^{2,e,+}_{2,--} + 2A^{2,h}_{2,--} - 2A^{2,e,-}_{2,--} + A^{+}_{4,-} - A^{-}_{4,-}.
\end{aligned}
$$

Proof. By inspection of all 141 co-orientable bifurcations of the two previous subsections. ∎

There are three relations on the previous invariants

$$\begin{aligned} I^+_{c^+_+} &= I^+_{c^+_-} + I^+_{c^-_-} - I^+_{c^-_+}; \\ I^-_{c^+_+} &= I^-_{c^+_-} + I^-_{c^-_-} - I^-_{c^-_+}; \\ I_{\ell'_-} &= I_{\ell'_+} + I^+_{c^-_+} + I^-_{c^+_-} - I^+_{c^+_-} - I^-_{c^-_+}. \end{aligned}$$

hence only 16 of them are linearly independent.

2.5 Bifurcations in 2-parameter families

Our proof of Theorems 2.3.1 and 2.3.2 is based on the study of bifurcations in generic 2-parameter families of fronts. The bifurcation diagram of each family gives a linear equation on the increments of our local invarinats across the codimension 1 strata: the equation states that the total increment along a small generic loop in $\mathcal{L}$ around the codimension 2 stratum must vanish. Any solution to the whole system of these equations is a coefficient set of a linear combination of codimension 1 strata in $\mathcal{L}$ which is discriminantal cycle.

We denote the increment across a particular stratum as the stratum itself, but in small characters. Increments which may be non-zero only in the mod2 case will be kept in square brackets, as well as non-co-orientable strata in formulas (but not in figures).

2.5.1 Gluing codimension 1 strata together

We start with all 145 strata, four of which – $A^{4,++--}_{1,++--}, A^{4,++--}_{1,--++}$, $TA^{2,h,1}_{++}$ and $TA^{2,h,1}_{--}$ – we have failed to co-orient in $\mathcal{L}$. Our initial goal is to reduce the number of unknown increments.

2.5.1.1 Extra A_1 component

First of all we consider the easiest kind of codimension 2 bifurcations when an extra generic A_1 sheet of $\mathcal{F}$ passes through a point of a codimension 1 bifurcation S. For the cases of the table below, the planar discriminants are of the form shown in Figure 2.21. The vertical coordinate there is the parameter in bifurcation S, and the horizontal measures the position of the A_1 sheet. Such a discriminant gives the equation $u = v$ for the increments. The equations obtained at this stage allow us to consider in what follows sums of the strata differing only by certain indices in their notation. As we have mentioned, such bigger strata will be denoted by one representative from each class. If one of the summands in a big stratum is non-co-orientable, then the increment of any integer invariant across the big stratum is zero. We make no difference between the expressions *planar discriminants* and *bifurcation diagrams*.

No.	S	equation	big stratum
1	$TA^{3,\alpha_1\alpha_2\alpha_3}_{1,\beta_1\beta_2\beta_3}$	$a^{4,\alpha_1\alpha_2\alpha_3\delta}_{1,\beta_1\beta_2\beta_3\gamma} = a^{4,-\delta\alpha_1\alpha_2\alpha_3}_{1,-\gamma\beta_1\beta_2\beta_3}$	$[A^{4,++++}_{1,++++}]$, $[A^{4,++++}_{1,+++-}]$, $[A^{4,++++}_{1,++--}]$, $[A^{4,++++}_{1,+---}]$, $[A^{4,++++}_{1,----}]$
2	$TA^{2,e,\alpha_1\alpha_2}_{1,\ \ \beta_1\beta_2}$	$ta^{3,\alpha_1\alpha_2\delta}_{1,\beta_1\beta_2\gamma} = ta^{3,\alpha_1\alpha_2-\delta}_{1,\beta_1\beta_2-\gamma}$	$TA^{3,+++}_{1,+++}$, $TA^{3,+++}_{1,++-}$, $TA^{3,+++}_{1,+--}$, $TA^{3,+++}_{1,---}$

No.	S	equation	big stratum
3	$TA_{2\sigma}A^{e,\alpha}_{1,\beta}$	$a_{2\sigma}a^{2,\delta\alpha}_{1,\gamma\beta} = a_{2\sigma}a^{2,\alpha-\delta}_{1,\beta-\gamma}$	$A_{2\sigma}A^{2,++}_{1,++}$, $A_{2\sigma}A^{2,++}_{1,+-}$, $A_{2\sigma}A^{2,++}_{1,-+}$, $A_{2\sigma}A^{2,++}_{1,--}$
4	$A^{e,\alpha}_{3,\beta}$	$a_{3,\beta}{}^{\alpha}a_{1,\gamma}{}^{\delta} = a_{3,\beta}{}^{\alpha}a_{1,-\gamma}{}^{-\delta}$	$A_{3,\beta}{}^{\alpha}A_{1,+}{}^{+}$, $A_{3,\beta}{}^{\alpha}A_{1,-}{}^{+}$

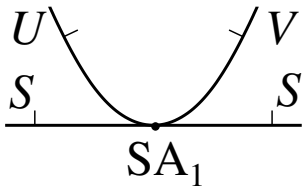

Figure 2.21: Bifurcation diagram of the families SA_1 obtained from interaction of a generic smooth sheet A_1 with a codimension 1 bifurcation S.

2.5.1.1.1 Gluing up the TA^3_1 strata: We illustrate how the table above was obtained on the example of its second line. We consider a smooth sheet $A_{1,\gamma}{}^{\delta}$ passing through a $TA^{2,e,\alpha_1\alpha_2}_{1,\ \ \beta_1\beta_2}$ bifurcation. Assume the sheets of the $TA^{2,e}_1$ family are $v = u^2 + w^2 - \lambda$ and the horizontal sheet $v = 0$. Let the equation of the extra smooth sheet be $u = \mu$, where λ, μ are the family parameters. It is clear that TA^3_1 points only occur when $\lambda > 0$ and $w = 0$, see Figure 2.22. Now we want the smooth sheet A_1 passing through the intersection of $v = u^2 - \lambda$ and $v = 0$, where $\lambda > 0$. So, the meeting is at $u^2 - \lambda = 0$ and $u = \mu$. Hence, $\mu^2 = \lambda$ is the equation of the TA^3_1 strata in the space of parameters (λ, μ). Therefore, apart from the μ-axis, the planar discriminant of the family is the parabola, and its two branches correspond to the $TA^{3,\alpha_1\alpha_2\delta}_{1,\beta_1\beta_2\gamma}$ and $TA^{3,\alpha_1\alpha_2-\delta}_{1,\beta_1\beta_2-\gamma}$ strata as it is shown in Figure 2.23. The equation is:

$$ta^{3,\alpha_1\alpha_2\delta}_{1,\beta_1\beta_2\gamma} = ta^{3,\alpha_1\alpha_2-\delta}_{1,\beta_1\beta_2-\gamma}.$$

Due to this equation we are able to glue up the elementary TA_1^3 strata into the four big strata according to the number of faces of the bounded region appearing after the bifurcation that are framed in the co-orienting directions (see the table above).

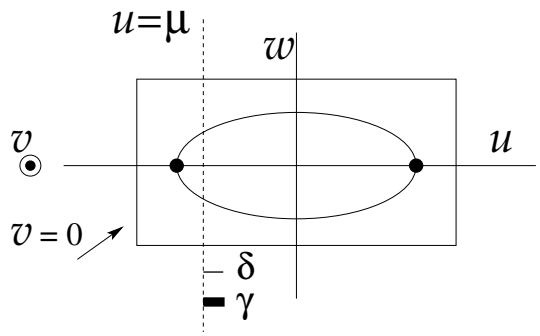

Figure 2.22: The intersection of the $TA_1^{2,e}A_1$ sheets in $v = 0$.

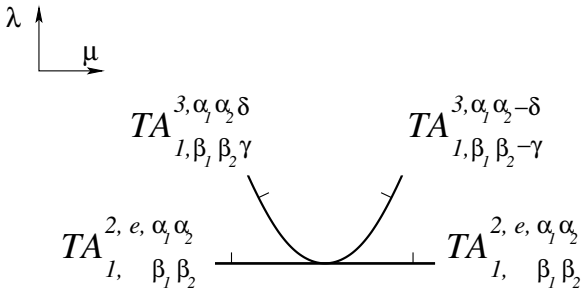

Figure 2.23: Bifurcation diagram of the intersection of the $TA_1^{2,e}$ family with a generic smooth sheet.

2.5.1.1.2 Extra A_1 component passing through A_4 and D_4 bifurcations: In the A_4A_1 and D_4A_1 families the bifurcation diagram is different

from the previous cases.

We have the normal form of $A_{4,\beta}^{\alpha}$ as $\alpha u = x^5 - \lambda x^3 + vx^2 + wx$, and let $v = \mu$ be the equation of the extra smooth sheet $A_{1,\gamma}^{\delta}$ (see figure 2.24). The normal form is quasi-homogeneous if we assign weights to the parameters as $\lambda \sim 2$ and $\mu \sim 3$. Observing Figure 2.25 we notes there are only two types of codimension 1 strata appearing: A_3A_1 when the sheet meets the swallowtail points, and $A_2A_1^2$ when the sheet meets points o f A_2A_1 of the A_4 stratum. Therefore, the A_3A_1 and $A_2A_1^2$ strata in the bifurcation diagram of the A_4A_1 family are semicubical parabolas $\lambda^3 = \text{const}\cdot\mu^2$, see Figure 2.25. The equation obtained from the diagram is

$$\mathbf{5}.\ a_{3,\ \beta}^{-\alpha} a_{1,\gamma}^{\ \delta} - a_{3,\beta}^{\alpha} a_{1,-\gamma}^{\ -\delta} + a_{2^\beta} a_{1,\gamma-\beta}^{2,\delta\ \alpha} - a_{2^\beta} a_{1,\beta\gamma}^{2,\alpha\delta} = 0$$

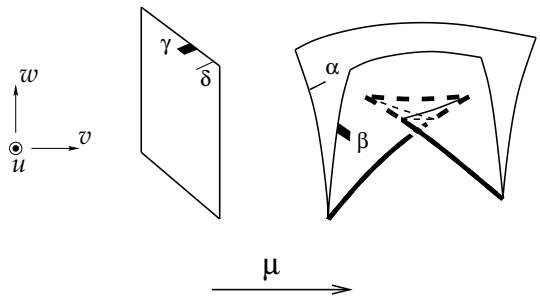

Figure 2.24: A smooth sheet passing through the A_4 bifurcation.

Figure 2.26 shows the bifurcation diagrams of the $D_4^{\pm}A_{1,\gamma}^{\ \delta}$ families. The two equations obtained from the diagrams coincide, so we have

$$6.\ ta_{2-\beta} a_{1,\gamma}^{e,\delta} - ta_{2\beta} a_{1,\gamma}^{e,\delta} + a_{3,\beta}^{\ +} a_{1,\gamma}^{\ \delta} - a_{3,-\beta}^{\ -} a_{1,\gamma}^{\ \delta} = 0$$

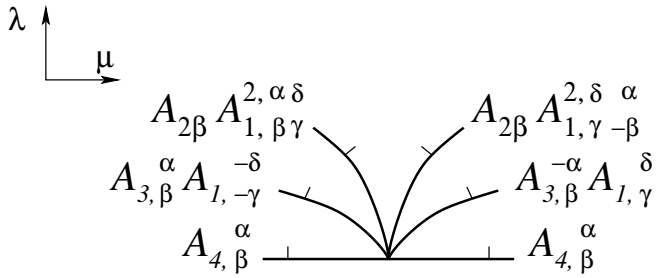

Figure 2.25: Bifurcation diagram of the A_4A_1 family.

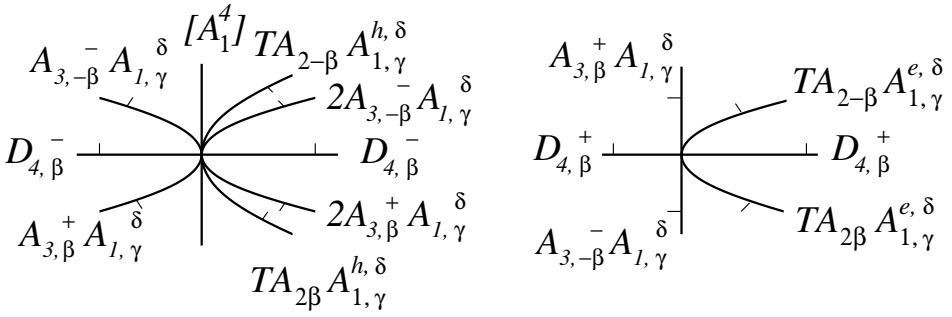

Figure 2.26: Bifurcation diagrams of the $D_4^{\pm}A_1$ families.

A possibility to ignore all types of A_1^4 bifurcations comes from a later consideration of interaction of a swallowtail with a transversal intersection of two smooth sheets (Section 2.5.3.2).

2.5.2 Cubic bifurcations

The $A_3^{e/h}$ singularities have the normal forms $u = x^4 \pm v^2x^2 + wx$. Writing v^3 instead of the $\pm v^2$, we obtain a codimension 2 uni-germ, with a versal deformation $u = x^4 \pm (v^3 + \lambda v + \mu)x^2 + wx$. Its planar discriminant is a semi-cubical parabola $4\lambda^3 + 27\mu^2 = 0$, and yields coincidence of the increments across its half-branches [17]. Similarly replacing quadratic configurations by cubic in some other codimension 1 bifurcations S, we obtain a list like in the previous subsection:

No.	S	equations	big stratum
7	$A^{e,\alpha}_{3,\beta}$	$a^{e,\alpha}_{3,\beta} = a^{h,\alpha}_{3,\beta}$	$A^{e/h,\alpha}_{3,\ \beta}$
8	$TA_{2\sigma}A^{e,\alpha}_{1,\beta}$	$ta_{2\sigma}a^{e,\alpha}_{1,\beta} = ta_{2\sigma}a^{h,-\alpha}_{1,-\beta}$	
9	$TA^{2,e,\alpha_1\alpha_2}_{1,\ \ \beta_1\beta_2}$	$ta^{2,e,\alpha_1\alpha_2}_{1,\ \ \beta_1\beta_2} = ta^{2,h,0}_{1,\beta_1\beta_2} = -ta^{2,e,-\alpha_1-\alpha_2}_{1,\ \ -\beta_1-\beta_2}$, $ta^{2,e,+-}_{1,\ \ ++} = ta^{2,h,1}_{1,+-} = -ta^{2,e,+-}_{1,\ \ --}$, $ta^{2,e,+-}_{1,\ \ +-} = [ta^{2,h,1}_{1,++}]$, $ta^{2,e,+-}_{1,\ \ -+} = [ta^{2,h,1}_{1,--}]$.	$TA^{2,e,++}_{1,\ \ ++}$, $TA^{2,e,++}_{1,\ \ +-}$, $TA^{2,e,++}_{1,\ \ --}$, $TA^{2,e,+-}_{1,\ \ ++}$, $[TA^{2,e,+-}_{1,\ \ +-}]$, $[TA^{2,e,+-}_{1,\ \ -+}]$

2.5.3 Particular multi-germ families

So far we have reduced the number of unknown increments down to 61, out of which 7 may be non-trivial only mod2. We will write all equations we obtain

from now in terms of the big strata from Section 2.4.3, for example we will write $a_{2+}a_{1,+}^{e,+}$ instead of $a_{2+}a_{1,-}^{h,-}$.

2.5.3.1 Non-transversal interaction with a cuspidal edge

We will study three codimension 2 events when the plane tangent to a front $\mathcal{F}$ at its edge point is in a special position with another local component of $\mathcal{F}$. We have three cases here:

(1) the plane coincides with the plane tangent to a smooth A_1 sheet;

(2) the plane contains the tangent direction of the line of transversal intersection of two A_1 sheets;

(3) the plane contains the tangent direction of another cuspidal edge.

In all three cases the calculations will be exactly the same, they only differ by the strata involved in the planar discriminant. So we will do all cases simultaneously.

First, we chose coordinate x, y, z, in which the cuspidal edge S is $x^3+y^2 = 0$. From the other local components T we will need a line L. This will be the singular set in the case of A_1^2 and the cuspidal edge, and the critical point set of the projection along z-direction of the A_1 sheet.

At the most degenerate moment L meets the edge line of S, and is tangent to the tangent plane to S at this point. However, due to the genericity of our 2-parameter family, L cannot be tangent to the cuspidal line of S.

Take a smooth surface S' containing the line L and transversal to the cuspidal line of S, S' has the equation $z = \Phi(x, y)$. The diffeomorphism $z_{new} = z - \Phi(x, y)$, brings S' to $z_{new} = 0$ and preserves the equation of S (see Figure 2.27)

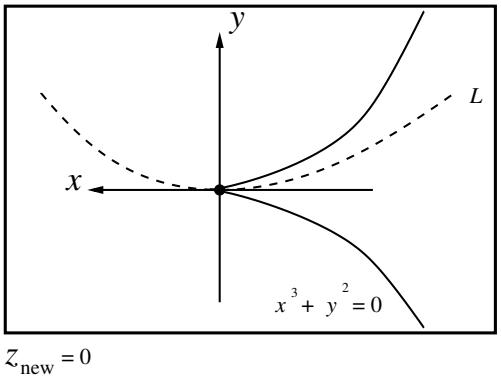

Figure 2.27: The curves in the smooth surface S'.

In the plane $z_{new} = 0$, the line L has the form:

$$y + Ax^2 + Bx^3 + ... = 0$$

Therefore, the union of $(S \cap S')$ with L has the equation $\Psi(x, y) = (x^3 + y^2)(y + Ax^2 + Bx^3 + ...) = 0$, whose principal part is the E_7 singularity. Hence, we can find new coordinates x', y' instead of x, y in which Ψ is $y'(y'^2 + x'^3)$. Thus, the line L is the x'-axis. Now omitting the dashes from x', y', we deform L as $y = \mu x + \lambda$, and move the surface T rigidly with the line. The bifurcation diagram for this deformations consists of those values (λ, μ) for which the line is either tangent to the cuspidal curve $S \cap S' = \{x^3 + y^2 = 0\}$ or passes through the origin.

For example, consider a smooth sheet interacting with a cuspidal edge (we will omit the decorations for simplicity). If the parameters λ and μ are positive then at the tangency we will have $TA_1^{2,e}$ points when assuming the image of the projection of the smooth sheet onto $z = 0$ is the halfplane above the line. Similarly for the other cases of λ and μ (see Figure 2.28).

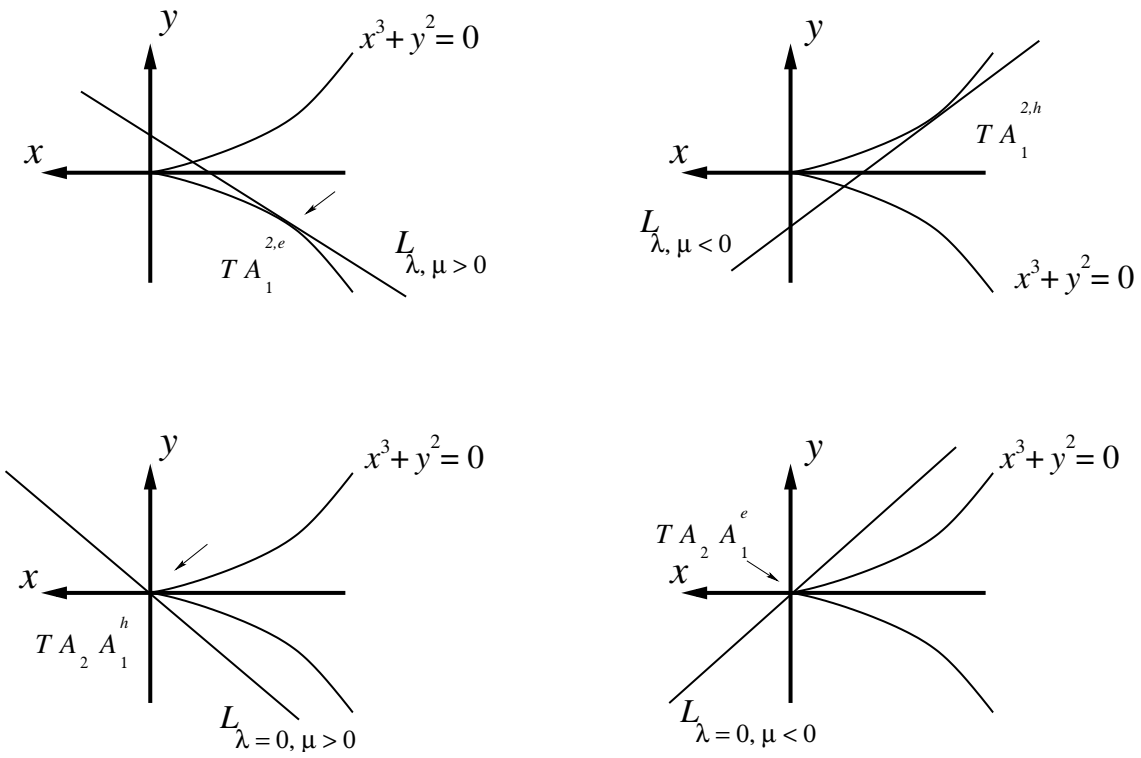

Figure 2.28: A smooth sheet interacting with a cuspidal edge as seen in the xy-plane.

The $TA_1^{2,e}$ and $TA_1^{2,h}$ strata in the bifurcation diagram form a cubic curve due to the weights of the parameters, which gives us the equation $\lambda = \text{const} \cdot \mu^3$ (see Figure 2.29).

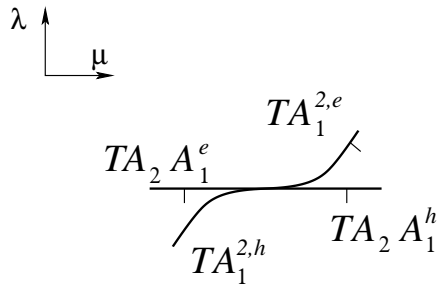

Figure 2.29: Bifurcation diagrams of non-transversal interaction of a smooth sheet with a cuspidal edge.

Adding the framing and orientation to the participating front components, we get the bifurcation diagrams shown in Figures 2.30, 2.31 and 2.32.

The equations obtained from the diagrams are:

$$
\begin{aligned}
\textbf{10}.\quad & ta_{2\sigma}a^{e,-}_{1,-\alpha} - ta_{2\sigma}a^{e,+}_{1,\alpha} + ta^{2,e,++}_{1,\ \alpha-\sigma} + ta^{2,h,0}_{1,\alpha\sigma} &&= 0\\
\textbf{11}.\quad & ta_{2\sigma}a^{e,+}_{1,-\alpha} - ta_{2\sigma}a^{e,-}_{1,\alpha} + ta^{2,e,+-}_{1,\ -\sigma\alpha} + \sigma ta^{2,h,1}_{1,\sigma-\alpha} &&= 0\\
\textbf{12}.\quad & ta_{2\sigma}a^{e,-}_{1,-\alpha} - ta_{2\sigma}a^{e,+}_{1,\alpha} + ta^{2,e,+-}_{1,\ \alpha-\sigma} + \sigma ta^{2,h,1}_{1,\alpha-\sigma} &&= 0\\
\textbf{13}.\quad & ta_{2\sigma}a^{e,+}_{1,-\alpha} - ta_{2\sigma}a^{e,-}_{1,\alpha} + ta^{2,e,--}_{1,\ \alpha-\sigma} - ta^{2,h,0}_{1,-\alpha-\sigma} &&= 0\\
\textbf{14}.\quad & a_{2\sigma}a^{2,-\delta-\alpha}_{1,-\gamma-\beta} + a_{2\sigma}a^{2,-\alpha-\delta}_{1,-\beta-\gamma} - ta^{3,-\delta\alpha}_{1,\sigma\gamma\beta} - ta^{3,+\delta\alpha}_{1,\sigma\gamma\beta} &&= 0\\
\textbf{15}.\quad & a^{2,e,-}_{2,\alpha\sigma} + a^{2,h}_{2,\sigma\alpha} - ta_{2\sigma}a^{e,+}_{1,-\alpha} - ta_{2\sigma}a^{e,+}_{1,\alpha} &&= 0\\
\textbf{16}.\quad & a^{2,e,+}_{2,\alpha\sigma} - a^{2,h}_{2,\alpha\sigma} - ta_{2\sigma}a^{e,+}_{1,-\alpha} - ta_{2\sigma}a^{e,+}_{1,\alpha} &&= 0\\
\textbf{17}.\quad & a^{2,e,+}_{2,\alpha\sigma} - a^{2,h}_{2,\alpha\sigma} - ta_{2\sigma}a^{e,-}_{1,-\alpha} - ta_{2\sigma}a^{e,-}_{1,\alpha} &&= 0\\
\textbf{18}.\quad & a^{2,e,-}_{2,\alpha\sigma} + a^{2,h}_{2,\sigma\alpha} - ta_{2\sigma}a^{e,-}_{1,-\alpha} - ta_{2\sigma}a^{e,-}_{1,\alpha} &&= 0
\end{aligned}
$$

2.5.3.2 Interaction with a swallowtail

In this section we study codimension 2 events involving a swallowtail S and another local fragment Q of a front. We assume that, in local coordinates

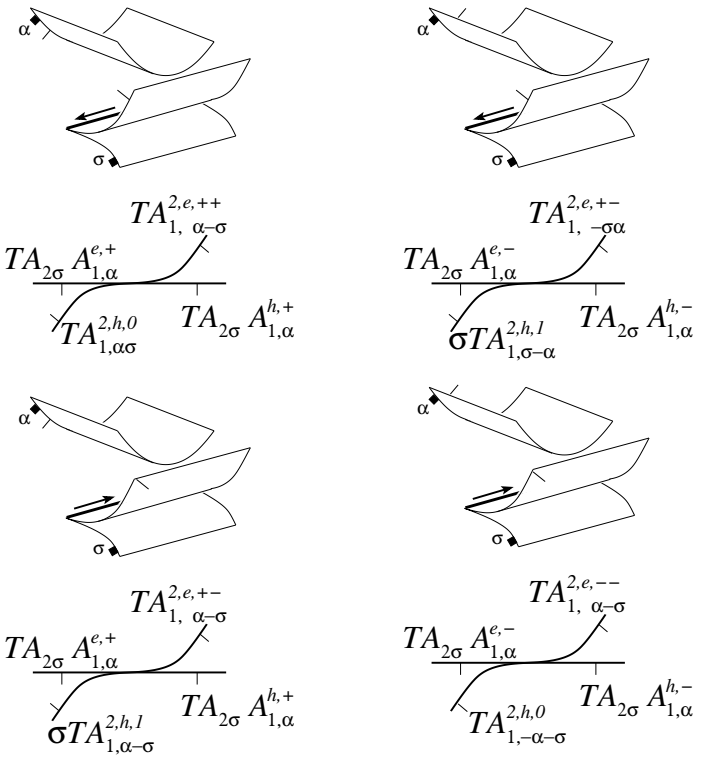

Figure 2.30: Bifurcation diagrams of smooth sheet interactions with cuspidal edge.

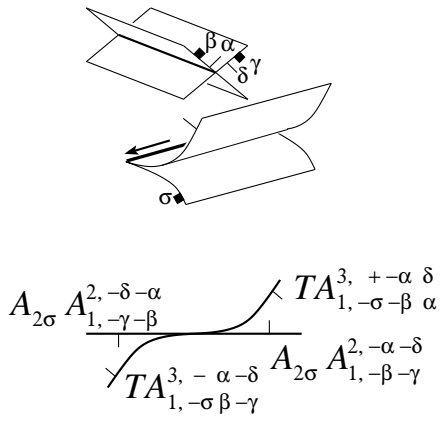

Figure 2.31: Transversal intersection of two smooth sheets interacting with a cuspidal edge.

a, b, c on $\mathbb{R}^3$, the swallowtail is the set of all triplets (a, b, c) of the coefficients of polynomials $\frac{1}{4}x^4+\frac{1}{2}ax^2+bx+c$ with multiple roots. At the most degenerate moment, the additional fragment Q will be passing through the origin of $\mathbb{R}^3_{a,b,c}$, and will be as follows:

(1) a smooth sheet tangent to the self-intersection curve of S but transversal to the tangent plane $c = 0$ to S at the origin;

(2) two smooth sheets meeting transversally along a line L passing through the origin transversally to $c = 0$;

(3) a cuspidal edge whose edge curve passes through the origin transversally to $c = 0$;

We deal with these cases one by one.

Case 1

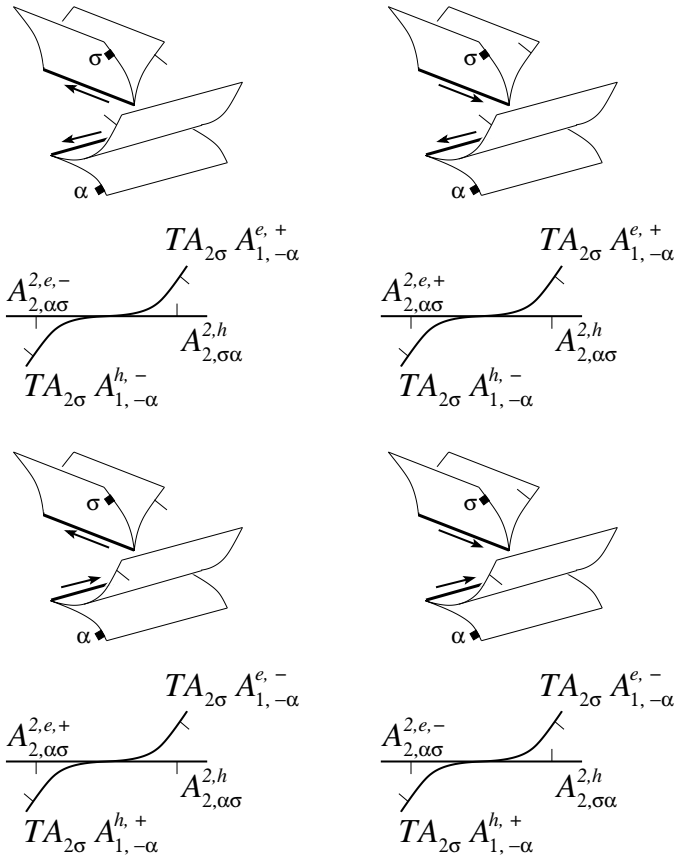

Figure 2.32: A cuspidal edge interacting with another cuspidal edge.

Following [10], under the conditions we have on the smooth sheet Q, there exists a coordinate change in $\mathbb{R}^3_{a,b,c}$ preserving S after which the equation of Q in its most degenerate position is $b + a^2 = 0$.

Also [10] tells us that for a versal deformation of the function $b + a^2$ with respect to the subgroup of the contact equivalence group preserving S we can take $F_\lambda = b - \lambda_2 + (a - \lambda_1)^2$. Bifurcations in the family of surfaces $F_\lambda = 0$ in $\mathbb{R}^3_{a,b,c}$ in presence of S are better seen after projection onto $\mathbb{R}^2_{a,b}$. The projection means that we study the bifurcations of the curves $F_\lambda = 0$ in $\mathbb{R}^2_{a,b}$ with respect to the image of the singular locus of S which consists of the cuspidal curve $4a^3 + 27b^2 = 0$ and the negative $a-$semiaxis (see Figure 2.33).

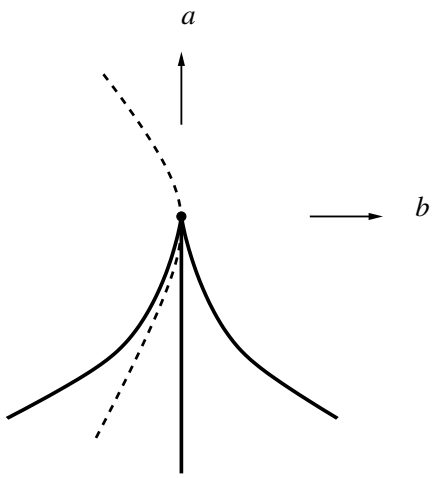

Figure 2.33: Projection of the swallowtail and the smooth sheet to the ab-plane.

We have three degenerations here:

(a) A curve $F_\lambda = 0$ is tangent to the negative $a-$axis (see Figure 2.34) which

happens if $\lambda_1 < 0$, $\lambda_2 = 0$. This corresponds to a TA_1^3 front singularity.

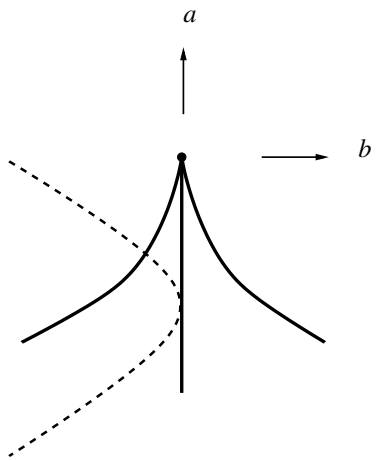

Figure 2.34: TA_1^3 points.

(b) A curve $F_\lambda = 0$ contains the cusp point (the origin), that is $-\lambda_2 + \lambda_1^2 = 0$ (Figure 2.35). This provides an A_3A_1 front singularity.

(c) A curve $F_\lambda = 0$ is tangent to the cuspidal curve meaning the front has a TA_2A_1 singularity. This happens if the following system of equations is satisfied:

$$\begin{aligned} b - \lambda_2 + (a - \lambda_1)^2 &= 0 \\ 4a^3 + 27b^2 &= 0 \\ \begin{vmatrix} 2(a-\lambda_1) & 1 \\ 12a^2 & 54b \end{vmatrix} &= 0 \end{aligned}$$

Excluding a, b we obtain

$$\left(64{\lambda_1}^3 - {\lambda_1}^2 - 72\lambda_2\lambda_1 + \lambda_2 + 432{\lambda_2}^2\right)\left(-\lambda_2 + {\lambda_1}^2\right)^2 = 0$$

The first factor here provides an equation for the TA_2A_1 stratum, while

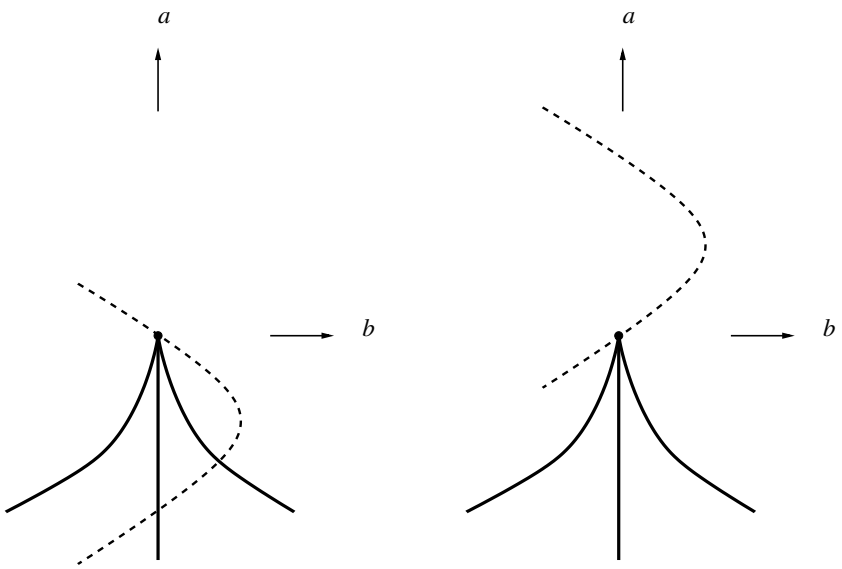

Figure 2.35: A_3A_1 points.

the second is the A_3A_1 equation. In Figure 2.36 we see the tangency between the strata is cubic.

Adding the framings and orientations to the participating front components, we get bifurcation diagrams shown in Figure 2.36.

Case 2

From [15], it follows that the transversality of L to $c = 0$ implies that we can make a coordinate change in $\mathbb{R}^3_{a,b,c}$ preserving S and making Q (in its most degenerate position) a cylinder in the $c-$direction, that is having the equation $F_0 = 0$ where

$$F_0(a, b) = (a + k_1 b + \text{ h.o.t in } b)^2 + k_2 b^2 + \text{ h.o.t in } b \qquad (2.1)$$

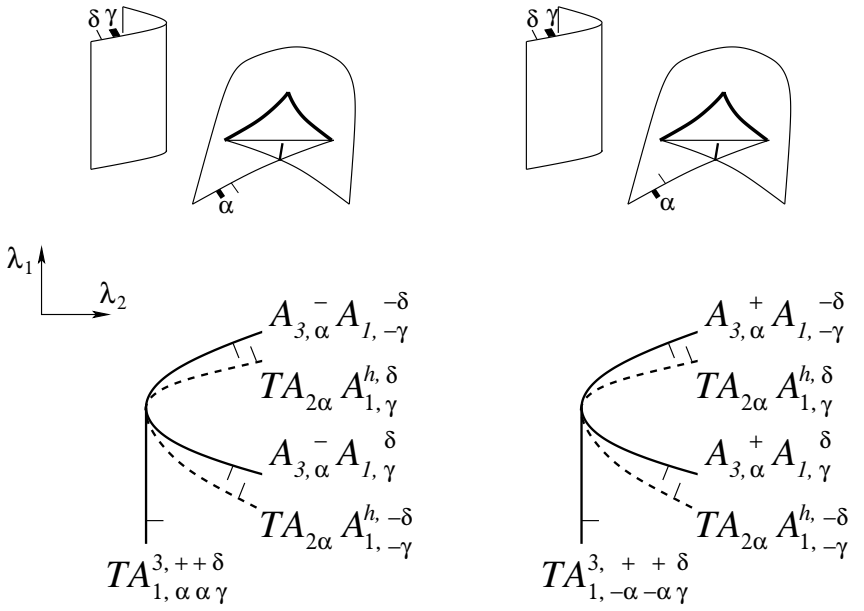

Figure 2.36: 2-parameter bifurcations involving a swallowtail and a smooth sheet, in the big strata notation.

in which k_1, k_2 are real constants, and $k_2 < 0$.

Similar to case 1, we introduce a two-parameter family $F_\lambda(a,b) = F_0(a - \lambda_1, b - \lambda_2)$ and analyse bifurcations with the swallowtail S in terms of the projection to the ab-plane.

This gives the following strata in the $\lambda_1\lambda_2$-parameter space:

- A_1^4: the negative λ_1-semiaxis, corresponding to the singular point of the $F_\lambda(a,b) = 0$ curve being on the negative $a-$simiaxis.
- A_3A_1: the curve $F_0(-\lambda_1, -\lambda_2) = 0$, corresponding to the $F_\lambda(a,b) = 0$ passing through the origin of the $ab-$plane.
- $A_2A_1^2$: $\{4\lambda_1^3 + 27\lambda_2^2 = 0\}$, corresponding to the singular point of the curve $F_\lambda(a,b) = 0$ being on the projection of the cuspidal edge of S.

The illustrations including the framings and orientations of the fronts components are given in Figure 2.37.

Case 3

It goes absolutely similar to case 2, but we must replace the term k_2b^2 in expression (2.1) with k_2b^3, $k \neq 0$, and strata A_1^4 and $A_2A_1^2$ with respectively $A_2A_1^2$ and A_2^2. See Figure 2.38.

The bifurcations in Figures 2.36, 2.37 and 2.38 provide the following equations on the invariants increments:

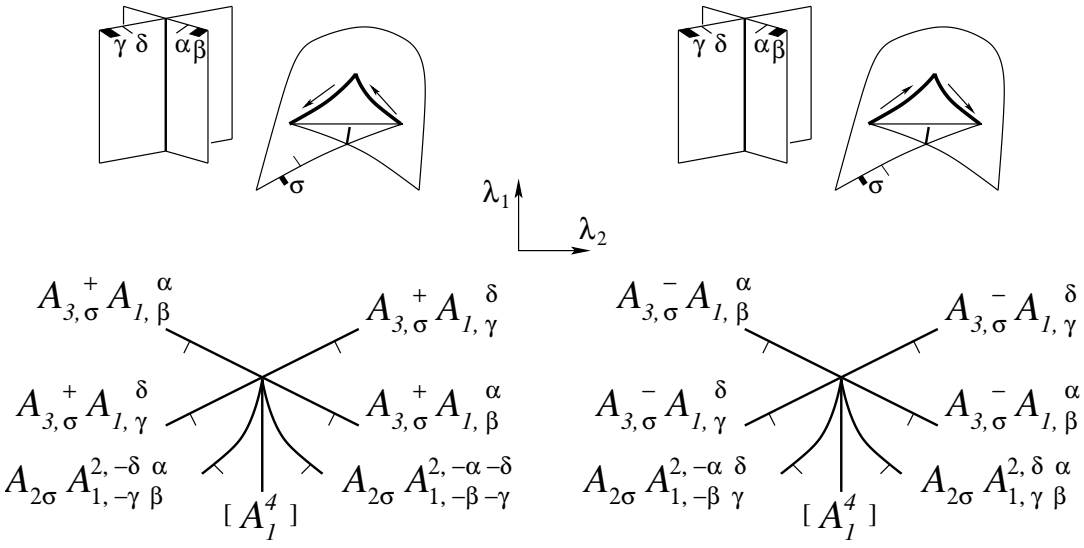

Figure 2.37: Bifurcation diagrams involving a swallowtail and a transversal intersection of two smooth sheets.

19.	$2a_{3,\ \alpha}^{-}a_{1,\gamma}^{\delta} - ta_{2\alpha}a_{1,\gamma}^{e,\delta} - ta_{2\alpha}a_{+,-\gamma}^{e,-\delta} - ta_{1,\alpha\alpha\gamma}^{3,++\delta}$	$=$	0
20.	$2a_{3,\ \alpha}^{+}a_{1,\gamma}^{\delta} - ta_{2\alpha}a_{1,\gamma}^{e,\delta} - ta_{2\alpha}a_{+,-\gamma}^{e,-\delta} - ta_{1,-\alpha-\alpha\gamma}^{3,+\ +\ \delta}$	$=$	0
21.	$[a_1^4]$	$=$	0
22.	$a_{3,\ \alpha}^{+}a_{1,-\beta}^{+} + a_{3,\ \alpha}^{+}a_{1,\beta}^{+} + a_{2,\beta\alpha}^{2,h} - a_{2,\alpha\beta}^{2,e,+} - a_{2\beta}a_{1,-\alpha-\alpha}^{2,++}$	$=$	0
23.	$a_{3,\ \alpha}^{+}a_{1,-\beta}^{-} + a_{3,\ \alpha}^{+}a_{1,\beta}^{-} - a_{2,\alpha\beta}^{2,h} - a_{2,\alpha\beta}^{2,e,-} - a_{2\beta}a_{1,\alpha\alpha}^{2,--}$	$=$	0
24.	$a_{3,\ \alpha}^{-}a_{1,-\beta}^{+} + a_{3,\ \alpha}^{-}a_{1,\beta}^{+} - a_{2,\alpha\beta}^{2,h} - a_{2,\alpha\beta}^{2,e,-} - a_{2\beta}a_{1,-\alpha-\alpha}^{2,--}$	$=$	0
25.	$a_{3,\ \alpha}^{-}a_{1,-\beta}^{-} + a_{3,\ \alpha}^{-}a_{1,\beta}^{-} + a_{2,\beta\alpha}^{2,h} - a_{2,\alpha\beta}^{2,e,+} - a_{2\beta}a_{1,\alpha\alpha}^{2,++}$	$=$	0

Remark 4. Summands of all 5 big A_1^4 strata appear as particular cases of the equation **21**. This is why in equations **6** (Section 2.5.1.1.2) the A_1^4 summands are dropped.

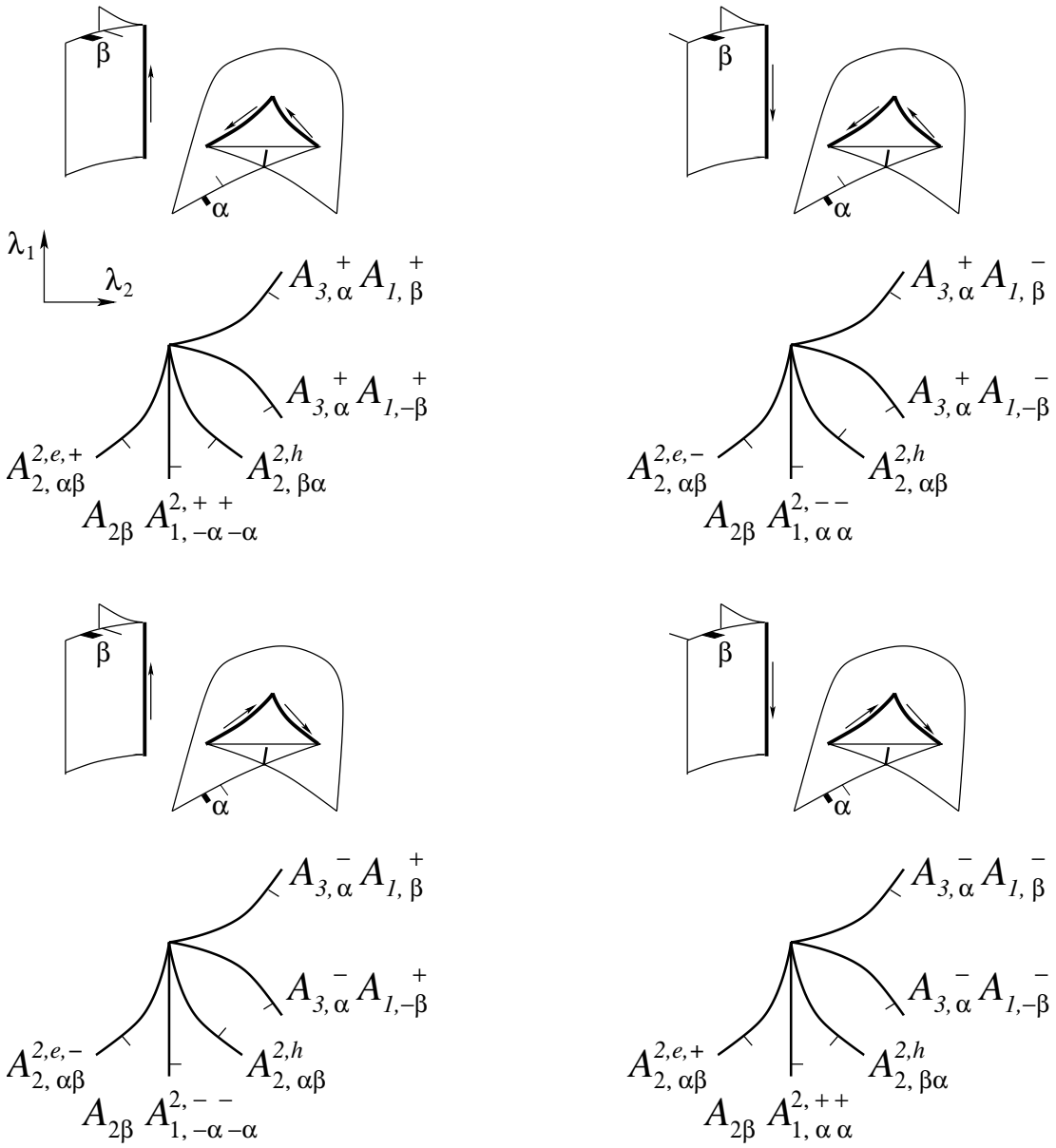

Figure 2.38: Bifurcation diagrams involving a swallowtail and a cuspidal edge.

2.5.4 Uni-germs of codimension 2

Following [21] a generic 2-parameter family of fronts in $\mathbb{R}^3$ may be gathered into a big front in $\mathbb{R}^5$ with a stable singularity. Therefore, we have to consider how such big front singularities may be sliced over $\mathbb{R}^2$ in a generic way. This means that we must analyse slicings of discriminants of A_5 and D_5 function singularities and of the cylinders over the D_4 and $A_{\leq 4}$ discriminants. The slicings must satisfy two conditions:

- they should not be trivial extensions by an extra parameter of the slicings corresponding to generic 1-parameter families of fronts.
- the topology of the source surface parameterising the front should not change.

These two conditions rule out of our consideration all cylindrical big fronts in $\mathbb{R}^5$ except for the cylinder over the A_4 discriminant.

We now consider in turns the three cases we have singled out.

The A_5 family

A versal deformation of A_5 is $F : x^6+\alpha x^4+\beta x^3+\gamma x^2+\delta x+\varepsilon$, and its discriminant $\Sigma(A_5)$ is a hypersurface in $\mathbb{R}^5_{\alpha,\ldots,\varepsilon}$ corresponding to the polynomials in x with multiple roots. Consider a generic map $\lambda : \mathbb{R}^5_{\alpha,\ldots,\epsilon} \longmapsto \mathbb{R}^2_{\lambda_1,\lambda_2}$. Due to [10] up to a diffeomorphism of $\mathbb{R}^5$ preserving Σ and a coordinate choice on $\mathbb{R}^2$, we may assume that:

$$\begin{aligned} \lambda_1 &= \alpha \\ \lambda_2 &= \beta + \text{higher weight terms} \end{aligned}$$

We take the weights of $\alpha, \beta, \gamma, \delta, \varepsilon$ here to be $2, 3, 4, 5, 6$ respectively. The bifurcation diagram of the 2-parameter family of fronts consists of the λ-images of all 1-dimensional strata of $\Sigma(A_5)$. So, let us find parametrizations of these strata: A_4, A_3A_1 and A_2^2. Assuming $x = t$ is the root of F of maximal multiplicity corresponding to one of these cases, we have that F is respectively

$$\begin{aligned} A_4 &: (x-t)^5(x+5t) &&= x^6 - 15t^2x^4 + 40t^3x^3 - ... \\ A_3A_1 &: (x-t)^4(x+2t)^2 &&= x^6 - 6t^2x^4 + 4t^3x^3 + ... \\ A_2^2 &: (x-t)^3(x+t)^3 &&= x^6 - 3t^2x^4 + 3t^4x^2 - t^6. \end{aligned}$$

Respectively, the (α, β)-parts of the strata parametrizations are:

A_4 :	A_3A_1 :	A_2^2 :
$\alpha = -15t^2;$	$\alpha = -6t^2;$	$\alpha = -3t^2;$
$\beta = 40t^3.$	$\beta = 4t^3.$	$\beta = 0.$

Hence the non-decorated bifurcation diagram of the A_5 family is as shown in Figure 2.39, left. Adding the framing and orientation, we get the decorated A_5 diagrams of Figure 2.39. The decoration of an A_5 diagram depends on the choice of an A_4 type on the branches of the outer semicubical parabola of the bifurcation diagram.

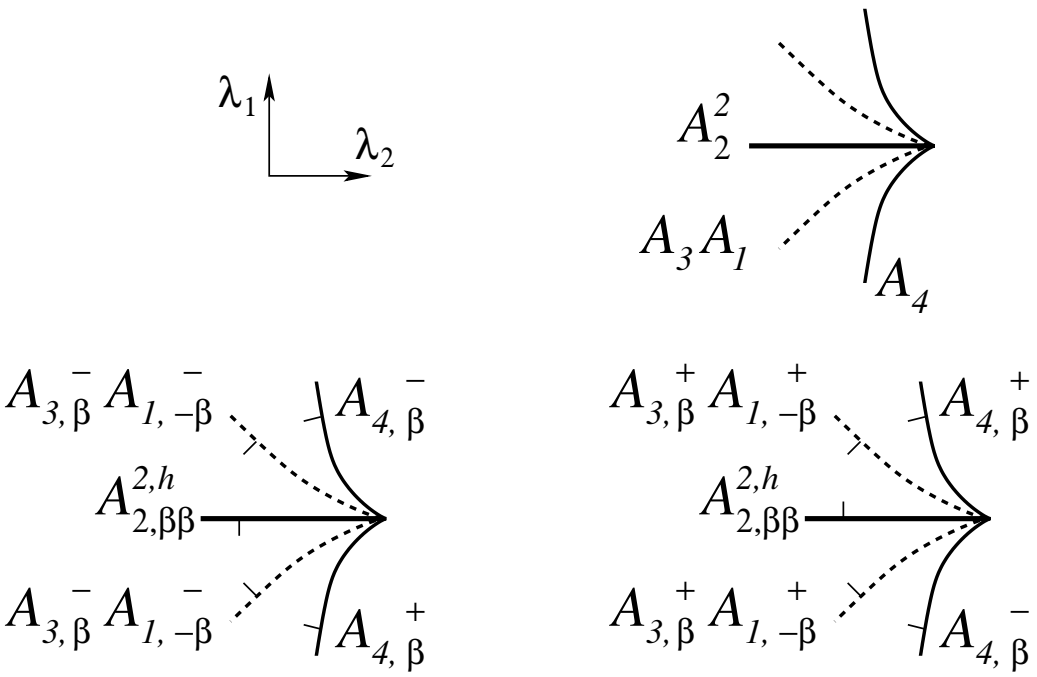

Figure 2.39: Bifurcation diagrams of A_5 families.

The A_4 family

We now consider functions on the base $\mathbb{R}^4_{\alpha,\beta,\gamma,\delta}$ of a versal deformation

$$x^5 + \alpha x^3 + \beta x^2 + \gamma x + \delta \qquad (1)$$

of the A_4 family. According to [10], a generic function vanishing at the origin may be reduced by a diffeomorphism of $\mathbb{R}^4$ preserving $\Sigma(A_4)$ to α (this defines the A_4 front transformation in Figure 2.20). The function next in the order of degeneracy may be reduced by the subgroup of the contact group preserving $\Sigma(A_4)$ to $-\beta \pm \alpha^2$, and has a versal deformation $-\beta \pm \alpha^2 + \lambda_1\alpha + \lambda_2$. In this case we may set $\beta = \pm\alpha^2 + \lambda_1\alpha + \lambda_2$ in (1) and the formula is a generating function for a 2-parameter family of fronts in $\mathbb{R}^3_{\alpha,\gamma,\delta}$.

The bifurcation diagram of this family consists of those values of (λ_1, λ_2) for which the hypersurface

$$\beta = \pm\alpha^2 + \lambda_1\alpha + \lambda_2 \qquad (2)$$

in $\mathbb{R}^4_{\alpha,\beta,\gamma,\delta}$ is not transversal to the stratification of $\Sigma(A_4)$. This means that either the hypersurface contains the A_4 stratum (that is the origin, hence $\lambda_2 = 0$) or is tangent to one of the 1-dimensional strata (A_3 or A_2A_1).

Now we parameterise the strata:

$$\begin{aligned} A_3 \;&:\; (x-t)^4(x+4t) &&= x^5 - 10t^2x^3 + 20t^3x^2 - ... \\ A_2A_1 \;&:\; (x-2t)^3(x+3t)^2 &&= x^5 - 15t^2x^3 + 10t^3x^2 + ... \end{aligned}$$

In each case, we equate the parametrisation to (1) to find the values of t for the intersections of the hypersurface (2) with the stratum. Hence the tan-

gencies with the strata A_3 and A_2A_1 occur when respectively the polynomials

$$-20t^3 \pm 100t^4 - 10\lambda_1 t^2 + \lambda_2$$
$$-10t^3 \pm 225t^4 - 15\lambda_1 t^2 + \lambda_2$$

have non-zero multiple roots. The t^4-terms here do not affect the shape of the bifurcation diagram, and its non-decorated version is in Figure 2.40, left. On the right of the same figure, we show the effect of framing and orientation choices.

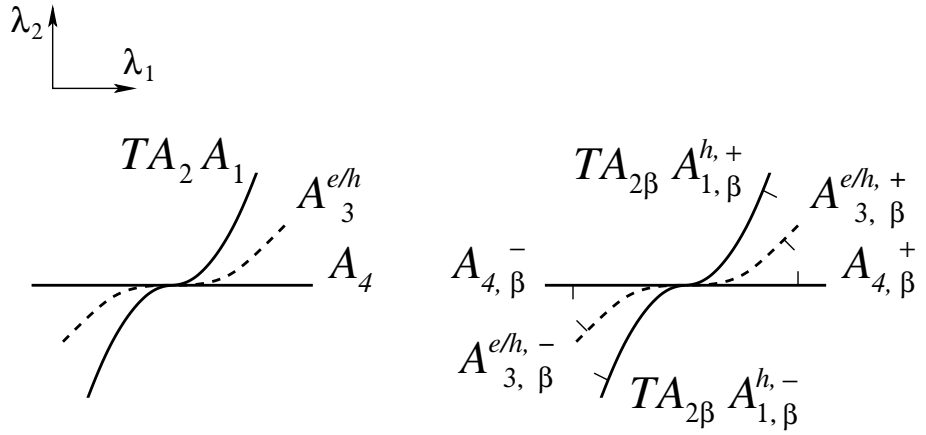

Figure 2.40: Bifurcation diagrams of the family $x^5 + \alpha x^3 + (\pm\alpha^2 + \lambda_1\alpha + \lambda_2)x^2 + \gamma x + \delta$.

The D_5 family

It goes similar to the A_5 case. We have the generating family $x^2y + y^4 + \alpha y^3 + \beta y^2 + \gamma y + \delta x + \varepsilon$, and we consider a generic map $\lambda : \mathbb{R}^5_{\alpha,\ldots,\varepsilon} \longmapsto \mathbb{R}^2_{\lambda_1,\lambda_2}$. Like in the A_5 case, we can assume that

$$\begin{aligned} \lambda_1 &= \alpha \\ \lambda_2 &= \beta + \text{higher weight terms} \end{aligned}$$

where the weights of $\alpha, \beta, \gamma, \delta, \varepsilon$ are $2, 4, 6, 5, 8$. All the 1-dimensional strata of $\Sigma(D_5)$ are quasihomogeneous curves, and their λ-images are

$$\lambda_2 = c_2\lambda_1^2 + c_{5/2}\lambda_1^{5/2} + \text{ higher order terms in } \lambda_1,$$

where c_2, $c_{5/2}$ are some constants. The curves will be just parabolas $\lambda_2 = c_2\lambda_1^2$ if we take a not very generic but straight map $\lambda^0 = (\alpha, \beta)$. MAPLE calculations give the λ^0-images of the strata shown in Figure 2.41, top, and also provide the decorated versions which are in the middle and bottom of Figure 2.41. The A_4 stratum there is doubled. This shows that the λ^0 map is of infinite codimension. However, the higher weight terms in λ will only split the A_4 stratum and cannot affect the strata ordering in any other sense. Due to this observation, we stick to the bifurcation diagram provided by λ^0.

Figures 2.39, 2.40 and 2.41 provide the following equations:

26. $a_{4,\beta}^{-} - a_{4,\beta}^{+} + a_{2,\beta\beta}^{2,h} = 0$

27. $a_{4,\beta}^{+} - a_{4,\beta}^{-} - a_{2,\beta\beta}^{2,h} = 0$

28. $a_{4,\beta}^{+} + a_{4,\beta}^{-} - a_{3,\ \beta}^{e/h,+} - a_{3,\ \beta}^{e/h,-} - ta_{2\beta}a_{1,-\beta}^{e,-} - ta_{2\beta}a_{1,-\beta}^{e,+} = 0$

29. $d_{4,\beta}^{-} + a_{3,\beta}^{+}a_{1,\beta}^{-} + a_{3,\beta}^{+}a_{1,-\beta}^{-} + a_{3,\ -\beta}^{e/h,-} + a_{3,\ \beta}^{e/h,-} - a_{2\beta}a_{1,-\beta-\beta}^{2,++}$
$-a_{4,\beta}^{+} - a_{4,\beta}^{-} - d_{4,\beta}^{+} = 0$

30. $d_{4,\beta}^{+} + a_{3,-\beta}^{-}a_{1,\beta}^{+} + a_{3,-\beta}^{-}a_{1,-\beta}^{+} + a_{3,\ \beta}^{e/h,+} + a_{3,\ -\beta}^{e/h,+} - a_{2-\beta}a_{1,-\beta-\beta}^{2,++}$
$-a_{4,\beta}^{+} - a_{4,\beta}^{-} - d_{4,\beta}^{-} = 0$

2.6 Proofs of Theorem 2.3.1 and 2.3.2

We have now obtained enough relations between the increments to prove the classification claims made in Section 2.3. Any further generic 2-parameter

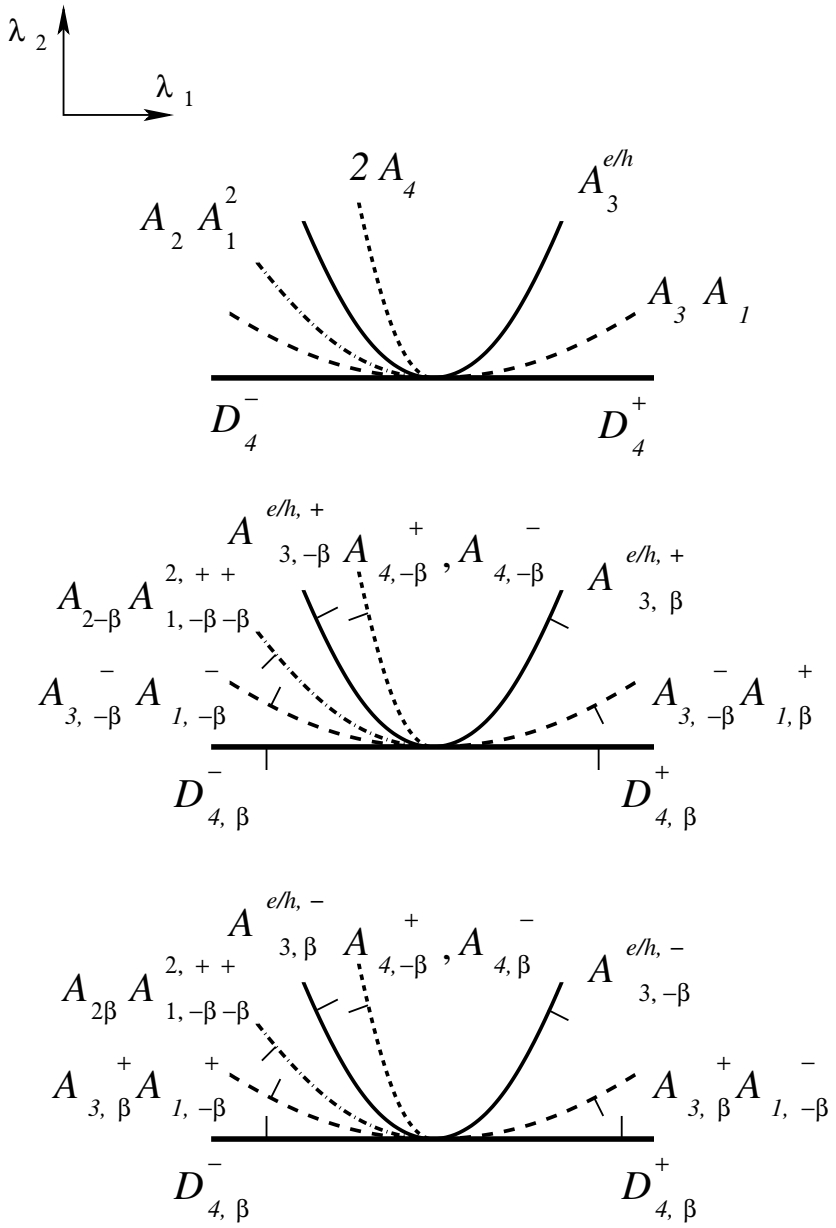

Figure 2.41: Bifurcation diagrams of D_5 families.

families of fronts (for example, passage of an extra A_1 sheet through $A_2^{2,e}$ or $TA_2A_1^h$ bifurcations) are not able to provide us with any equations on the increments independent from those we have already obtained. The equations **5,6,10–30** give us a system of more than 80 equations, depending on the signs of the decorations $\alpha, \ldots, \gamma$. However, only 35 of them are linearly independent, and these are:

$$
\begin{array}{rlccccc}
 & & \alpha & \beta & \delta & \gamma & \sigma \\
5(3): & a_{3,+}^{\ -}a_{1,-}^{\ +} - a_{3,+}^{\ +}a_{1,-}^{\ +} - a_{2+}a_{1,+-}^{2,++} + a_{2+}a_{1,--}^{2,++} = 0 & + & + & + & - & \\
5(4): & a_{3,+}^{\ -}a_{1,-}^{\ +} - a_{3,+}^{\ +}a_{1,-}^{\ +} - a_{2+}a_{1,-+}^{2,++} + a_{2+}a_{1,--}^{2,++} = 0 & + & + & - & + & \\
5(5): & a_{3,-}^{\ -}a_{1,-}^{\ +} - a_{3,-}^{\ +}a_{1,-}^{\ +} - a_{2-}a_{1,--}^{2,++} + a_{2-}a_{1,+-}^{2,++} = 0 & + & - & + & - & \\
5(6): & a_{3,-}^{\ -}a_{1,-}^{\ +} - a_{3,-}^{\ +}a_{1,-}^{\ +} - a_{2-}a_{1,--}^{2,++} + a_{2-}a_{1,-+}^{2,++} = 0 & + & - & - & + & \\
5(7): & a_{3,+}^{\ -}a_{1,+}^{\ +} - a_{3,+}^{\ +}a_{1,+}^{\ +} - a_{2+}a_{1,++}^{2,++} + a_{2+}a_{1,-+}^{2,++} = 0 & + & + & - & - & \\
5(8): & a_{3,-}^{\ -}a_{1,+}^{\ +} - a_{3,-}^{\ +}a_{1,+}^{\ +} - a_{2-}a_{1,+-}^{2,++} + a_{2-}a_{1,++}^{2,++} = 0 & + & - & - & - & \\
6(2): & ta_{2+}a_{1,+}^{e,+} - ta_{2-}a_{1,+}^{e,+} + a_{3,-}^{\ +}a_{1,+}^{\ +} - a_{3,+}^{\ -}a_{1,+}^{\ +} = 0 & & - & + & + & \\
6(4): & ta_{2+}a_{1,-}^{e,+} - ta_{2-}a_{1,-}^{e,+} + a_{3,-}^{\ +}a_{1,-}^{\ +} - a_{3,+}^{\ -}a_{1,-}^{\ +} = 0 & & - & + & - & \\
6(5): & ta_{2-}a_{1,+}^{e,-} - ta_{2+}a_{1,+}^{e,-} + a_{3,+}^{\ +}a_{1,-}^{\ +} - a_{3,-}^{\ -}a_{1,-}^{\ +} = 0 & & + & - & + & \\
6(6): & ta_{2+}a_{1,+}^{e,-} - ta_{2-}a_{1,+}^{e,-} + a_{3,-}^{\ +}a_{1,-}^{\ +} - a_{3,+}^{\ -}a_{1,-}^{\ +} = 0 & & - & - & + & \\
6(7): & ta_{2-}a_{1,-}^{e,-} - ta_{2+}a_{1,-}^{e,-} + a_{3,+}^{\ +}a_{1,+}^{\ +} - a_{3,-}^{\ -}a_{1,+}^{\ +} = 0 & & + & - & - & \\
6(8): & ta_{2+}a_{1,-}^{e,-} - ta_{2-}a_{1,-}^{e,-} + a_{3,-}^{\ +}a_{1,+}^{\ +} - a_{3,+}^{\ -}a_{1,+}^{\ +} = 0 & & - & - & - & \\
10(1): & ta_{2+}a_{1,-}^{e,-} - ta_{2+}a_{1,+}^{e,+} + ta_{1,\ +-}^{2,e,++} + ta_{1,\ ++}^{2,e,++} = 0 & + & & & & + \\
12(4): & ta_{2-}a_{1,+}^{e,-} - ta_{2-}a_{1,-}^{e,+} - ta_{1,\ ++}^{2,e,+-} + [ta_{1,\ -+}^{2,e,+-}] = 0 & - & & & & -
\end{array}
$$

		α	β	δ	γ	σ
$13(2)$	$: ta_{2-}a^{e,+}_{1,-} - ta_{2-}a^{e,-}_{1,+} - ta^{2,e,++}_{1,\ \ --} - ta^{2,e,++}_{1,\ \ +-}$	$= 0$	$+$			$-$
$18(3)$	$: a^{2,e,-}_{2,+-} + a^{2,h}_{2,-+} - ta_{2-}a^{e,-}_{1,-} - ta_{2-}a^{e,-}_{1,+}$	$= 0$	$+$			$-$
$18(4)$	$: a^{2,e,-}_{2,--} + a^{2,h}_{2,--} - ta_{2-}a^{e,-}_{1,+} - ta_{2-}a^{e,-}_{1,-}$	$= 0$	$-$			$-$
$20(1)$	$: 2a_{3,\ +}^{\ \ +}a_{1,+}^{\ \ +} - ta_{2+}a^{e,+}_{1,+} - ta_{2+}a^{e,-}_{1,-} - ta^{3,+++}_{1,+--}$	$= 0$	$+$	$+$	$+$	
$20(2)$	$: 2a_{3,\ -}^{\ \ +}a_{1,+}^{\ \ +} - ta_{2-}a^{e,+}_{1,+} - ta_{2-}a^{e,-}_{1,-} - ta^{3,+++}_{1,+++}$	$= 0$	$-$	$+$	$+$	
$20(3)$	$: 2a_{3,\ +}^{\ \ +}a_{1,-}^{\ \ +} - ta_{2+}a^{e,+}_{1,-} - ta_{2+}a^{e,-}_{1,+} - ta^{3,+++}_{1,---}$	$= 0$	$+$	$+$	$-$	
$20(4)$	$: 2a_{3,\ -}^{\ \ +}a_{1,-}^{\ \ +} - ta_{2-}a^{e,+}_{1,-} - ta_{2-}a^{e,-}_{1,+} - ta^{3,+++}_{1,++-}$	$= 0$	$-$	$+$	$-$	
$24(1)$	$: a_{3,\ +}^{\ \ -}a_{1,-}^{\ \ +} + a_{3,\ +}^{\ \ -}a_{1,+}^{\ \ +} - a^{2,h}_{2,++} - a^{2,e,-}_{2,++} - a_{2+}a^{2,++}_{1,++}$	$= 0$	$+$	$+$		
$24(3)$	$: a_{3,\ -}^{\ \ -}a_{1,-}^{\ \ +} + a_{3,\ -}^{\ \ -}a_{1,+}^{\ \ +} - a^{2,h}_{2,-+} - a^{2,e,-}_{2,+-} - a_{2+}a^{2,++}_{1,--}$	$= 0$	$-$	$+$		
$24(4)$	$: a_{3,\ -}^{\ \ -}a_{1,+}^{\ \ +} + a_{3,\ -}^{\ \ -}a_{1,-}^{\ \ +} - a^{2,h}_{2,--} - a^{2,e,-}_{2,--} - a_{2-}a^{2,++}_{1,--}$	$= 0$	$-$	$-$		
$25(1)$	$: a_{3,\ +}^{\ \ -}a_{1,-}^{\ \ -} + a_{3,\ +}^{\ \ -}a_{1,+}^{\ \ -} + a^{2,h}_{2,++} - a^{2,e,+}_{2,++} - a_{2+}a^{2,++}_{1,++}$	$= 0$	$+$	$+$		
$25(2)$	$: a_{3,\ +}^{\ \ -}a_{1,+}^{\ \ -} + a_{3,\ +}^{\ \ -}a_{1,-}^{\ \ -} + a^{2,h}_{2,-+} - a^{2,e,+}_{2,+-} - a_{2-}a^{2,++}_{1,++}$	$= 0$	$+$	$-$		
$25(3)$	$: a_{3,\ -}^{\ \ -}a_{1,-}^{\ \ -} + a_{3,\ -}^{\ \ -}a_{1,+}^{\ \ -} + a^{2,h}_{2,+-} - a^{2,e,+}_{2,+-} - a_{2+}a^{2,++}_{1,--}$	$= 0$	$-$	$+$		
$25(4)$	$: a_{3,\ -}^{\ \ -}a_{1,+}^{\ \ -} + a_{3,\ -}^{\ \ -}a_{1,-}^{\ \ -} + a^{2,h}_{2,--} - a^{2,e,+}_{2,--} - a_{2-}a^{2,++}_{1,--}$	$= 0$	$-$	$-$		
$26(1)$	$: a_{4,+}^{\ \ -} - a_{4,+}^{\ \ +} + a^{2,h}_{2,++}$	$= 0$		$+$		
$26(2)$	$: a_{4,-}^{\ \ -} - a_{4,-}^{\ \ +} + a^{2,h}_{2,--}$	$= 0$		$-$		
$28(1)$	$: a_{4,+}^{\ \ +} + a_{4,+}^{\ \ -} - a^{e/h,+}_{3,\ \ +} - a^{e/h,-}_{3,\ \ +} - ta_{2+}a^{e,-}_{1,-} - ta_{2+}a^{e,+}_{1,-}$	$= 0$		$+$		
$28(2)$	$: a_{4,-}^{\ \ +} + a_{4,-}^{\ \ -} - a^{e/h,+}_{3,\ \ -} - a^{e/h,-}_{3,\ \ -} - ta_{2-}a^{e,-}_{1,+} - ta_{2-}a^{e,+}_{1,+}$	$= 0$		$-$		
$29(1)$	$: d^{-}_{4,-} + a^{\ \ +}_{3,-}a_{1,+}^{\ \ +} + a^{\ \ +}_{3,-}a_{1,-}^{\ \ +} + a^{e/h,-}_{3,\ \ -} + a^{e/h,-}_{3,\ \ +}$ $-a_{2-}a^{2,++}_{1,++} - a_{4,-}^{\ \ +} - a_{4,-}^{\ \ -} - d^{+}_{4,-}$	$= 0$		$+$		
$29(2)$	$: d^{-}_{4,+} + a^{\ \ +}_{3,+}a_{1,+}^{\ \ +} + a^{\ \ +}_{3,+}a_{1,-}^{\ \ +} + a^{e/h,-}_{3,\ \ -} + a^{e/h,-}_{3,\ \ +}$ $-a_{2+}a^{2,++}_{1,--} - a_{4,+}^{\ \ +} - a_{4,+}^{\ \ -} - d^{+}_{4,+}$	$= 0$		$-$		
$30(2)$	$: d^{+}_{4,+} + a^{\ \ -}_{3,-}a_{1,+}^{\ \ +} + a^{\ \ -}_{3,-}a_{1,-}^{\ \ +} + a^{e/h,+}_{3,\ \ +} + a^{e/h,+}_{3,\ \ -}$ $-a_{2-}a^{2,++}_{1,--} - a_{4,-}^{\ \ +} - a_{4,-}^{\ \ -} - d^{-}_{4,+}$	$= 0$		$-$		

On the other hand, in the integer case, the number of big strata is 54. Along with the ones mentioned in Section 2.4.3 they are

$$A^{2,e,+}_{2,++},\quad A^{2,e,+}_{2,+-},\quad A^{2,e,+}_{2,--},\quad A^{2,e,-}_{2,++},\quad A^{2,e,-}_{2,+-},\quad A^{2,e,-}_{2,--},\quad A^{2,h}_{2,++},\quad A^{2,h}_{2,+-},\quad A^{2,h}_{2,-+},$$

$$A^{2,h}_{2,--},\quad A_{4,+}{}^{+},\quad A_{4,-}{}^{+},\quad A_{4,+}{}^{-},\quad A_{4,-}{}^{-},\quad D^{+}_{4,+},\quad D^{+}_{4,-},\quad D^{-}_{4,+},\quad D^{-}_{4,-}$$

Therefore, the rank of the space of integer discriminantal cycles is 19. This proves Theorem 2.3.1.

Proof of Theorem 2.3.2. Over $\mathbb{Z}_2$ we have the same strata along with $TA^{2,+-}_{1,+-}$ and $TA^{2,-+}_{1,+-}$ which may have non-trivial increments only mod2. Equation **20** tells us that the increments across A^4_1 strata are equal to zero, hence all types of A^4_1 strata are excluded from the total number of big strata over $\mathbb{Z}_2$. The number of linearly independent equations is 36, the same equations as over the integers together with

$$11(3):\ ta_{2+}a^{e,+}_{1,+} - ta_{2+}a^{e,-}_{1,-} - ta^{2,e,+-}_{1,\ ++} + ta^{2,e,+-}_{1,\ +-} = 0 \quad (\alpha = -, \sigma = +).$$

Thus, the rank of the space of mod2 discriminantal cycles is 20. Our proof of Theorem 2.3.2 is finished. The derivatives of the basic invariants are shown in Lemma 4.4.1, apart from $I^{+'}_{\Sigma^2}$, $I^{-'}_{\Sigma^2}$ I'_{opp} and I'_{dir} which may happen to be non-trivial cycles in $\mathcal{L}$. The four derivatives are

$$\begin{aligned}
I^{+'}_{\Sigma^2} &: D^{+}_{4,+} + D^{-}_{4,+};\\
I^{-'}_{\Sigma^2} &: D^{+}_{4,-} + D^{-}_{4,-};\\
I'_{opp} &: TA^{2,e,++}_{1,++} - TA^{2,e,++}_{1,+-} + TA^{2,e,++}_{1,--};\\
I'_{dir} &: TA^{2,e,+-}_{1,++} + TA^{2,e,+-}_{1,+-} + TA^{2,e,+-}_{1,-+}.
\end{aligned}$$

Proof of Corollary 2.3.1. In $\mathcal{L}_1$, the set of all Legendrian maps without corank 2 points, equations **6, 29** and **30** are prohibited. The number of unknowns over the integers will be 50 (we exclude all four types of D_4). The number of linearly independent equations in $\mathcal{L}_1$ drops to 33, equations 5(3), 5(4), 5(5), 5(6), 5(7), 5(8), 10(1), 12(4), 13(2), 18(3), 18(4), 20(1), 20(2), 20(3), 20(4), 24(1), 24(3), 24(4), 25(1), 25(2), 25(3), 25(4), 26(1), 26(2), 28(1), 28(2) along with:

$$\begin{array}{lll} & & \alpha\ \ \beta\ \ \delta\ \ \gamma\ \ \sigma \\ 10(2): & ta_{2-}a^{e,-}_{1,-} - ta_{2-}a^{e,+}_{1,+} + ta^{2,e,++}_{1,\ ++} + ta^{2,e,++}_{1,\ +-} & = 0\ +\ \ \ \ \ - \\ 10(3): & ta_{2+}a^{e,-}_{1,+} - ta_{2+}a^{e,+}_{1,-} + ta^{2,e,++}_{1,\ --} + ta^{2,e,++}_{1,\ +-} & = 0\ -\ \ \ \ \ + \\ 11(3): & ta_{2+}a^{e,+}_{1,+} - ta_{2+}a^{e,-}_{1,-} + ta^{2,e,+-}_{1,\ ++} + [ta^{2,e,+-}_{1,\ +-}] & = 0\ -\ \ \ \ \ + \\ 14(1): & 2a_{2+}a^{2,++}_{1,++} - ta^{3,+++}_{1,++-} - ta^{3,+++}_{1,+++} & = 0\ +\ +\ +\ +\ + \\ 14(2): & a_{2+}a^{2,++}_{1,+-} + a_{2+}a^{2,++}_{1,-+} - ta^{3,+++}_{1,+--} - ta^{3,+++}_{1,++-} & = 0\ +\ +\ +\ -\ + \\ 14(3): & 2a_{2+}a^{2,++}_{1,--} - ta^{3,+++}_{1,---} - ta^{3,+++}_{1,+--} & = 0\ +\ -\ +\ -\ + \\ 14(5): & a_{2-}a^{2,++}_{1,+-} + a_{2-}a^{2,++}_{1,-+} - ta^{3,+++}_{1,+--} - ta^{3,+++}_{1,++-} & = 0\ +\ +\ +\ -\ - \end{array}$$

Thus, the space of integer discriminantal cycles in $\mathcal{L}_1$ has rank 17, which proves Corollary 2.3.1.

In $\mathcal{L}_1$ over $\mathbb{Z}_2$ we have the following

Corollary 2.6.1. *The space of mod 2 discriminantal cycles in $\mathcal{L}_1(M,N)$ has rank 20. Its basis is formed by the derivatives of the invariants*

$$I_{t_{+++}},\quad I_{t_{++-}},\quad I_{t_{+--}},\quad I_{t_{---}},$$

$$I_{s^+_+},\quad I_{s^+_-},\quad (I_{s^+_-} - I_{s^-_-})/2,\quad (I_{s^+_+} - I_{s^-_+})/2,$$

$$I^+_{c^+_-},\quad I^+_{c^-_+},\quad I^+_{c^-_-},\quad I^-_{c^+_+},\quad I^-_{c^+_-},\quad (I^+_{c^+_-} + I^+_{c^-_+} + I^-_{c^+_-} + I_{s^+_-} + I_{s^-_+} - I^-_{c^-_+})/2,$$

$$(I_{\ell'_+} + I_{s^-_+})/2, \quad ,(I_{\ell'_-} + I_{s^+_-})/2, \quad ((I_{s^+_+} + I^+_{c^+_-} + I^+_{c^-_+} - I_\ell))/2,$$
$$I_{opp}, \quad I_{dir}, \quad I_{ds_+}.$$

Proof. The proof is straightforward. Over $\mathbb{Z}_2$ the number of unknowns, in $\mathcal{L}_1$, is 52. Only 32 equations from the previous system, after excluding all D_4 components, are linearly independent. Hence, the rank of the space of mod2 discriminantal cycles is 20. ∎

The invariant I_{ds_+} (and similarly its twin I_{ds_-}) is dual to the sum of mod2 degrees of swallowtail points with positive (negative) orientation. The way we calculate the jumps of I_{ds_+}, I_{ds_-} invariants is as follows. First we shift the swallowtail point to a small sphere as shown in Figure 2.42. After that we project radially all the front onto the sphere. Then we take the degree of this map for $deg(s)$. The derivatives of I_{ds_+} and I_{ds_-} are:

$$\begin{aligned} I_{ds_+} &: A_{3,+}{}^+A_{1,+}{}^+ + A_{3,+}{}^+A_{1,-}{}^+ + A_{3,+}{}^-A_{1,+}{}^+ + A_{3,+}{}^-A_{1,-}{}^+; \\ I_{ds_-} &: A_{3,-}{}^+A_{1,+}{}^+ + A_{3,-}{}^+A_{1,-}{}^+ + A_{3,-}{}^-A_{1,+}{}^+ + A_{3,-}{}^-A_{1,-}{}^+. \end{aligned}$$

The two invariants I_{ds^+} and I_{ds^-} satisfy the relation

$$I_{t_{+++}} + I_{t_{++-}} + I_{t_{+--}} + I_{t_{---}} + I_{ds_+} + I_{ds_-} = 0$$

2.7 Classification of the discriminantal cycles and invariants over $\mathbb{Q}$

Switching from the integer coefficients to rational allows to consider simplified bases of the invariant spaces and emphasize the geometrical sense of the basic invariants. For framed and oriented fronts we obtain

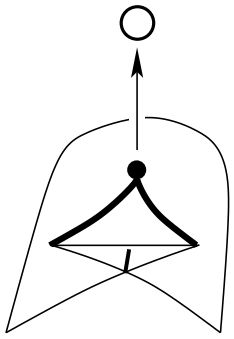

Figure 2.42: Shifting a swallowtail point.

Theorem 2.7.1. *For any surface M and oriented 3-manifold N, the space of rational discriminantal cycles in $\mathcal{L}(M,N)$ has rank 19. Its basis is formed by the derivatives of the invariants*

$$I_{t_{+++}},\quad I_{t_{++-}},\quad I_{t_{+--}},\quad I_{t_{---}},\quad I_{s^+_+},\quad I_{s^+_-},\quad I_{s^-_+},\quad I_{s^-_-},\quad I^+_{\Sigma^2},\quad I^-_{\Sigma^2},$$

$$I^+_{c^+_-},\quad I^+_{c^-_+},\quad I^+_{c^-_-},\quad I^-_{c^+_-},\quad I^-_{c^-_+},\quad I^-_{c^-_-},\quad I_{\ell'_+},\quad I_{\ell},\quad I_{opp}.$$

Considering $\mathcal{L}_1(M,N)$, the set of all Legendrian maps without corank 2 points, we have

Corollary 2.7.1. *The space of rational discriminantal cycles in $\mathcal{L}_1(M,N)$ has rank 17. Its basis is formed by the derivatives of the invariants*

$$I_{t_{+++}},\quad I_{t_{++-}},\quad I_{t_{+--}},\quad I_{t_{---}},\quad I_{s^+_+},\quad I_{s^+_-},\quad I_{s^-_+},\quad I_{s^-_-},$$

$$I^+_{c^+_-},\quad I^+_{c^-_+},\quad I^+_{c^-_-},\quad I^-_{c^+_-},\quad I^-_{c^-_+},\quad I^-_{c^-_-},\quad I_{\ell'_+},\quad I_{\ell},\quad I_{opp}.$$

Chapter 3

Local invariants of framed fronts

In this chapter we omit the front orientation used earlier. Namely, we assume that the source of our Legendrian maps is a non-oriented compact surface. As a result, we will get additional unions into big strata, hence the numbers of unknowns and equations comparing with Chapter 2 will be reduced.

3.1 Stratification of generic framed fronts in oriented 3-manifolds

In this setting, there are two ways to frame a smooth sheet. The other types of stable singularities are:

A_1^2 , transversal intersections of two smooth sheets;

A_1^3 , same for three sheets;

A_2 , cuspidal edges; similar to Chapter 2, the framing defines the natural orientation of the edge (upward in the left half of Figure 3.1 below);

$A_2A_1^{\pm}$, transversal intersections of edges with regular sheets;

$A_3^{\pm}$, swallowtail points.

The signs in the notations of the last two pairs of singularities distinguish between different framing choices as shown in Figure 3.1.

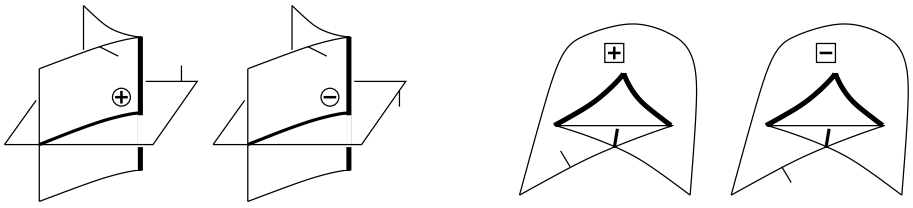

Figure 3.1: Singularises $A_2A_1^{\pm}$ and $A_3^{\pm}$.

Local generating families of hypersurfaces for the one-component singularities are:

$$A_1 :\ u = x^2\,, \qquad A_2 :\ u = x^3 + vx\,, \qquad A_3^{\pm} :\ \pm u = x^4 + vx^2 + wx\,.$$

3.2 Integer invariants in the framed setting

In this setting M will always be a non-oriented compact surface, and N an oriented 3-manifold, both without boundaries. We denote by $\mathcal{L}^{fr} = \mathcal{L}^{fr}(M, N)$ the space of all such Legendrian maps $M \to N$.

Example 8. Similar to the case of framed and oriented fronts, the number of isolated singularities of $\mathcal{F}$ of a particular type is a local invariant. The only difference between this case and the previous one is the number of types:

I_t, *the number of triple points* A_1^3;

$I_{s^\pm}$, *the numbers of positive and negative swallowtails*;

$I_{c^\pm}$, *the numbers of* $A_2A_1^\pm$ *points*;

$I_{\ell'}$, *the self-linking number of the oriented link defined by the cuspidal edge of* $\mathcal{F}$ *in* $\mathbb{R}^3$ *or* S^3.

3.3 Classification of the discriminantal cycles and invariants in the framed case

The first main result of this chapter is

Theorem 3.3.1. *The space of integer discriminantal cycles in* $\mathcal{L}^{fr}(M,N)$ *has rank 6. Its basis is formed by the derivatives of the invariants*

$$I_t\,,\quad (I_{s^+}\pm I_{s^-})/2\,,\quad (I_{c^+}+I_{c^-})/2\,,\quad I_{\Sigma^2}\,,\quad (2I_{s^+}+I_{c^+}-I_{c^-}-6I_{\Sigma^2})/4\,.$$

This implies

Corollary 3.3.1. *The space of integer local invariants of framed fronts in* N *parametrised by* M *has rank either 6 or 5.*

The exact value of the rank here depends on I'_{Σ^2} being or not being a trivial cycle.

Let $\mathcal{L}_1^{fr}\subset\mathcal{L}^{fr}(M,N)$ be the set of all Legendrian maps without corank 2 points. Discriminantal cycles in $\mathcal{L}_1^{fr}$ do not contain any summands of I'_{Σ^2}. Our proof of Theorem 3.3.1 yields

Corollary 3.3.2. *The space of integer discriminantal cycles in $\mathcal{L}_1^{fr}(M,N)$ has rank 5. Its basis is formed by the derivatives of the invariants*

$$I_t\,,\quad (I_{s^+}\pm I_{s^-})/2\,,\quad (I_{c^+}+I_{c^-})/2\,,\quad (2I_{s^+}+I_{c^+}-I_{c^-})/4\,.$$

Respectively, these five invariants form a basis of the space of all integer local invariants on $\mathcal{L}_1^{fr}(M,N)$.

In the $\mathbb{Z}_2$ case we have

Theorem 3.3.2. *The space of mod2 discriminantal cycles in $\mathcal{L}^{fr}(M,N)$ has rank 8. Its basis is formed by I'_{dir}, I'_{opp} and the reduced basic derivatives of Theorem 3.3.1.*

Prohibition of corank 2 points in homotopies cuts here the rank down to 7 and excludes I'_{Σ^2}.

Depending on how many of the linear combinations of the mod2 discriminantal cycles I'_{dir}, I'_{opp} and I'_{Σ^2} turn out to be trivial, we have

Corollary 3.3.3. *The space of $\mathbb{Z}_2$-valued local invariants of framed fronts in N parametrised by M has rank at least 5 and at most 8.*

Both theorems are proved in Section 3.5.

3.4 Codimension 1 bifurcations

The list of codimension 1 discriminantal strata in $\mathcal{L}^{fr}(M,N)$ becomes shorter than in Section 2.4. We are now listing all codimension 1 singularities.

3.4.1 Multi-germs

All multi-germs lose the signs of the orientation in their notation, and the corresponding strata are now the sums of the former strata along the whole range of the lost signs. The notations will be very similar to the previous setting. A new feature that we introduce now will be letter r which stays for the number of faces of the bounded region appearing *after* the bifurcation, which are framed outward the region. While listing the codimension 1 singularities, we will use the equations obtained in Sections 2.5.1 and 2.5.2 to glue the strata together. In some cases will be using $\bullet$ to emphases the front orientation from Chapter 2, which is now ignored. So, we have (see Figure 3.2):

$A_1^{4,r}$, $r = 2, 3, 4$, the pre-bifurcation tetrahedral region has $4-r$ faces framed outwards. Therefore, the $r = 2$ stratum $A_1^{4,2}$ is not co-orientable in $\mathcal{L}^{fr}$ by local means. According to equation **1** in Section 2.5.1.1 the $A^{4,\alpha_1\alpha_2\alpha_3\alpha_4}_{1,\beta_1\beta_2\beta_3\beta_4}$ strata were united into 5 big ones distinguished by the number of indices i for which $\alpha_i = \beta_i$. In our current situation we are summing up the $A^{4,\alpha_1\alpha_2\alpha_3\alpha_4}_{1,\beta_1\beta_2\beta_3\beta_4}$ along the β_i when passing to the elementary strata in the new setting. Each of the latter sums contains at least one summand from each of the 5 former. Therefore, all our new $A_1^{4,r}$ strata glue up into one A_1^4, which is not coorientable since $A_1^{4,2}$ is not.

$TA_1^{3,r}$, $r = 0, 1, 2, 3$, again, each of the $TA_1^{3,r}$ strata contains an elementary summand from each of the four big TA_1^3 strata we had in Chapter 2 according to the equations **2** of Section 2.5.1.1. Therefore, all new elementary strata make up one new big stratum TA_1^3.

$TA_1^{2,e,r}$, $r = 0, 1, 2$, elliptic tangency of two smooth sheets. The value of r indicates the number of pluses α_i in the notation $TA_{1,\ \beta_1\beta_2}^{2,e,\alpha_1\alpha_2}$ of the previous settings. For example, the stratum $TA_1^{2,e,2}$ is the sum of the $TA_{1,\ \beta_1\beta_2}^{2,e,++}$ along the $\beta_i = \pm$.

$TA_1^{2,h,r}$, $r = 0, 1$, same, but hyperbolic. We write $r = 1$ if the sheets have the same framings, and $r = 0$ if the framings are opposite. For $r = 1$, we fail to locally co-orient the stratum in $\mathcal{L}^{fr}$. Using equation **9** in Section 2.5.2 we have:

$$\begin{aligned} TA_1^{2,e,2} &= TA_{1,\ \bullet\bullet}^{2,e,++} + TA_{1,\bullet\bullet}^{2,h,0} - TA_{1,\ \bullet\bullet}^{2,e,--}; \\ TA_1^{2,e,1} &= TA_{1,\ \bullet\bullet}^{2,e,+-} + [TA_{1,\bullet\bullet}^{2,h,1}]. \end{aligned}$$

The right hand side of the two equations cover all types of TA_1^2 in our current setting. Hence, all types of TA_1^2 join into two classes which we will call $TA_1^{2,opp}$ and $[TA_1^{2,dir}]$.

$A_2A_1^{2,\pm,\pm}$, cuspidal edge meets the intersection of two smooth sheets. The two signs are the signs of the two A_2A_1 points after the bifurcation, in the order in which the points are locally on the cuspidal edge if we follow the edge orientation. The table in Section 2.4.3 lists 8 big strata in the sense of Chapter 2. Each of them has a summand $A_{2\bullet}A_{1,\bullet\bullet}^{2,++}$. Therefore, in the current sense all types of $A_2A_1^2$ strata are now glued up into one big stratum $A_2A_1^2$.

$A_2^{2,e,\pm}$, two edges meet face-to-face. During the bifurcation the crossing sign of the two local oriented edges changes. The sign in the notation of the stratum is the crossing sign after the bifurcation. The $A_2^{2,e,\sigma}$, $\sigma = \pm$, stratum will be the sum of $A_{2,\beta_1\beta_2}^{2,e,\sigma}$ along the whole range of the β_i.

$A_2^{2,h}$, one of the edges is overtaking the other. The crossing sign of the two edges after the bifurcation is plus. Similarly, we have $A_2^{2,h}$ stratum as the sum of the $A^{2,h}_{2,\beta_1\beta_2}$, along $\beta_i = \pm$. Thus, we only have one type of $A_2^{2,h}$.

$A_3^{\pm}A_1^{\pm}$, a smooth sheet passes through a swallowtail. The meaning of the A_1 sign is clear from Figure 3.2. According to equation **4** in Section 2.5.1.1 we have for example,

$$\begin{aligned} A_3^+A_1^+ &= A_{3,\bullet}{}^+A_{1,\bullet}{}^+ + A_{3,\bullet}{}^+A_{1,\bullet}{}^-; \\ A_3^-A_1^+ &= A_{3,\bullet}{}^-A_{1,\bullet}{}^+ + A_{3,\bullet}{}^-A_{1,\bullet}{}^-. \end{aligned}$$

which allows us to join all types of the A_3A_1 bifurcations into two classes $A_3^+A_1$ and $A_3^-A_1$.

$TA_2A_1^{e,\pm}$, cuspidal edge becomes tangent to a smooth sheet so that the two local components of $\mathcal{F}$ do not intersect before the bifurcation. The two cases differ by the framing of the smooth sheet.

$TA_2A_1^{h,\pm}$, the hyperbolic version of the previous. We decorate A_1 with plus if the framing coincides with the way the edge is orientated, and minus otherwise. From equation **8** in Section 2.5.2 we have,

$$\begin{aligned} TA_2A_1^{e,+/h,-} &= TA_{2\bullet}A_{1,\bullet}^{e,+} + TA_{2\bullet}A_{1,\bullet}^{h,-}; \\ TA_2A_1^{e,-/h,+} &= TA_{2\bullet}A_{1,\bullet}^{e,-} + TA_{2\bullet}A_{1,\bullet}^{h,+}. \end{aligned}$$

3.4.2 Uni-germs

In Figure 3.3 we show the modifications of Figure 2.20. The majority of the uni-germ transitions are straightforward:

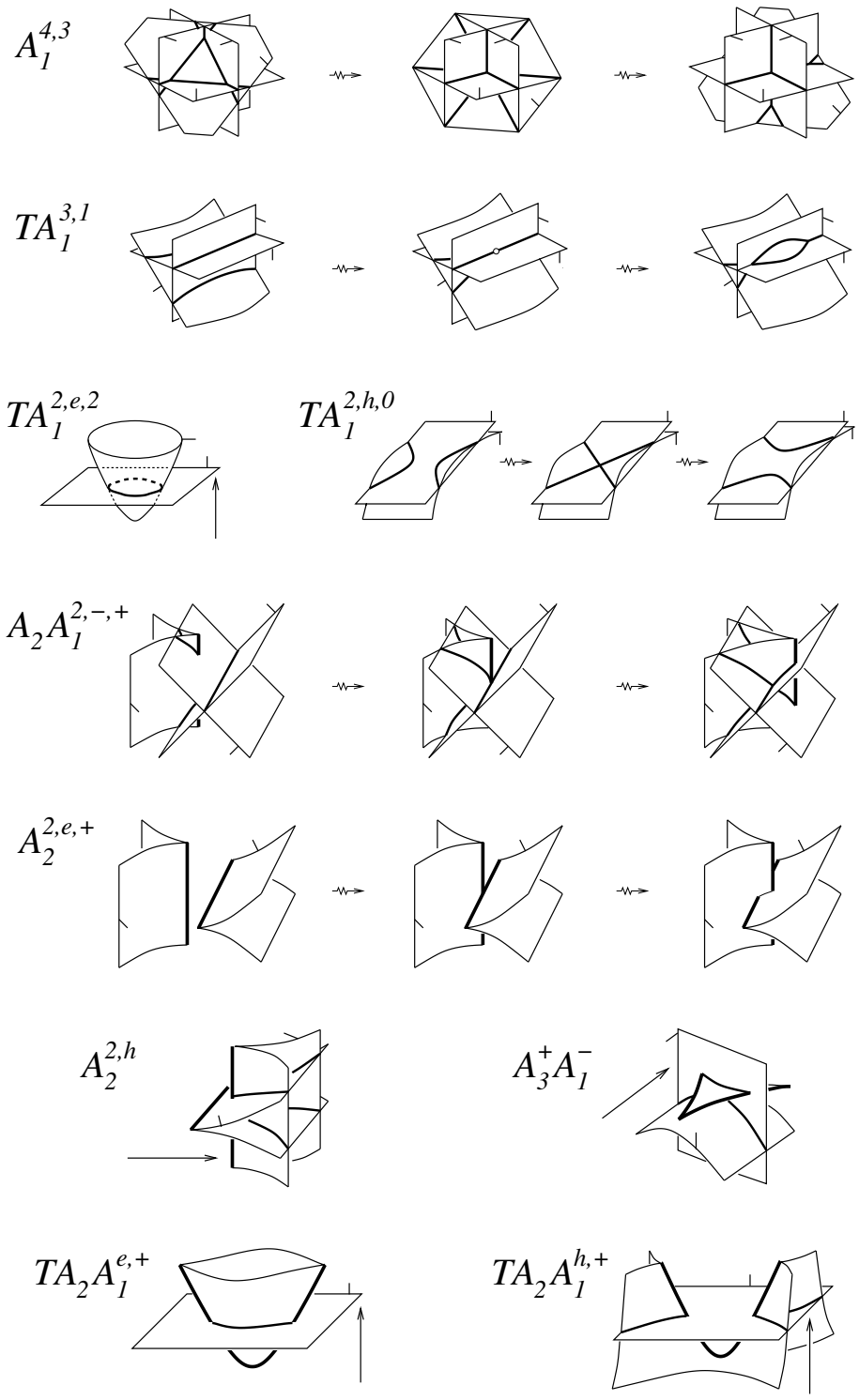

Figure 3.2: Codimension 1 framed multi-germs.

$A_3^{e/h,\pm}$, with the new understanding of the swallowtail sign;

$A_4^{\pm}$, here the sign is the local crossing number of the edge after the bifurcation. It coincides with the signs of the two A_2A_1 points appearing.

$D_4^{\pm}$, the swallowtails after the bifurcations are positive.

3.4.3 The integer invariants in terms of linear combinations of the strata

The next table shows the classes of the elementary strata which we were able to join together and the notations of their big strata in the framed-only case. Strata with classes of their own are not included in the table.

No.	Big Stratum Notation	Class
1	$[A_1^4]$	$[A_1^{4,2}] + A_1^{4,3} + A_1^{4,4}$
2	TA_1^3	$TA_1^{3,0} + TA_1^{3,1} + TA_1^{3,2} + TA_1^{3,3}$
3	$TA_1^{2,opp}$	$TA_1^{2,e,2} + TA_1^{2,h,0} - TA_1^{2,e,0}$
4	$[TA_1^{2,dir}]$	$TA_1^{2,e,1} + [TA_1^{2,h,1}]$
5	$A_2A_1^2$	$A_2A_1^{2,++} + A_2A_1^{2,+-} + A_2A_1^{2,--} + A_2A_1^{2,-+}$
6	$A_3^+A_1$	$A_3^+A_1^+ + A_3^+A_1^-$
7	$A_3^-A_1$	$A_3^-A_1^+ + A_3^-A_1^-$
8	$TA_2A_1^{e,+/h,-}$	$TA_2A_1^{e,+} + TA_2A_1^{h,-}$
9	$TA_2A_1^{e,-/h,+}$	$TA_2A_1^{e,-} + TA_2A_1^{h,+}$
10	$A_3^{e/h,+}$	$A_3^{e,+} + A_3^{h,+}$
11	$A_3^{e/h,-}$	$A_3^{e,-} + A_3^{h,-}$

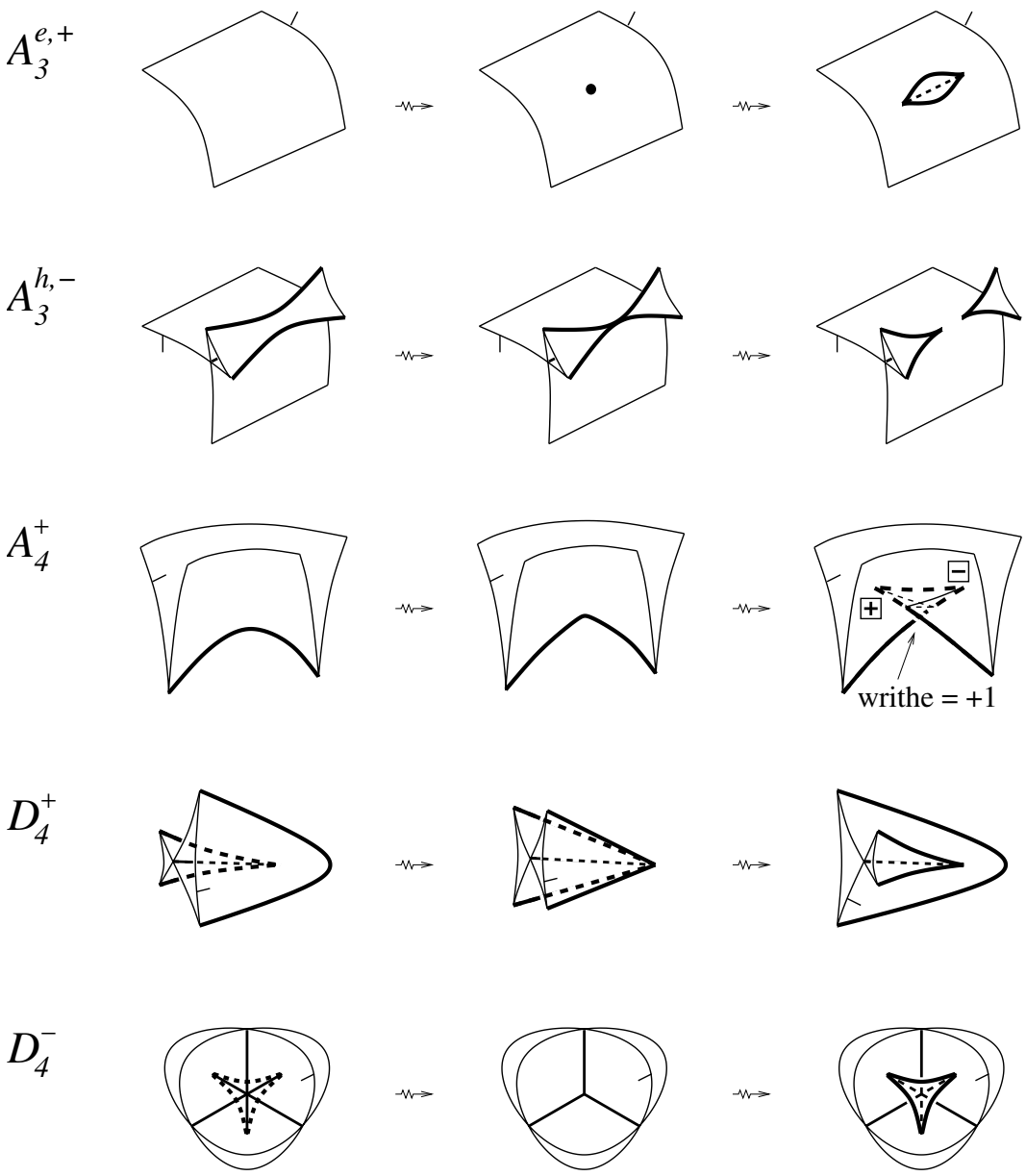

Figure 3.3: Codimension 1 framed uni-germs.

Within these settings, inspection of Figures 3.2 and 3.3 implies

Lemma 3.4.1. *The derivatives of the numbers of points of isolated singularity types of generic fronts and of the edge self-linking number are*

$$\begin{aligned}
I_s/2 &= (I_{s^+}+I_{s^-})/2 \;:\; A_3^{e/h,+}+A_3^{e/h,-}+A_4^+ + A_4^-,\\
\widehat{I}_s/2 &= (I_{s^+}-I_{s^-})/2 \;:\; A_3^{e/h,+}-A_3^{e/h,-}+D_4^+ + 3D_4^-,\\
I_c/2 &= (I_{c^+}+I_{c^-})/2 \;:\; 2A_2^{2,e,+}+2A_2^{2,e,-}+A_3^+A_1+A_3^-A_1+TA_2A_1\\
&\qquad\qquad +A_4^+ + A_4^-,\\
\widehat{I}_c/2 &= (I_{c^+}-I_{c^-})/2 \;:\; 2A_2^{2,e,+}-2A_2^{2,e,-}+2A_2^{2,h}+A_4^+ - A_4^-,\\
& I_t \;:\; 2TA_1^3+2A_2A_1^2+A_3^+A_1+A_3^-A_1,\\
& I_{\ell'} \;:\; 2A_2^{2,e,+}-2A_2^{2,e,-}+2A_2^{2,h}+A_4^+ - A_4^-.
\end{aligned}$$

In particular, we see that in $\mathbb{R}^3$ or S^3, up to an additive constant, $I_{\ell'} = (I_{c^+}-I_{c^-})/2$.

3.4.4 Equations on the increments

Like before, we start with the easiest kind of codimension 2 bifurcations when an extra generic A_1 sheet of $\mathcal{F}$ passes through a point of a codimension 1 bifurcation. As we have mentioned, most of the equations obtained from such bifurcations and also from the cubic bifurcations were used earlier when listing the codimension 1 singularities.

However, in this setting the bifurcation diagram of the A_4A_1 family in Figure 2.25 when $\alpha,\sigma=+$, gives us the equation $a_3^+a_1^- = a_3^-a_1^+$ which allows to unite $A_3^+A_1^-$ and $A_3^-A_1^+$ together. On the other hand, we were able to glue $A_3^+A_1^-$ with $A_3^+A_1^+$ and $A_3^-A_1^-$ with $A_3^-A_1^+$ (via $A_3^{e/h,+}A_1$ and $A_3^{e/h,-}A_1$).

Hence, all types of A_3A_1 have the same increments of the invariants.

So far the number of unknown integer increments is 17, out of which two may be non-trivial only mod2: $[A_1^4], [TA_1^{2,dir}]$.

We now consider the modifications for the current setting of the 2-parameter families we studied for framed and oriented fronts in Sections 2.5.3 and 2.5.4. The modified bifurcation diagrams are shown in Figures 3.4, 3.5 and 3.6. In each case there we are illustrating one of possible choices of the framing. The diagrams for all other framing options can be easily obtained by dropping the lower indices of the codimension 2 bifurcations diagrams of Chapter 2.

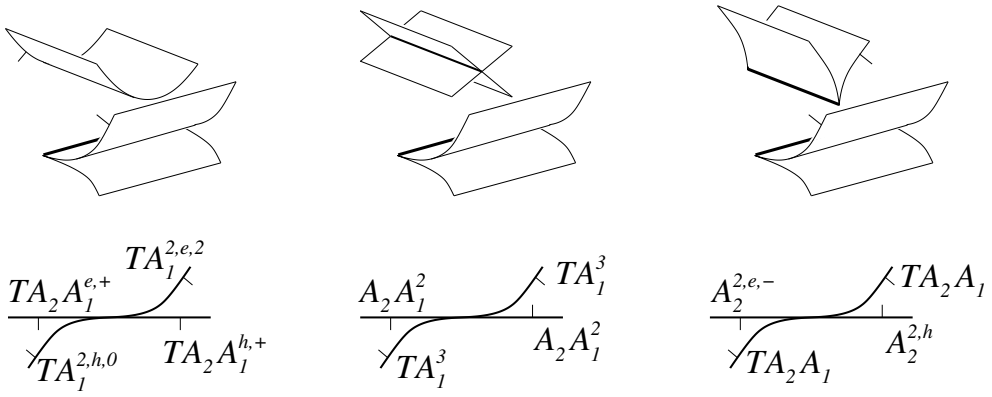

Figure 3.4: Codimension 2 degenerations due to special positions with respect to the tangent plane at an edge point. The reason to omit the TA_2A_1 decorations in the last diagram is given at the end of this section.

Respectively, we obtain new equations for the increments (the numbering of the equations correspond to the numbering of the Chapter 2 equations):

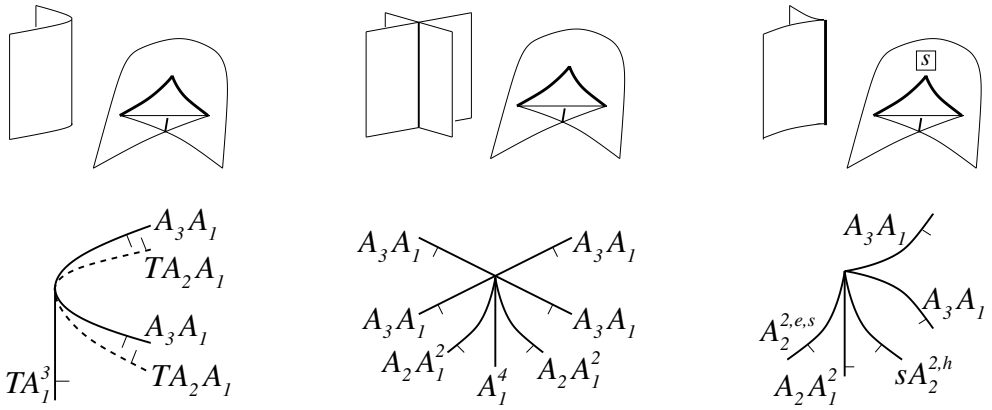

Figure 3.5: Codimension 2 degenerations involving swallowtails.

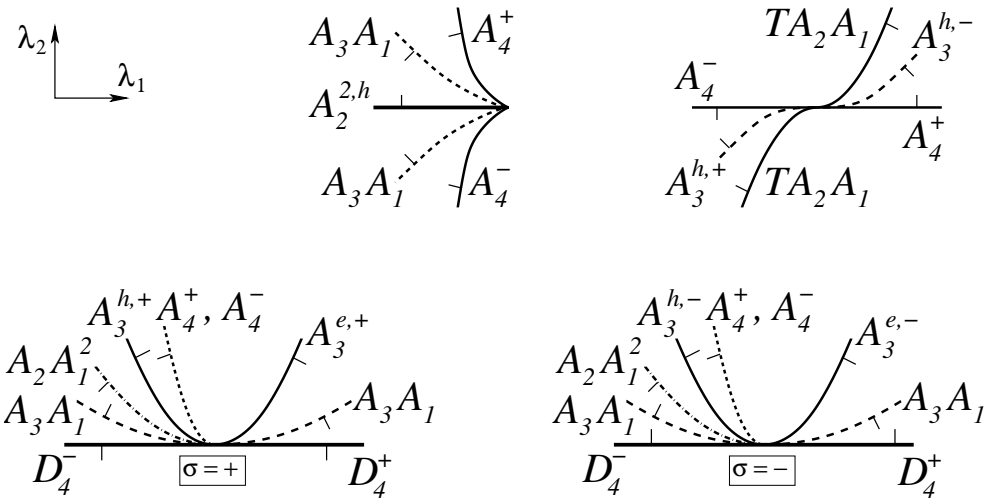

Figure 3.6: Uni-germs of codimension 2

$$
\begin{aligned}
\textbf{10}.\quad & t a_2 a_1^{e,-} - t a_2 a_1^{e,+} + 2 t a_1^{2,dir} && = 0 \\
\textbf{11}.\quad & t a_2 a_1^{e,+} - t a_2 a_1^{h,+} && = 0 \\
\textbf{12}.\quad & t a_2 a_1^{e,-} - t a_2 a_1^{h,-} && = 0 \\
\textbf{13}.\quad & t a_2 a_1^{e,-} - t a_2 a_1^{h,-} - 2 t a_1^{2,dir} && = 0 \\
\textbf{14}.\quad & 2 a_2 a_1^2 - 2 t a_1^3 && = 0 \\
\textbf{15}.\quad & a_2^{2,e,-} + a_2^{2,h} - 2 t a_2 a_1 && = 0 \\
\textbf{16}.\quad & a_2^{2,e,+} - a_2^{2,h} - 2 t a_2 a_1 && = 0 \\
\textbf{19}.\quad & 2 a_3 a_1 - 2 t a_2 a_1 - t a_1^3 && = 0 \\
\textbf{21}.\quad & [a_1^4] && = 0 \\
\textbf{22}.\quad & a_2^{2,e,+} + a_2 a_1^2 - a_2^{2,h} - 2 a_3 a_1 && = 0 \\
\textbf{23}.\quad & a_2^{2,e,-} + a_2 a_1^2 + a_2^{2,h} - 2 a_3 a_1 && = 0 \\
\textbf{27}.\quad & a_4^+ - a_4^- - a^{2,h} && = 0 \\
\textbf{28}.\quad & a_4^+ + a_4^- - 2 t a_2 a_1 - a_3^{e/h,+} - a_3^{e/h,-} && = 0 \\
\textbf{29}.\quad & d_4^- - 2 a_3 a_1 - 2 a_3^{e/h,+} + a_4^+ + a_4^- + a_2 a_1^2 - d_4^+ && = 0 \\
\textbf{30}.\quad & d_4^+ - 2 a_3 a_1 - 2 a_3^{e/h,-} + a_4^+ + a_4^- + a_2 a_1^2 - d_4^- && = 0
\end{aligned}
$$

Equations **11** and **12** allow us to unite in one all codimension 1 strata TA_2A_1 (which we are using already in equations **15, 16, 19** and **28** also in Figures 3.4, 3.5 and 3.6):

3.5 Proofs of the classification results in the framed case

The equations we have obtained are sufficient to prove the classification claims made in Section 3.3. All other 2-parameter bifurcations of framed fronts fail to add equations independent from those we have already written out.

In the integer case, after joining elementary strata into the bigger ones, we have now 14 strata

$$TA_1^3,\ A_2A_1^2,\ A_3A_1,\ TA_2A_1,\ A_2^{2,e,+},\ A_2^{2,e,-},\ A_2^{2,h},\ A_4^+,\ A_4^-,\ A_3^{e/h,+},$$

$$A_3^{e/h,-},\ TA_1^{2,opp},\ D_4^+,\ D_4^-.$$

We collect equations **13**–**30** (equation **10** just repeats **13**) into the tables below, for arbitrary and mod2 coefficients. The first table contains the equations themselves in the order they have appeared (we are using dots for zero coefficients). The bars indicate the equations which are integer linear combinations of the others. The second table lists the discriminantal cycles as linear combinations of the strata (with the notations as in Lemma 3.4.1).

$\mathbb{Z}$	13	$\overline{14}$	15	16	19	22	$\overline{23}$	27	28	29	$\overline{30}$
TA_1^3	.	-2	.	.	-1	.	.	.	.	.	.
$TA_1^{2,opp}$	-2	.	.	.	.	.	.	.	.	.	.
$A_2A_1^2$	.	2	.	.	.	1	1	.	.	1	1
A_3A_1	.	.	.	.	2	-2	-2	.	.	-2	-2
TA_2A_1	.	.	-2	-2	-2	.	.	.	-2	.	.
$A_3^{e/h,+}$	.	.	.	.	.	.	.	.	-1	-2	.
$A_3^{e/h,-}$	.	.	.	.	.	.	.	.	-1	.	-2
$A_2^{2,e,+}$	.	.	.	1	.	1	.	.	.	.	.
$A_2^{2,e,-}$	.	.	1	.	.	.	1	.	.	.	.
$A_2^{2,h}$	.	.	1	-1	.	-1	1	-1	.	.	.
A_4^+	.	.	.	.	.	.	.	1	1	1	1
A_4^-	.	.	.	.	.	.	.	-1	1	1	1
D_4^+	.	.	.	.	.	.	.	.	.	-1	1
D_4^-	.	.	.	.	.	.	.	.	.	1	-1

$\mathbb{Z}$	$I'_s/2$	$\widehat{I'}_s/2$	$I'_c/2$	$\widehat{I}'_c/2$	I'_t	I'_{Σ^2}	I'_0
TA_1^3	.	.	.	.	2	.	.
$TA_1^{2,opp}$	.	.	.	.	.	.	.
$A_2A_1^2$	.	.	.	.	2	.	.
A_3A_1	.	.	1	.	1	.	.
TA_2A_1	.	.	1	.	.	.	.
$A_3^{e/h,+}$	1	1	.	.	.	.	1
$A_3^{e/h,-}$	1	-1	.	.	.	.	.
$A_2^{2,e,+}$	.	.	2	2	.	.	1
$A_2^{2,e,-}$	.	.	2	-2	.	.	-1
$A_2^{2,h}$	.	.	.	2	.	.	1
A_4^+	1	.	1	1	.	.	1
A_4^-	1	.	1	-1	.	.	.
D_4^+	.	1	.	.	.	1	1
D_4^-	.	3	.	.	.	1	.

Here $I'_0 = (I'_s/2 + \widehat{I}'_s/2 + \widehat{I}'_c/2 - 3I'_{\Sigma^2})/2 = (2I'_{s^+} + I'_{c^+} - I'_{c^-} - 6I'_{\Sigma^2})/4$.

The rank count of the first table shows that the space of integer discriminantal cycles is 6-dimensional, and the second table tells us that a basis of this integer space is formed by the 6 cycles excluding $\widehat{I}'_c/2$. This proves Theorem 3.3.1.

In $\mathbb{Z}_2$ setting we have the same strata as in the $\mathbb{Z}$ case along with $A_1^{2,dir}$ and A_1^4 which may have non-trivial increments only mod2. Adjusting the above tables to the $\mathbb{Z}_2$ case, we use equations **15** and **16** to make a big stratum

$A_2^{2.e/h}$, then exclude the $[A_1^4]$, TA_1^3 and $A_2A_1^2$ strata (along with the equations **19**, **21** and **22** in which exactly one of them appears now on its own), and drop the duplicate and $0 = 0$ equations. This leaves us with 3 independent equations in 11 unknowns. The table consists of two parts. The left one contains the equations, while the right lists the discriminantal cycles as linear combinations of the strata.

$\mathbb{Z}_2$	27	28	29	$I'_s/2$	$\widehat{I}'_s/2$	$I'_c/2$	$\widehat{I}'_c/2$	I'_t	I'_{Σ^2}	I'_{opp}	I'_{dir}	I'_0
$TA_1^{2,opp}$	.	.	.	.	.	.	.	.	.	1	.	.
$TA_1^{2,dir}$	.	.	.	.	.	.	.	.	.	.	1	.
A_3A_1	.	.	.	.	.	1	.	1	.	.	.	.
TA_2A_1	.	.	.	.	.	1	.	.	.	.	.	.
$A_3^{e/h,+}$	.	1	.	1	1	.	.	.	.	.	.	1
$A_3^{e/h,-}$	.	1	.	1	1	.	.	.	.	.	.	.
$A_2^{2,e/h}$	1	.	.	.	.	.	.	.	.	.	.	1
A_4^+	1	1	1	1	.	1	1	.	.	.	.	1
A_4^-	1	1	1	1	.	1	1	.	.	.	.	.
D_4^+	.	.	1	.	1	.	.	.	1	.	.	1
D_4^-	.	.	1	.	1	.	.	.	1	.	.	.

The space of mod2 invariants has rank 8. There is one relation on the 9 discriminantal cycles listed in the table: $I'_s/2 + \widehat{I}'_s/2 + \widehat{I}'_c/2 + I'_{\Sigma^2} \equiv 0$. The two further invariants I'_{opp}, I'_{dir} are the derivatives of the $\mathbb{Z}_2$-valued functions counting the parities of the self-tangency of two smooth sheets in homotopies. Our proof of Theorem 3.3.2 is finished.

3.6 Classification over $\mathbb{Q}$

Similar to Chapter 2, our results over the rational numbers are:

Theorem 3.6.1. *For any surface M and oriented 3-manifold N, the space of rational discriminantal cycles in $\mathcal{L}^{fr}(M,N)$ has rank 6. Its basis is formed by the derivatives of the invariants*

$$I_t\,, \quad I_{s_+}\,, \quad I_{s_-}\,, \quad I_{c_+}\,, \quad I_{c_-}\,, \quad I_{\Sigma^2}\,.$$

Considering $\mathcal{L}_1^{fr}(M,N)$, the set of all Legendrian maps without corank 2 points, we have

Corollary 3.6.1. *The space of all rational local invariants on $\mathcal{L}_1^{fr}(M,N)$ has rank 5. Its basis is formed by the derivatives of the invariants*

$$I_t\,, \quad I_{s_+}\,, \quad I_{s_-}\,, \quad I_{c_+}\,, \quad I_{c_-}\,.$$

Chapter 4

Local invariants of oriented fronts

We now consider oriented fronts with no framing. This corresponds to Legendrian maps $M \looparrowright PT^*N \to N$, of immersed Legendrian submanifolds in the space of non-framed contact elements of N, where M is a compact oriented surface. We denote the set of all such maps by $\mathcal{L}_{or} = \mathcal{L}_{or}(M, N)$. Similarly to Chapter 3, such modifications will lead to the reduced number of unknowns and equations comparing to Chapter 2.

4.1 Stable singularities of oriented fronts

An orientation of a front equips its smooth sheets A_1 with a co-orientation, exactly like it was explained in Section 2.1. The notations of the strata are inherited from Chapter 2, where the upper signs are omitted since they are responsible for the fronts framing which is now ignored.

A_1^2, transversal intersections of two smooth sheets;

A_1^3, same for three sheets;

$A_{2\pm}$, cuspidal edges as in Figure 4.1, we note that now the edge is not oriented;

$A_{2\pm}A_1$, transversal intersections of edges with regular sheets;

$A_{3,\pm}$, swallowtail points, on the edges of the same sign, as in Figure 4.1.

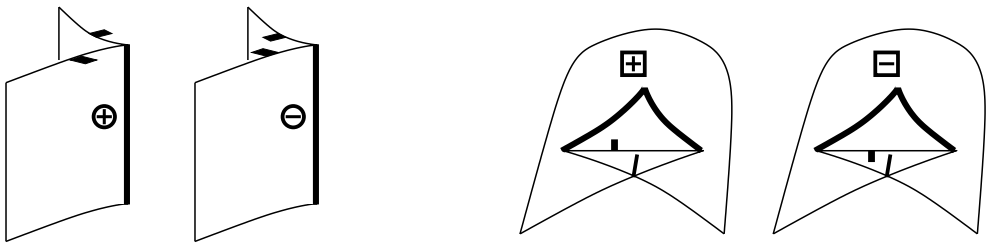

Figure 4.1: Types of stable singularities of oriented fronts: $A_{2\pm}$ and $A_{3,\pm}$.

4.2 Integer invariants in the oriented setting

Example 9. We will repeat the same invariants as in Chapter 3 with the only difference in the numbers of types.

I_t, *the number of triple points* A_1^3;

$I_{s_\pm}$, *the numbers of positive and negative swallowtails*;

$I_{c_\pm}$, *the numbers of* $A_{2\pm}A_1$ *points*;

Cuspidal edges of $\mathcal{F}$ are not oriented, hence the integer *linking* and *self-linking numbers* are not defined in $\mathcal{L}_{or}$. However, in the mod2 setting, via an

arbitrary choice of the orientation of the edges of $\mathcal{F}$, the I_ℓ, $I_{\ell'_+}$, $I_{\ell'_-}$ invariants are well-defined in $\mathbb{R}^3$ or S^3.

In Section 4.5 we will adapt the integral invariant $I_\int$ described in Section 0.4.1 to the case of oriented fronts in $\mathbb{R}^3$.

4.3 Classification of the discriminantal cycles and invariants in the oriented setting

The first main result of this chapter is

Theorem 4.3.1. *The space of integer discriminantal cycles in $\mathcal{L}_{or}(M, \mathbb{R}^3)$ has rank 7. Its basis is formed by the derivatives of the invariants*

$$(I_{s_+} - 3I_{\Sigma^2})/2,\ (I_{s_-} + I_{\Sigma^2})/2,\ I_{c_+}/2,\ I_{c_-}/2,\ I_t,\ I_{\Sigma^2},\ ((I_{s_+} + I_{s_-})/2 + I_t - I_\int)/2.$$

This implies

Corollary 4.3.1. *The space of integer local invariants of oriented fronts in $\mathbb{R}^3$ parametrised by M has rank either 7 or 6.*

The exact value of the rank here depends on I'_{Σ^2} being or not being a trivial cycle.

Let $\mathcal{L}^1_{or} \subset \mathcal{L}_{or}(M, N)$ be the set of all Legendrian maps without corank 2 points. Our proof of Theorem 4.3.1 yields

Corollary 4.3.2. *The space of integer discriminantal cycles in $\mathcal{L}^1_{or}(M, \mathbb{R}^3)$ has rank 6. Its basis is formed by the derivatives of the invariants*

$$I_{s_+}/2,\ I_{s_-}/2,\ I_{c_+}/2,\ I_{c_-}/2,\ I_t,\ ((I_{s_+} + I_{s_-})/2 + I_t - I_\int)/2.$$

Respectively, these six invariants form a basis of the space of all integer local invariants on $\mathcal{L}^1_{or}(M,N)$.

In the $\mathbb{Z}_2$ case we have

Theorem 4.3.2. *The space of mod2 discriminantal cycles in* $\mathcal{L}_{or}(M,\mathbb{R}^3)$ *has rank 11. Its basis is formed by* I'_ℓ, $I'_{\ell'_+}$, $I'_{\ell'_-}$, $I'_{dir}+I'_{opp}$ *and the reduced basic derivatives of Theorem 4.3.1.*

Depending on how many of the linear combinations of the mod2 discriminantal cycles $I'_{dir}+I'_{opp}$ and I'_{Σ^2} turn out to be trivial, we have

Corollary 4.3.3. *The space of* $\mathbb{Z}_2$*-valued local invariants of framed fronts in* $\mathbb{R}^3$ *parametrised by* M *has rank at least 9 and at most 11.*

The proofs of the theorems are in Section 4.3.

4.4 Codimension 1 bifurcations

4.4.1 Multi-germs

All codimension 1 singularities involving smooth sheets are exactly the same as the ones we had in Section 3.4, with the only difference in the notations that we write the letter r in the lower indices.

$$A^4_{1,r}, r=2,3,4, \quad TA^3_{1,r}, r=0,1,2,3, \quad TA^{2,e}_{1,r}, r=0,1,2, \quad TA^{2,h}_{1,r}, r=0,1,$$

Using the arrangement from Section 3.4 we glue up these elementary strata into A^4_1, TA^3_1, $TA^2_{1,opp}$ and $[TA^2_{1,dir}]$.

We further modify the bifurcations of Section 2.4 keeping the order unchanged (the positive direction of a transition is the same as in Chapter 2 unless specified). Also, in some cases we will be using $\bullet$ for the summation along all possible elementary choices of the front framings from Chapter 2, which are now being ignored.

So, we now have the following list of multi-germ codimension 1 bifurcations:

$A_{2\pm}A^2_{1,r}$, $r = 0, 1, 2$, where the sign is that of the cuspidal edge, and r is the number of the outwards oriented A_1 faces of the newborn finite region. We have for example,

$$A_{2+}A^2_{1,1} = A_{2+}A^{2,\bullet\bullet}_{1,+-} + A_{2+}A^{2,\bullet\bullet}_{1,-+}$$

According to equation **3** in Section 2.5.1.1 the elementary $A_2A^2_1$ strata were united into 8 big ones in the sense of Chapter 2. Four of them were with a positive cuspidal edge sign and the other four with negative. Each of these four positive (negative) strata has a summand $A_{2+}A^{2,\alpha_1\alpha_2}_{1,++}$ ($A_{2-}A^{2,\alpha_1\alpha_2}_{1,++}$). Therefore, in our current situation the 8 big classes are united into two classes distinguished by the sign of the cuspidal edge: $A_{2\pm}A^2_1$;

$A^{2,e}_{2,\pm\pm}$, where the signs are the signs of the meeting edges. We will use $A^{2,e}_{2,+-}$, not $A^{2,e}_{2,-+}$;

$A^{2,h}_{2,\pm\pm}$, with the same understanding and use of the signs as in the elliptic case. The strata $A^{2,h,}_{2,++}$ and $A^{2,h}_{2,--}$ are non-co-orientable, and we assume that

the positive direction of the $A^{2,h}_{2,+-}$ transformation is towards creation of two $A_{2+}A_1$ points;

$A_{3,\pm}A_{1,\pm}$, where the first sign is that of the swallowtail, while the second is similar to its use in Chapter 2. Using equation **4** from Section 2.5.1.1 we have:

$$\begin{aligned} A_{3,+}A_1 &= A_{3,+}^{\bullet}A_{1,+}^{\bullet} + A_{3,+}^{\bullet}A_{1,-}^{\bullet}; \\ A_{3,-}A_1 &= A_{3,-}^{\bullet}A_{1,+}^{\bullet} + A_{3,-}^{\bullet}A_{1,-}^{\bullet}. \end{aligned}$$

Thus, all A_3A_1 types are joined into two classes distinguished by the sign of the swallowtail.

$TA_{2\pm}A^e_{1,\pm}$, where the first sign is that of the cuspidal edge, and the second represents the co-orientation of the smooth sheet;

$TA_{2\pm}A^h_{1,\pm}$, all similar to the elliptic case. Using equation **8** in Section 2.5.2 we glue up:

$$\begin{aligned} TA_{2+}A^{e/h}_{1,+/-} &= TA_{2+}A^{e,\bullet}_{1,+} + TA_{2+}A^{h,\bullet}_{1,-}; \\ TA_{2+}A^{e/h}_{1,-/+} &= TA_{2+}A^{e,\bullet}_{1,-} + TA_{2+}A^{h,\bullet}_{1,+}; \\ TA_{2-}A^{e/h}_{1,+/-} &= TA_{2-}A^{e,\bullet}_{1,+} + TA_{2-}A^{h,\bullet}_{1,-}; \\ TA_{2-}A^{e/h}_{1,-/+} &= TA_{2-}A^{e,\bullet}_{1,-} + TA_{2-}A^{h,\bullet}_{1,+}; \end{aligned}$$

Hence, in the oriented settings there are these 4 types of TA_2A_1.

4.4.2 Uni-germs

Figure 4.3 shows codimension 1 oriented uni-germs.

$A^{e/h}_{3,\pm}$, are now running with the new understanding of the swallowtail sign $\pm$;

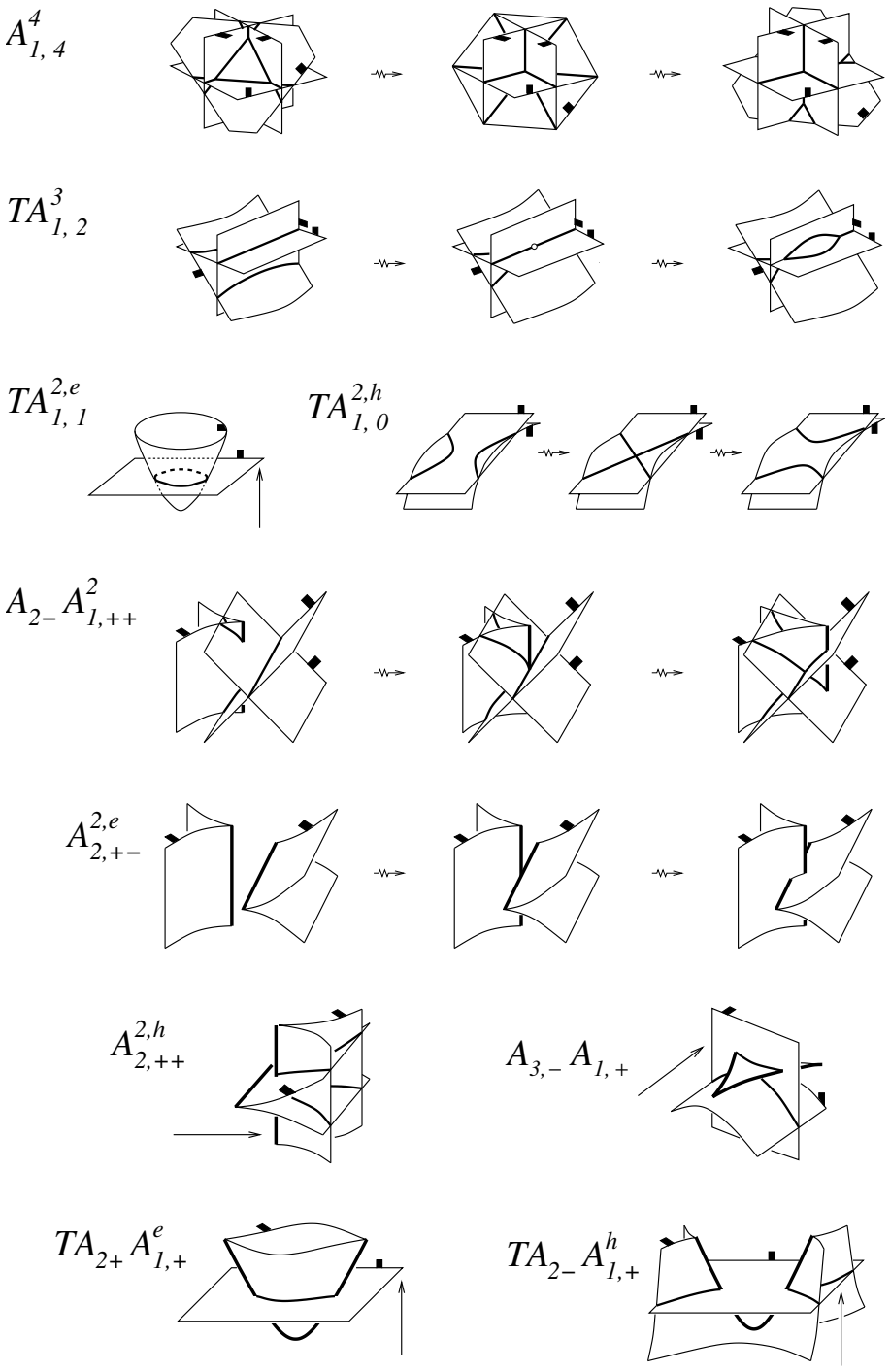

Figure 4.2: Codimension 1 oriented multi-germs.

$A^{\sigma}_{4,s}$, $s = \pm$, $\sigma = \pm$, occurs on an A_{2s} edge which obtains the local writhe σ after the bifurcation (the two appearing swallowtails are $A_{3,s}$);

$D^{\pm}_4$, are again directed towards creation of positive swallowtails, with the positivity of this setting. Note that the superscript decoration is still due to the sign in the normal form $D^{\pm}_4 = x^2y \pm y^3$.

4.4.3 The integer invariants in terms of linear combinations of the strata

The table below shows the notations of the big strata in the oriented setting. Strata with classes of their own are not included in the table.

No.	Big Stratum Notation	Class
1	$[A^4_1]$	$[A^4_{1,2}] + A^4_{1,3} + A^4_{1,4}$
2	TA^3_1	$TA^3_{1,0} + TA^3_{1,1} + TA^3_{1,2} + TA^3_{1,3}$
3	$TA^2_{1,opp}$	$TA^{2,e}_{1,2} + TA^{2,h}_{1,0} - TA^{2,e}_{1,0}$
4	$[TA^2_{1,dir}]$	$TA^{2,e}_{1,1} + [TA^{2,h}_{1,1}]$
5	$A_{2+}A^2_1$	$A_{2+}A^2_{1,++} + A_{2+}A^2_{1,+-} + A_{2+}A^2_{1,-+} + A_{2+}A^2_{1,--}$
6	$A_{2-}A^2_1$	$A_{2-}A^2_{1,++} + A_{2-}A^2_{1,+-} + A_{2-}A^2_{1,-+} + A_{2-}A^2_{1,--}$
7	$A_{3,+}A_1$	$A_{3,+}A_{1,+} + A_{3,+}A_{1,-}$
8	$A_{3,-}A_1$	$A_{3,-}A_{1,+} + A_{3,-}A_{1,-}$
9	$TA_{2+}A^{e/h}_{1,+/-}$	$TA_{2+}A^e_{1,+} + TA_{2+}A^h_{1,-}$
10	$TA_{2+}A^{e/h}_{1,-/+}$	$TA_{2+}A^e_{1,-} + TA_{2+}A^h_{1,+}$

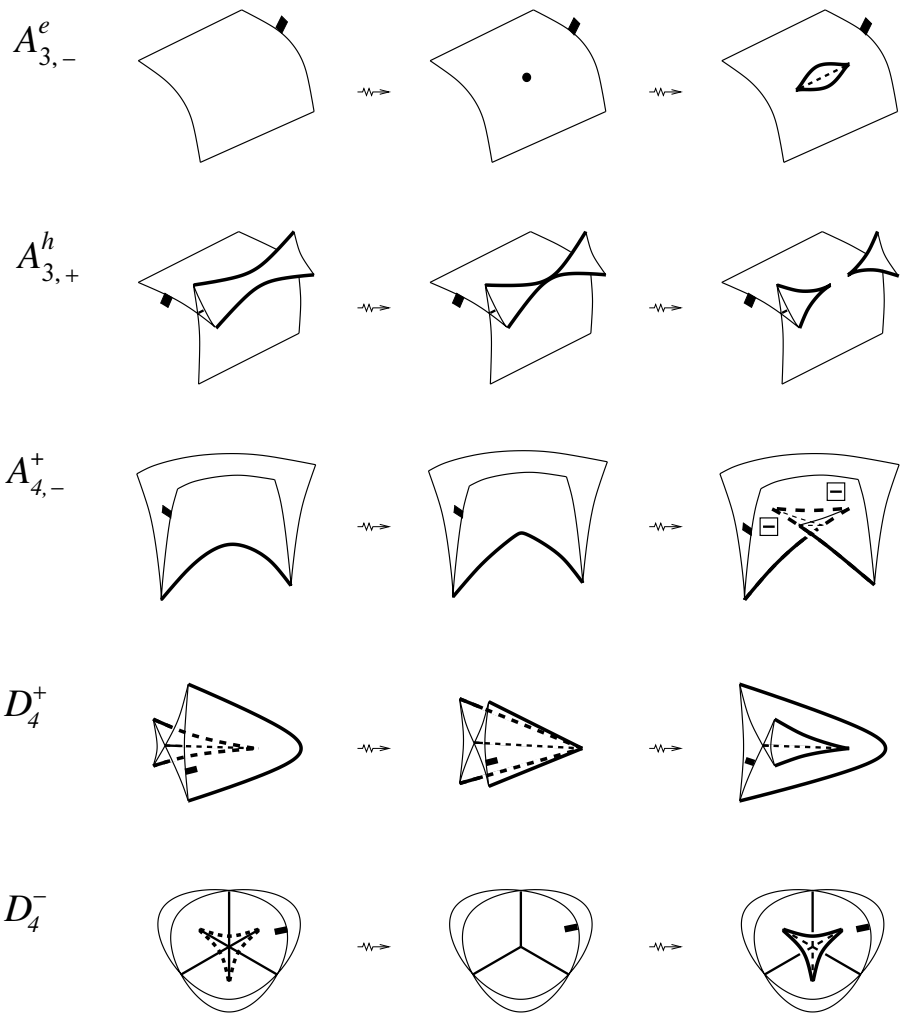

Figure 4.3: Codimension 1 oriented uni-germs.

No.	Big Stratum Notation	Class
11	$TA_{2-}A_{1,+/-}^{e/h}$	$TA_{2-}A_{1,+}^{e} + TA_{2-}A_{1,-}^{h}$
12	$TA_{2-}A_{1,-/+}^{e/h}$	$TA_{2-}A_{1,-}^{e} + TA_{2-}A_{1,+}^{h}$
13	$A_{3,+}^{e/h}$	$A_{3,+}^{e} + A_{3,+}^{h}$
11	$A_{3,-}^{e/h}$	$A_{3,-}^{e} + A_{3,-}^{h}$

Inspection of Figures 4.2 and 4.3 immediately implies

Lemma 4.4.1. *The derivatives of the numbers of points of isolated singularity types of generic fronts are*

$$\begin{aligned}
I_s/2 = (I_{s_+} + I_{s_-})/2 &: A_{3,+}^{e/h} + A_{3,-}^{e/h} + A_{4,+}^{+} + A_{4,+}^{-} + A_{4,-}^{+} + A_{4,-}^{-},\\
(I_{s_+} - I_{s_-})/2 &: A_{3,+}^{e/h} - A_{3,-}^{e/h} + A_{4,+}^{+} + A_{4,-}^{+} - A_{4,+}^{-} - A_{4,-}^{-}\\
&\quad + D_4^{+} + 3D_4^{-},\\
I_c/2 = (I_{c_+} + I_{c_-})/2 &: 2A_{2,++}^{2,e} + 2A_{2,+-}^{2,e} + 2A_{2,--}^{2,e} + A_{3,+}A_1 + A_{3,-}A_1\\
&\quad + TA_{2+}A_{1,+/-}^{e/h} + TA_{2-}A_{1,+/-}^{e/h} + TA_{2+}A_{1,-/+}^{e/h}\\
&\quad + TA_{2-}A_{1,-/+}^{e/h} + A_{4,+}^{+} + A_{4,+}^{-} + A_{4,-}^{+} + A_{4,-}^{-},\\
(I_{c_+} - I_{c_-})/2 &: 2A_{2,++}^{2,e} - 2A_{2,--}^{2,e} - 2A_{2,+-}^{2,h} + A_{3,+}A_1 - A_{3,-}A_1\\
&\quad + TA_{2+}A_{1,+/-}^{e/h} - TA_{2-}A_{1,+/-}^{e/h} + TA_{2+}A_{1,-/+}^{e/h}\\
&\quad - TA_{2-}A_{1,-/+}^{e/h} + A_{4,+}^{+} + A_{4,+}^{-} - A_{4,-}^{+} - A_{4,-}^{-},\\
I_t &: 2TA_1^3 + 2A_{2+}A_1^2 + 2A_{2-}A_1^2 + A_{3,+}A_1 + A_{3,+}A_1.
\end{aligned}$$

4.5 The integral invariant

We introduce now an invariant of generic oriented fronts in oriented $\mathbb{R}^3$ that is very similar to the integral in Goryunov's invariants of mappings of surfaces into three-space [16], which was described in detail in Section 0.4.1.

Following Goryunov's definition, we set:

$$I_{\int}(\mathcal{F}) = \int_{\mathbb{R}^3 \setminus \mathcal{F}} deg(u) d\chi + \sum_t deg(t) + \frac{1}{2} \sum_s deg(s),$$

where t and s run through all triple and swallowtail points of the fronts $\mathcal{F}$.

As it was said in Section 0.4.1, $deg(t)$ is the arithmetical mean of the degrees of the 8 local connected components of the complement of the front. For example if we set the degree of the 8 components of a transversal intersection of three oriented smooth sheets to be $(d, d-1, d-1, d-1, d-2, d-2, d-2, d-3)$, then $deg(t) = d - \frac{3}{2}$. For the swallowtail degree, $deg(s)$, we take the degree of the largest of the three components around the swallowtail point s.

For example, the jump of $I_{\int}$ along $A^e_{3,-}$ is: (Figure 4.4)

$$\begin{aligned} I_{\int}(A^e_{3,-}) &= (-1)^3(d-1) + \tfrac{1}{2}(d+d) \\ &= 1 \end{aligned}$$

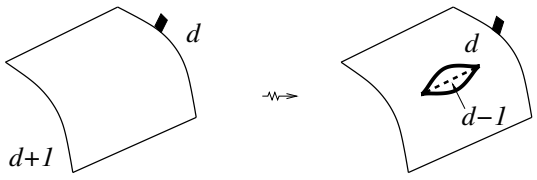

Figure 4.4: Distribution of degrees for $A^e_{3,-}$ bifurcation.

Another way to compute the jumps of $I_{\int}$ is to smoothen all cuspidal edges of $\mathcal{F}$ and replace swallowtails by Whitney umbrella, and then follow the calculations in [16]. See Figure 4.5.

The derivative of the integral invariant, $I_{\int}$, for oriented fronts in $\mathbb{R}^3$ is:

$$\begin{aligned} I_{\int} \ : \ & A^{e/h}_{3,-} - A^{e/h}_{3,+} - A^{+}_{4,+} - A^{-}_{4,+} + A^{+}_{4,-} + A^{-}_{4,-} - 2TA^{2,opp}_{1} - 2A^{2,e}_{2,++} + 2A^{2,e}_{2,--} \\ & - 2A^{2,h}_{2,+-} - A_{3,+}A_1 + A_{3,-}A_1 - 2TA_{2+}A^{e/h}_{1,+/-} + 2TA_{2-}A^{e/h}_{1,-/+} \end{aligned}$$

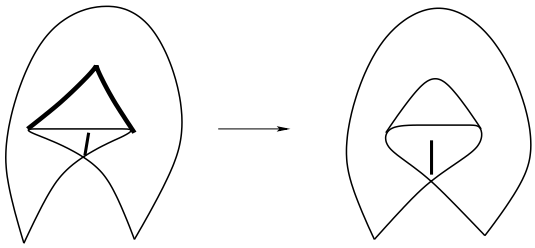

Figure 4.5: Transforming swallowtails to Whitney umbrellas.

4.6 Equations on the increments

The modified bifurcation diagrams are shown in Figure 4.6. Similarly to Chapter 3, we are only illustrating one of possible choices of the orientations.

In this setting the bifurcation diagram of an extra A_1 passes through a point of $A^e_{2,+-}$, gives us a new equation on the increments comparing with the framed fronts case (bifurcation **i** in Figure 4.6). The numbering of the other equations follows what we had in Chapter 2.

The equations obtained from the diagrams are:

$$\begin{array}{rll} & & \alpha\ \ \beta\ \ \gamma\ \ \sigma \\ \mathbf{i}: 2a_{2+}a_1^2 - 2a_{2-}a_1^2 & = 0 & \\ \mathbf{6(1)}: ta_{2-}a^e_{1,+} - ta_{2+}a^e_{1,+} + a_{3,+}a_1 - a_{3,-}a_1 & = 0 & +\ \ + \\ \mathbf{6(2)}: ta_{2-}a^e_{1,-} - ta_{2+}a^e_{1,-} + a_{3,+}a_1 - a_{3,-}a_1 & = 0 & +\ \ - \\ \mathbf{12(1)}: ta_{2+}a^e_{1,+} - ta_{2+}a^e_{1,-} - ta_1^{2,opp} + [a_1^{2,dir}] & = 0 & -\qquad + \\ \mathbf{12(2)}: ta_{2-}a^e_{1,+} - ta_{2-}a^e_{1,-} - ta_1^{2,opp} + [a_1^{2,dir}] & = 0 & -\ \ - \end{array}$$

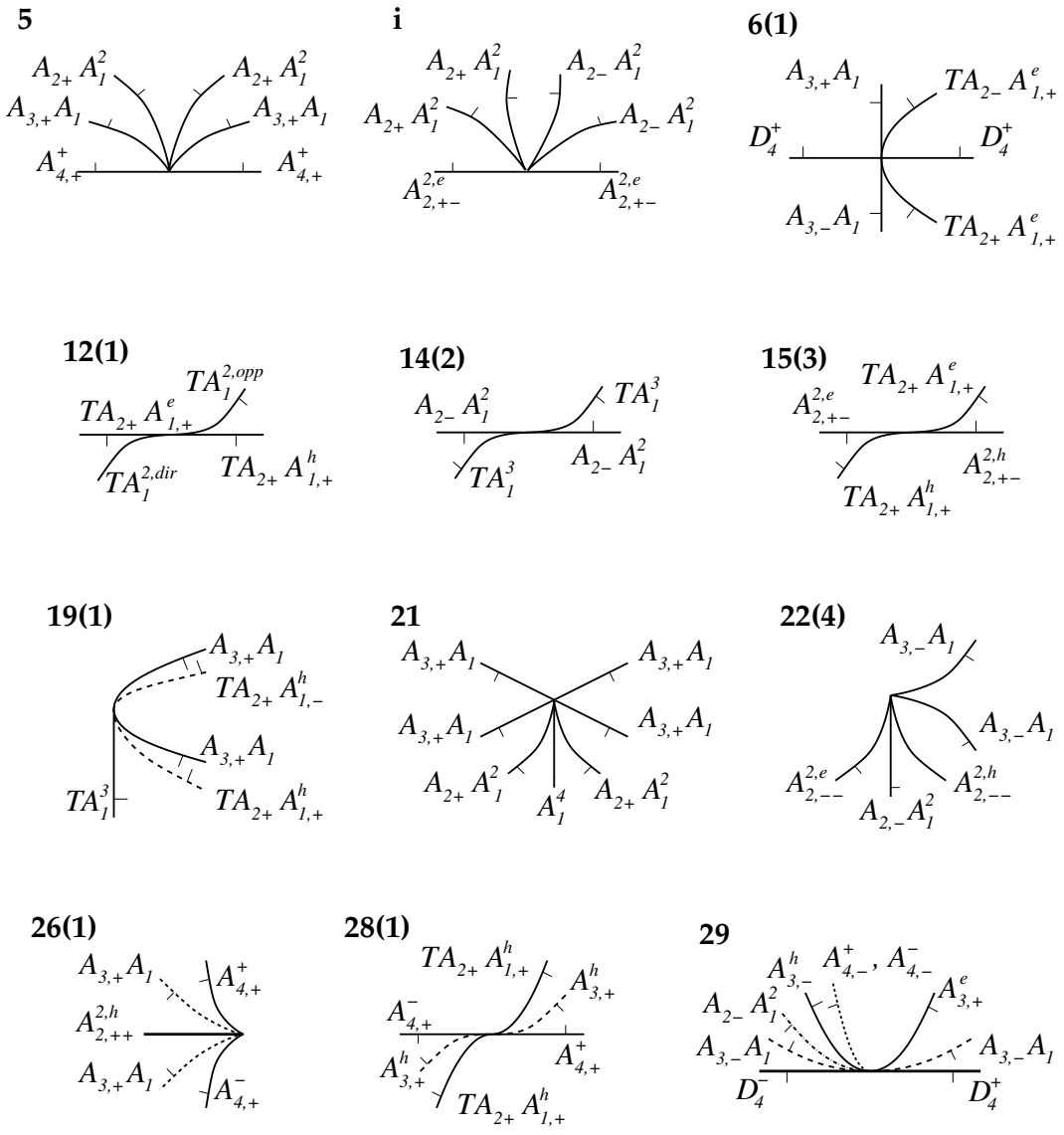

Figure 4.6: Bifurcation diagrams of 2-parameter families of oriented wave fronts.

		α	β	γ	σ
$\mathbf{14(1)} : 2a_{2+}a_1^2 - 2ta_1^3$	$= 0$				$+$
$\mathbf{14(2)} : 2a_{2-}a_1^2 - 2ta_1^3$	$= 0$				$-$
$\mathbf{15(1)} : a^{2,e}_{2,++} + [a^{2,h}_{2,++}] - ta_{2+}a^e_{1,+} - ta_{2+}a^e_{1,-}$	$= 0$	$+$			$+$
$\mathbf{15(2)} : a^{2,e}_{2,+-} - a^{2,h}_{2,+-} - ta_{2-}a^e_{1,-} - ta_{2-}a^e_{1,+}$	$= 0$	$+$			$-$
$\mathbf{15(3)} : a^{2,e}_{2,+-} + a^{2,h}_{2,+-} - ta_{2+}a^e_{1,+} - ta_{2+}a^e_{1,-}$	$= 0$	$-$			$+$
$\mathbf{15(4)} : a^{2,e}_{2,--} + [a^{2,h}_{2,--}] - ta_{2-}a^e_{1,-} - ta_{2-}a^e_{1,+}$	$= 0$	$-$			$-$
$\mathbf{19(1)} : 2a_{3,+}a_1 - ta_{2+}a^e_{1,-} - ta_{2+}a^e_{1,+} - ta_1^3$	$= 0$	$+$		$+$	
$\mathbf{19(2)} : 2a_{3,-}a_1 - ta_{2-}a^e_{1,-} - ta_{2-}a^e_{1,+} - ta_1^3$	$= 0$	$-$		$+$	
$\mathbf{21} : [a_1^4]$	$= 0$				
$\mathbf{22(1)} : 2a_{3,+}a_1 + [a^{2,h}_{2,++}] - a^{2,e}_{2,++} - a_{2+}a_1^2$	$= 0$	$+$	$+$		
$\mathbf{22(2)} : 2a_{3,+}a_1 - a^{2,h}_{2,+-} - a^{2,e}_{2,+-} - a_{2-}a_1^2$	$= 0$	$+$	$-$		
$\mathbf{22(3)} : 2a_{3,-}a_1 + a^{2,h}_{2,+-} - a^{2,e}_{2,+-} - a_{2+}a_1^2$	$= 0$	$-$	$+$		
$\mathbf{22(4)} : 2a_{3,-}a_1 + [a^{2,h}_{2,--}] - a^{2,e}_{2,--} - a_{2-}a_1^2$	$= 0$	$-$	$-$		
$\mathbf{26(1)} : a^+_{4,+} - a^-_{4,+} + [a^{2,h}_{2,++}]$	$= 0$		$+$		
$\mathbf{26(2)} : a^+_{4,-} - a^-_{4,-} + [a^{2,h}_{2,--}]$	$= 0$		$-$		
$\mathbf{28(1)} : a^+_{4,+} + a^-_{4,+} - 2ta_{2+}a^e_{1,-} - 2a^{e/h}_{3,+}$	$= 0$		$+$		
$\mathbf{28(2)} : a^+_{4,-} + a^-_{4,-} - 2ta_{2-}a^e_{1,+} - 2a^{e/h}_{3,-}$	$= 0$		$-$		
$\mathbf{29} : d_4^- - 2a_{3,-}a_1 - a^{e/h}_{3,+} + a^+_{4,-} + a^-_{4,-} - a^{e/h}_{3,-}$ $+a_{2-}a_1^2 - d_4^+$	$= 0$		$-$		
$\mathbf{30} : d_4^+ - 2a_{3,+}a_1 - a^{e/h}_{3,-} + a^+_{4,+} + a^-_{4,+} - a^{e/h}_{3,+}$ $+a_{2+}a_1^2 - d_4^-$	$= 0$		$+$		

4.7 Proofs of the classification of Section 4.3

The coefficients of the corresponding equations are collected in the two tables below. The A_4A_1 equations (number **5** in Figure 4.6) are not included since they are trivial. No other 2-parameter families provide non-independent equations.

$\mathbb{Z}$	**i**	**6(1)**	**6(2)**	**12(1)**	**12(2)**	**14(1)**	**14(2)**	**15(1)**	**15(2)**	**15(3)**	**15(4)**	**19(1)**
TA_1^3	.	.	.	.	.	-2	-2	.	.	.	.	-1
$TA_{1,opp}^2$	.	.	.	-1	-1	.	.	.	.	.	.	.
$A_{2+}A_1^2$	2	.	.	.	.	2	.	.	.	.	.	.
$A_{2-}A_1^2$	-2	.	.	.	.	.	2	.	.	.	.	
$A_{3,+}A_1$	.	1	1	.	.	.	.	.	.	.	.	2
$A_{3,-}A_1$	.	-1	-1	.	.	.	.	.	.	.	.	.
$TA_{2+}A_{1,+/-}^{e/h}$	.	-1	.	1	.	.	.	-1	.	-1	.	-1
$TA_{2+}A_{1,-/+}^{e/h}$	.	.	-1	-1	.	.	.	-1	.	-1	.	-1
$TA_{2-}A_{1,+/-}^{e/h}$	.	1	.	.	1	.	.	.	-1	.	-1	.
$TA_{2-}A_{1,-/+}^{e/h}$	.	.	1	.	-1	.	.	.	-1	.	-1	.
$A_{3,+}^{e/h}$	.	.	.	.	.	.	.	.	.	.	.	.
$A_{3,-}^{e/h}$	.	.	.	.	.	.	.	.	.	.	.	.
$A_{2,++}^{2,e}$	.	.	.	.	.	.	.	1	.	.	.	.
$A_{2,+-}^{2,e}$	.	.	.	.	.	.	.	.	1	1	.	.
$A_{2,--}^{2,e}$	.	.	.	.	.	.	.	.	.	.	1	.
$A_{2,+-}^{2,h}$	.	.	.	.	.	.	.	.	-1	1	.	.
$A_{4,+}^{+}$	.	.	.	.	.	.	.	.	.	.	.	.
$A_{4,+}^{-}$	.	.	.	.	.	.	.	.	.	.	.	.
$A_{4,-}^{+}$	.	.	.	.	.	.	.	.	.	.	.	.
$A_{4,-}^{-}$	.	.	.	.	.	.	.	.	.	.	.	.
D_4^+	.	.	.	.	.	.	.	.	.	.	.	.
D_4^-	.	.	.	.	.	.	.	.	.	.	.	.

$\mathbb{Z}$	**19(2)**	**21**	**22(1)**	**22(2)**	**22(3)**	**22(4)**	**26(1)**	**26(2)**	**28(1)**	**28(2)**	**29**	**30**
TA_1^3	-1		.	.	.	.	.	.	.	.	.	.
$TA_{1,opp}^2$	.	.	.	.	.	.	.	.	.	.	.	.
$A_{2+}A_1^2$	.	.	-1	.	-1	.	.	.	.	.	.	1
$A_{2-}A_1^2$	.	.	.	-1	.	-1	.	.	.	.	1	.
$A_{3,+}A_1$	.	.	2	2	.	.	.	.	.	.	.	-2
$A_{3,-}A_1$	2	.	.	.	2	2	.	.	.	.	-2	.
$TA_{2+}A_{1,+/-}^{e/h}$	.	.	.	.	.	.	.	.	.	.	.	.
$TA_{2+}A_{1,-/+}^{e/h}$	.	.	.	.	.	.	.	.	-2	.	.	.
$TA_{2-}A_{1,+/-}^{e/h}$	-1	.	.	.	.	.	.	.	.	-2	.	.
$TA_{2-}A_{1,-/+}^{e/h}$	-1	.	.	.	.	.	.	.	.	.	.	.
$A_{3,+}^{e/h}$	.	.	.	.	.	.	.	.	-2	.	-1	-1
$A_{3,-}^{e/h}$	.	.	.	.	.	.	.	.	.	-2	-1	-1
$A_{2,++}^{2,e}$	.	.	-1	.	.	.	.	.	.	.	.	.
$A_{2,+-}^{2,e}$	.	.	.	-1	-1	.	.	.	.	.	.	.
$A_{2,--}^{2,e}$	.	.	.	.	.	-1	.	.	.	.	.	.
$A_{2,+-}^{2,h}$	.	.	.	-1	1	.	.	.	.	.	.	.
$A_{4,+}^{+}$	.	.	.	.	.	.	1	.	1	.	.	1
$A_{4,+}^{-}$	.	.	.	.	.	.	-1	.	1	.	.	1
$A_{4,-}^{+}$	.	.	.	.	.	.	.	1	.	1	1	.
$A_{4,-}^{-}$	.	.	.	.	.	.	.	-1	.	1	1	.
D_4^+	.	.	.	.	.	.	.	.	.	.	-1	1
D_4^-	.	.	.	.	.	.	.	.	.	.	1	-1

The mod2 equations are collected in the next two tables. We have omitted there the strata which cannot contribute to the invariants (for example, A_1^4), and equations which are linear combinations of the others.

$\mathbb{Z}_2$	**6(2)**	**12(1)**	**15(1)**	**15(3)**	**15(4)**	**19(1)**	**22(1)**
TA_1^3	.	.	.	.	.	1	.
$TA_{1,opp}^2$	.	1	.	.	.	.	.
$TA_{1,dir}^2$	.	1	.	.	.	.	.
$A_{2+}A_1^2$	.	.	.	.	.	.	1
$A_{2-}A_1^2$	.	.	.	.	.	.	.
$A_{3,+}A_1$	1	.	.	.	.	.	.
$A_{3,-}A_1$	1	.	.	.	.	.	.
$TA_{2+}A_{1,+/-}^{e/h}$	.	1	1	1	.	1	.
$TA_{2+}A_{1,-/+}^{e/h}$	1	1	1	1	.	1	.
$TA_{2-}A_{1,+/-}^{e/h}$	.	.	.	.	1	.	.
$TA_{2-}A_{1,-/+}^{e/h}$	1	.	.	.	1	.	.
$A_{3,+}^{e/h}$	.	.	.	.	.	.	.
$A_{3,-}^{e/h}$	.	.	.	.	.	.	.
$A_{2,++}^{2,e}$	.	.	1	.	.	.	1
$A_{2,+-}^{2,e}$	.	.	.	1	.	.	.
$A_{2,--}^{2,e}$	.	.	.	.	1	.	.
$A_{2,++}^{2,h}$	.	.	1	.	.	.	1
$A_{2,+-}^{2,h}$	.	.	.	1	.	.	.
$A_{2,--}^{2,h}$	.	.	.	.	1	.	.
$A_{4,+}^{+}$	.	.	.	.	.	.	.
$A_{4,+}^{-}$	.	.	.	.	.	.	.
$A_{4,-}^{+}$	.	.	.	.	.	.	.
$A_{4,-}^{-}$	.	.	.	.	.	.	.
D_4^+	.	.	.	.	.	.	.
D_4^-	.	.	.	.	.	.	.

$\mathbb{Z}_2$	**22(2)**	**22(4)**	**26(1)**	**26(2)**	**28(1)**	**28(2)**	**30**
TA_1^3	.	.	.	.	.	.	.
$TA_{1,opp}^2$	.	.	.	.	.	.	.
$TA_{1,dir}^2$	.	.	.	.	.	.	.
$A_{2+}A_1^2$	.	.	.	.	.	.	1
$A_{2-}A_1^2$	1	1	.	.	.	.	.
$A_{3,+}A_1$	.	.	.	.	.	.	.
$A_{3,-}A_1$	.	.	.	.	.	.	.
$TA_{2+}A_{1,+/-}^{e/h}$	.	.	.	.	.	.	.
$TA_{2+}A_{1,-/+}^{e/h}$	.	.	.	.	.	.	.
$TA_{2-}A_{1,+/-}^{e/h}$	.	.	.	.	.	.	.
$TA_{2-}A_{1,-/+}^{e/h}$	.	.	.	.	.	.	.
$A_{3,+}^{e/h}$	.	.	.	.	.	.	1
$A_{3,-}^{e/h}$	.	.	.	.	.	.	1
$A_{2,++}^{2,e}$	.	.	.	.	.	.	.
$A_{2,+-}^{2,e}$	1	.	.	.	.	.	.
$A_{2,--}^{2,e}$	.	1	.	.	.	.	.
$A_{2,++}^{2,h}$	.	.	1	.	.	.	.
$A_{2,+-}^{2,h}$	1	.	.	.	.	.	.
$A_{2,--}^{2,h}$	.	1	.	1	.	.	.
$A_{4,+}^{+}$	.	.	1	.	1	.	.
$A_{4,+}^{-}$	.	.	1	.	1	.	.
$A_{4,-}^{+}$	.	.	.	1	.	1	.
$A_{4,-}^{-}$	.	.	.	1	.	1	.
D_4^+	.	.	.	.	.	.	1
D_4^-	.	.	.	.	.	.	1

The rank count of the previous tables shows that the spaces of integer and mod2 discriminantal cycles are 7- and 11-dimensional respectively, which proves Theorem 4.3.1 and 4.3.2.

The next table lists basic discriminantal cycles over the integers.

	$(I_{s_+}-3I_{\Sigma^2})/2$	$(I_{s_-}+I_{\Sigma^2})/2$	$I_{c_+}/2$	$I_{c_-}/2$	I_t	I_{Σ^2}	$((I_{s_+}+I_{s_-})/2+I_t-I_{\int})/2$
TA_1^3	.	.	.	.	2	.	1
$TA_{1,opp}^2$	.	.	.	.	.	.	1
$\left[TA_{1,dir}^2\right]$	.	.	.	.	.	.	.
$A_{2+}A_1^2$	.	.	.	.	2	.	1
$A_{2-}A_1^2$	.	.	.	.	2	.	1
$A_{3,+}A_1$	.	.	1	.	1	.	1
$A_{3,-}A_1$	.	.	.	1	1	.	.
$TA_{2+}A_{1,+/-}^{e/h}$	.	.	1	.	.	.	1
$TA_{2+}A_{1,-/+}^{e/h}$	.	.	1	.	.	.	.
$TA_{2-}A_{1,+/-}^{e/h}$	.	.	.	1	.	.	.
$TA_{2-}A_{1,-/+}^{e/h}$	.	.	.	1	.	.	-1
$A_{3,+}^{e/h}$	1	.	.	.	.	.	1
$A_{3,-}^{e/h}$	.	1	.	.	.	.	.
$A_{2,++}^{2,e}$	.	.	2	.	.	.	1
$A_{2,+-}^{2,e}$	.	.	2	2	.	.	.
$A_{2,--}^{2,e}$	.	.	.	2	.	.	-1
$\left[A_{2,++}^{2,h}\right]$	.	.	.	.	.	.	.
$A_{2,+-}^{2,h}$	.	.	-1	1	.	.	1
$\left[A_{2,--}^{2,h}\right]$	.	.	.	.	.	.	.
$A_{4,+}^{+}$	1	.	1	.	.	.	1
$A_{4,+}^{-}$	1	.	1	.	.	.	1
$A_{4,-}^{+}$	.	1	.	1	.	.	.
$A_{4,-}^{-}$	.	1	.	1	.	.	.
D_4^+	-1	.	.	.	.	1	.
D_4^-	.	-1	.	.	.	1	.

A basis of the discriminantal cycles over mod2 are formed by the reduced invariants of the previous table and by the derivatives of:

$$\begin{aligned} I_{\ell} &: A_{2,+-}^{2,e}+A_{2,+-}^{2,h}; \\ I_{\ell'_+} &: A_{4,+}^{+}+A_{4,+}^{-}; \\ I_{\ell'_-} &: A_{4,-}^{+}+A_{4,-}^{-}; \\ I_{tan} &: TA_1^{2,opp}+TA_1^{2,dir}. \end{aligned}$$

4.8 Classification of the discriminantal cycles and invariants over $\mathbb{Q}$

Our results over the rational numbers are:

Theorem 4.8.1. *For any oriented surface M and oriented 3-manifold N, the space of rational discriminantal cycles in $\mathcal{L}_{or}(M, \mathbb{R}^3)$ has rank 7. Its basis is formed by the derivatives of the invariants*

$$I_t\,, \quad I_{s_+}\,, \quad I_{s_-}\,, \quad I_{c_+}\,, \quad I_{c_-}\,, \quad I_{\Sigma^2}\,, \quad I_{\int}.$$

Considering $\mathcal{L}^1_{or}(M, \mathbb{R}^3)$, the set of all Legendrian maps without corank 2 points, we have

Corollary 4.8.1. *The space of all rational local invariants on $\mathcal{L}^1_{or}(M, \mathbb{R}^3)$ has rank 6. Its basis is formed by the derivatives of the invariants*

$$I_t\,, \quad I_{s_+}\,, \quad I_{s_-}\,, \quad I_{c_+}\,, \quad I_{c_-}\,, \quad I_{\int}.$$

List of Figures

Bibliography

[1] V. A. Vassiliev, *Cohomology of knot spaces* , Theory of singularities and its applications, Advances in Soviet Mathematics **1**, American Mathematical Society, Providence, RI, 1994, 225–262.

[2] V.A.Vassiliev, *Lagrange and Legendre characteristic classes,* Advanced Studies in Contemporary Mathematics **3**, Gordon and Breach Science Publishers, New York, 1988, x+268 pp.

[3] S. Chmutov, S. Duzhin and J. Mostovoy, *Introduction to Vassiliev Knot Invariants*, Cambridge University Press, May 2012, ISBN 978-1-107-02083-2.

[4] H. Whitney, *On regular closed curves in the plane*. Compositio Mathematica, 4 (1937), p. 276-284

[5] F. Aicardi, *Discriminants and local invariants of planar fronts*, The Arnold-Gelfand mathematical seminars. Geometry and singularity theory (eds V.I.Arnold, I.M.Gelfand, V.S.Retakh and M.Smirnov), Birkhäuser Boston, Boston, MA, 1997, 1–76.

[6] F. Aicardi, *On Mod2 Local Invariants of Maps Between 3-Manifiods*, pp:1-8, https://www.researchgate.net/publication/259189520.

[7] V. I. Arnold, *Plane curves, their invariants, perestroikas and classifications*, Advances in Soviet Mathematics 21 (1994), 3391.

[8] V. I. Arnold, *Mathematical Methods of Classical Mechanics*, Springer-Verlag, GTM 60, Berlin Heidelberg, Second edition, (1989).

[9] V. I. Arnold, *Geometrical Methods In The Theory of Ordinary Differential Equations*, Springer-Verlag, Berlin,(1988).

[10] V. I. Arnold, *Wave front evolution and equivariant Morse lemma*, Comm. Pure Appl. Math. **29** (1976) no. 6, 557–582.

[11] V. I. Arnold, S.M.Gusein-Zade and A.N.Varchenko, *Singularities of differentiable maps. Vol. I. The classification of critical points, caustics and wave fronts*, Monographs in Mathematics **82**, Birkhäuser Boston, Boston, MA, 1985, xi+382 pp.

[12] V. I. Arnold, *Singularities of caustics and wave fronts*, Mathematics and its Applications (Soviet Series) **62**, Kluwer, Dordrecht, 1990, xiv+259 pp. Apink, Auln

[13] V. I. Arnold, *Topological invariants of plane curves and caustics*, University Lecture Series **5** (American Mathematical Society, Providence, RI, 1994) viii+60 pp.

[14] V. I. Arnold, *Invarianty i perestroiki ploskih frontov*, Osobennosti gladkikh otobrazheniy s dopolnitel'nymi strukturami, Trudy Mat. Inst.

Steklov. **209** (1995) 14–64. English translation: *Invariants and perestroikas of wave fronts on the plane*, Singularities of smooth mappings with additional structures, *Proc. Steklov Inst. Math.* **209** (1995) 11–56.

[15] O. V. Lyashko, *Geometry of bifurcation diagrams*. Current problems in mathematics (Russian), Vol. 22, 94129, Itogi Nauki i Tekhniki, Akad. Nauk SSSR, Vsesoyuz. Inst. Nauchn. i Tekhn. Inform., Moscow, 1983.

[16] V. Goryunov, *Local invariants of mappings of surfaces into three-space*, The Arnold-Gelfand mathematical seminars. Geometry and singularity theory (eds V. I. Arnold, I. M. Gelfand, V. S. Retakh and M. Smirnov), Birkhäuser Boston, Boston, MA, 1997, 223–255.

[17] V. Goryunov, *Local invariants of maps between 3-manifolds*, Journal of Topology **6** (2013) 757–778.

[18] V. Goryunov, *Singularities of projections of complete intersections*, Current problems in mathematics, vol. 22, 167–206, Itogi Nauki i Tekhniki, Akad. Nauk SSSR, VINITI, Moscow, 1983 (Russian). English translation:*Journal of Soviet Mathematics* **27** (1984) no.3, 2785–2811.

[19] V. Goryunov and V. M. Zakalyukin, *Lagrangian and Legendrian Singularities*, Real and Complex Singularities, Trends in Mathematics, 169185, Birkhauger, 2006.

[20] V. Tchernov, *Arnold-type invariants of wave fronts on surfaces*, Topology **41** (2002) no. 1, 1–45.

[21] V. M. Zakalyukin, *Reconstructions of fronts and caustics depending on a parameter, and versality of mappings*, Current problems in mathemat-

ics, vol. 22, 56–93, Itogi Nauki i Tekhniki, Akad. Nauk SSSR, VINITI, Moscow, 1983 (Russian). English translation: *Journal of Soviet Mathematics* **27** (1984) no.3, 2713–2735.

[22] V. M. Zakalyukin, *Reconstructions of fronts and caustics depending one parameter*, Funct. Anal. Appl. (1976), 139140.

[23] V. M. Zakalyukin, *Lagrangian and Legendrian singularities*, Funct. Anal. Appl. (1976), 2331.